The Dissertation Committee for Joseph James Reczek Certifies that this is the approved version of the following dissertation:

Aromatic Electron Donor-Acceptor Interactions in Novel Supramolecular Assemblies

Committee:

Brent L. Iverson, Supervisor

C. Grant Willson

Jonathan L. Sessler

David A. Vanden Bout

Yueh-Lin Loo

Aromatic Electron Donor-Acceptor Interactions in Novel Supramolecular Assemblies

by

Joseph James Reczek, B.A.

Dissertation

Presented to the Faculty of the Graduate School of

The University of Texas at Austin

in Partial Fulfillment

of the Requirements

for the Degree of

Doctor of Philosophy

The University of Texas at Austin

December 2006

Dedication

To Julie and my family

Acknowledgements

I would like to thank my advisor, Professor Brent Iverson, for his years of guidance, patience, and support. The lessons he has taught, often by example, in chemistry, teaching, communication, thinking, perseverance, priorities, and the power of a positive attitude have made me a better scientist and a better person. He is truly a role model for the professional I hope to become.

I want to thank my friends in Austin who have aided me in both experiments and recreation, from the AFM to the WNDC. The cooperation and community here at UT make it a special place. In particular I would like to thank Sean McClure, Ron Houk, Bryan Kaehr, and Stephan Moldonado for their friendship, advice and beer.

I thank the Iverson group for their helpfulness and a pleasant working environment. Past members Greg Gabriel for all his help getting started in the group, and for a constant belief in what I was doing; and Karl Griswold for great conversations that no one should ever have. My contemporaries Navin Varadarajan and Yongjun Chu for always offering a friendly smile, good advice, and a pleasant conversation; and Valerie Bradford for both helpful and entertaining discussions. Finally the younger members; Chelsea Martinez for her candid point of view and editing skills, and Stevan Samuel for keeping me entertained and not asking *too many* questions. The future of the group's research is in good hands.

Most of all I would like to thank my family for their love and support. Often those Sunday morning phone calls were the highlight of my week. My Dad for always listening, advising, and supporting me, and my Mom for her love, worry, and caring conversations. And Julie, thank you for everything.

Aromatic Electron Donor-Acceptor Interactions in Novel Supramolecular Assemblies

Publication No._____

Joseph James Reczek, Ph.D.

The University of Texas at Austin, 2006

Supervisor: Brent L. Iverson

Molecular self-assembly using non-covalent interactions mediate the structure and function of many critical biological and synthetic molecules. Aromatic donor-acceptor interactions are a type of non-covalent interaction that have been utilized by the Iverson group in the development of aedamers, a class of foldamers that adopt specific secondary structures in aqueous solution. These molecules and their derivatives exploit the complexation of electron-rich 1,5-dialkoxy-naphthalene (Dan) with electron-deficient 1,4,5,8-naphthalene tetracarboxylic diimide (Ndi) within linear charged oligomers to achieve both *inter* and *intra*-molecular assemblies not found in nature.

This dissertation describes the use of the Dan:Ndi interaction in new systems and environments, expanding the potential and scope for applications of this chemistry. This work specifically focuses on *inter*-molecular assemblies, with novel molecular designs

for solution interactions as well as the group's first exploration of designed solid state and bulk properties.

Chapter 2 describes incorporation of either Dan or Ndi units into independent polymer strands. When mixed together, the Dan and Ndi polymers are shown to associate in solution and upon processing form macrostructures in films and fibers. Chapter 3 reports experiments in which a series of Dan and Ndi monomers are synthesized, melted together, and then allowed to cool to afford columnar mesophases. The results demonstrate the ability to predictably control the structure and phase transition temperatures of mesophases by mixing and matching Dan and Ndi components. Chapter 4 presents the solution phase synthesis of neutral Dan oligomers and describes their potential to increase the association constants of Dan and Ndi oligomers in aqueous solution. Chapter 5 describes work developing alternative designs in the structure and connectivity of Dan and Ndi units for intermolecular assembly.

Overall the work described herein implements aromatic electron donor-acceptor interactions in novel supramolecular chemistry, with a focus on the use of Dan and Ndi complexation in the formation of materials. These studies have taken the first difficult steps towards making uniquely controllable and functional materials based on non-covalent aromatic interactions a practical reality.

Table of Contents

List of Schemes

List of Figures

CHAPTER 1

Structural Assembly with Directed Aromatic Donor-Acceptor Interactions

1.1 MOLECULAR SELF ASSEMBLY: THINKING PAST THE COVALENT BOND

Much of the research in organic chemistry for over a century has been focused on the formation of novel or nature inspired molecules by developing ways to connect specific atoms with covalent bonds. However, molecular function is often dependent on non-covalent bonds. The natural world is filled with examples of functional non-covalent assemblies. Figure 1.1 represents just a few examples of natural assemblies, as well as some inspired synthetic designs. Both utilize the same non-covalent interactions, the most common of which are electrostatic, van der Waals, hydrogen bonding, metal coordination, and the centerpiece and focus of the work presented herein: aromatic-aromatic interactions.

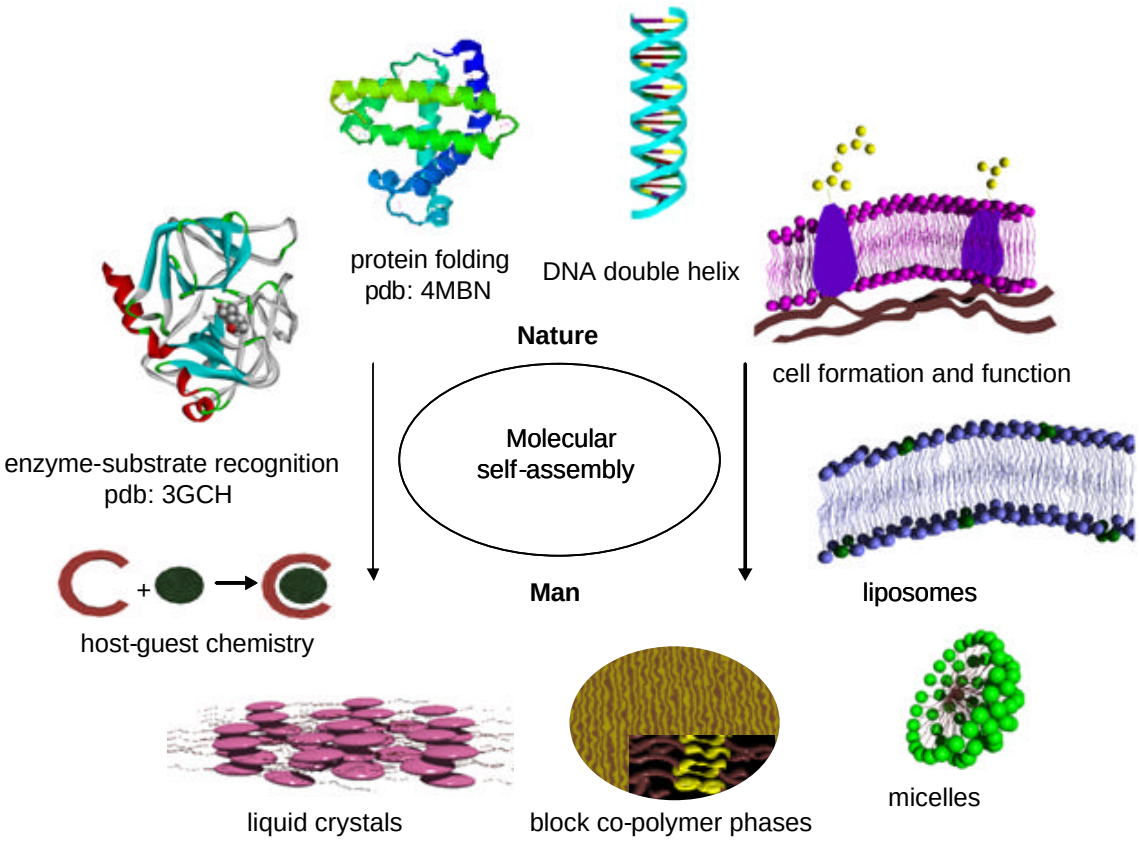

Figure 1.1 Schematic representations of molecular self-assembly in nature and some of the inspired synthetic assemblies.

Nature designs molecules to make use of one or several non-covalent interactions. One of the most commonly cited examples is that of the information storage capabilities of duplex DNA, which from just four basic building blocks, codes all the information of life. The solution structure of DNA exhibits two basic modes of molecular self-assembly through non-covalent bonds: intermolecular, or "supramolecular chemistry" (Lehn 1988), and intramolecular or "foldamer chemistry" (Gellman 1998). It has long been known that DNA adopts a double helical structure in solution based on specific *interstrand* hydrogen

bonding between base pairs. This is analogous to supramolecular chemistry, in which molecules are designed with the intent of specific interaction with other atoms, ions, or molecules to form complexes and assemblies. The stability of the DNA double helix is due largely to *intrastrand* aromatic-aromatic interaction between adjacent bases, analogous to foldamer chemistry, in which molecules are designed to exist in a specific secondary structure via intramolecular interactions (Baltzer 1999, McDonnell 1999). Other examples in biology cover an incredible functional range, from the amazing catalytic activity of enzymes that is derived in large part from their ability to specifically fold (foldamer chemistry) and then recognize substrate molecules (supramolecular chemistry), to the extremely high tensile strength and elasticity of spider silk, which is based on intermolecular and intramolecular hydrogen bonding (Winkler 2000, Kubik 2002). All are examples of covalent molecules, evolved in nature, to produce amazing properties and functions via molecular self-assembly.

Life exists due to the non-covalent folding, binding, and general assembly of biological molecules. To better understand these miracles of nature and creatively build on their concepts, we must better understand molecular self-assembly itself (Whitesides 2002). The arsenal of synthetic weapons and modeling tools developed over the years allow today's chemists to design and create synthetic self-assembling systems, and a multitude of intriguing, enlightening, and useful designs have been the result, in areas ranging from drug design and delivery to catalysis and even material science (Philp 1996, Reinhoudt 2002). Some systems closely resemble the natural designs which inspired them, and some move in new creative directions, all using one or more of the

directed non-covalent interactions found in nature to understand structure, and work toward function.

This introduction briefly discusses the origins and general scope of synthetic self-assembly in its intermolecular (supramolecular chemistry) and intramolecular (foldamer chemistry) forms, and then focuses on the concept and utility of self-assembly though aromatic-aromatic interactions. The previous studies of the Iverson group using directed donor-acceptor aromatic interactions are discussed in some detail as the precursors to the designs and experiments presented in the following chapters.

1.1.1 Supramolecular Chemistry

In the late 1960's, chemists started designing synthetic molecules with the specific intent of controlling interactions with other molecules via non-covalent interactions. The earliest examples of synthetically designed supramolecular chemistry, although it was not named so until later (Lehn 1988), are the crown ethers that Charles Pedersen designed to bind cations, shown in figure 1.2a (Pedersen 1967). The utility of the cyclic ethers was soon expanded to include complexation of small molecules, namely a-amino acids, by Cram and co-workers with binaphthalene corand systems (Figure 1.2b) (Helgeson 1973). A slightly different binding motif was then designed by Lehn and co-workers involving complete inclusion of cations with polyether cryptates (Figure 1.2c) (Cheney 1972).

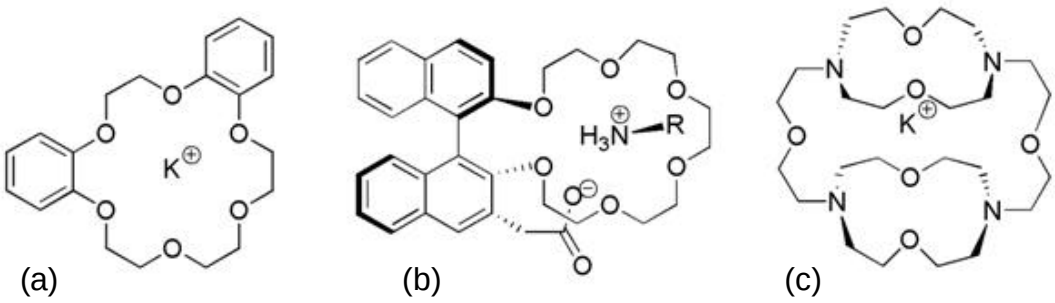

Figure 1.2 The origins of synthetic supramolecular chemistry.

The term “host-guest chemistry” or “molecular recognition” is commonly applied to molecules designed to bind a specific ion or small molecule, and this has become an incredibly rich and prolific field in its own right. Designing and synthesizing molecules for the purpose of ion and/or small molecule association and binding is truly looking past the covalent bond to the formation inter-molecular assemblies, and therefore supramolecular chemistry, and serves as the conceptual precursor to all types of synthetic self-assembly. Pedersen, Lehn, and Cram shared the 1987 Nobel prize in chemistry for the foundation of and further contribution to supramolecular chemistry. Much of the early work in this area can be found in several reviews (Lehn 1990, Amabilino 1995, Atwood 1996).

1.1.1.1 Polymers and Phases

Having more than one directed intermolecular interaction per molecule leads to a major branch of supramolecular self-assembly dealing with the organized control over polymolecular systems. These systems are generally what comes to mind today when considering supramolecular chemistry, and mainly consist of two types; supramolecular polymers and supramolecular phases (Lehn 2002).

Putting two or more directing non-covalent reaction sites on a single molecule can lead to the formation of extended "polymers" formed much like one would think from a traditional step growth polymerization. The most common non-covalent interactions utilized in these directed assemblies to date are hydrogen bonding and metal coordination due to their relative strength and directionality, discussed in respective reviews (Archer 2001, Edelmann 1999). For linear systems (Figure 1.3a), two ditopic monomers are synthesized with complementary reaction sites and are mixed in a 1:1 molar ratio in solution. The molecules interact and assemble due to the thermodynamic driving force of the designed interactions and associate to form extended assemblies. The structure of the linker between the interacting sites can be varied; for example it could be flexible or a rigid rod (Figure 1.3b), both of which have been shown to alter properties in resulting structures and films (Wegner 1992). Two and three dimensional cross linking structures have also been designed, illustrated schematically in figure 1.3, and show intriguing properties which include formation of gels and porous materials (Ciferri 2000). One example of non-covalent interacting groups for use in these architectures was designed by Lehn and co-workers and involves the tri-hydrogen bonding units shown in figure 1.3e (Fouquey 1990). Many more building blocks are available, and building blocks continue

to grow in number and variety for the supramolecular polymer chemist. The ability to mix and match components in a facile and dynamic manner offers an amazing variety of structures to explore, without the synthetic hardships and time drain of the covalent analogs (Lehn 2002, Ciferri 2000).

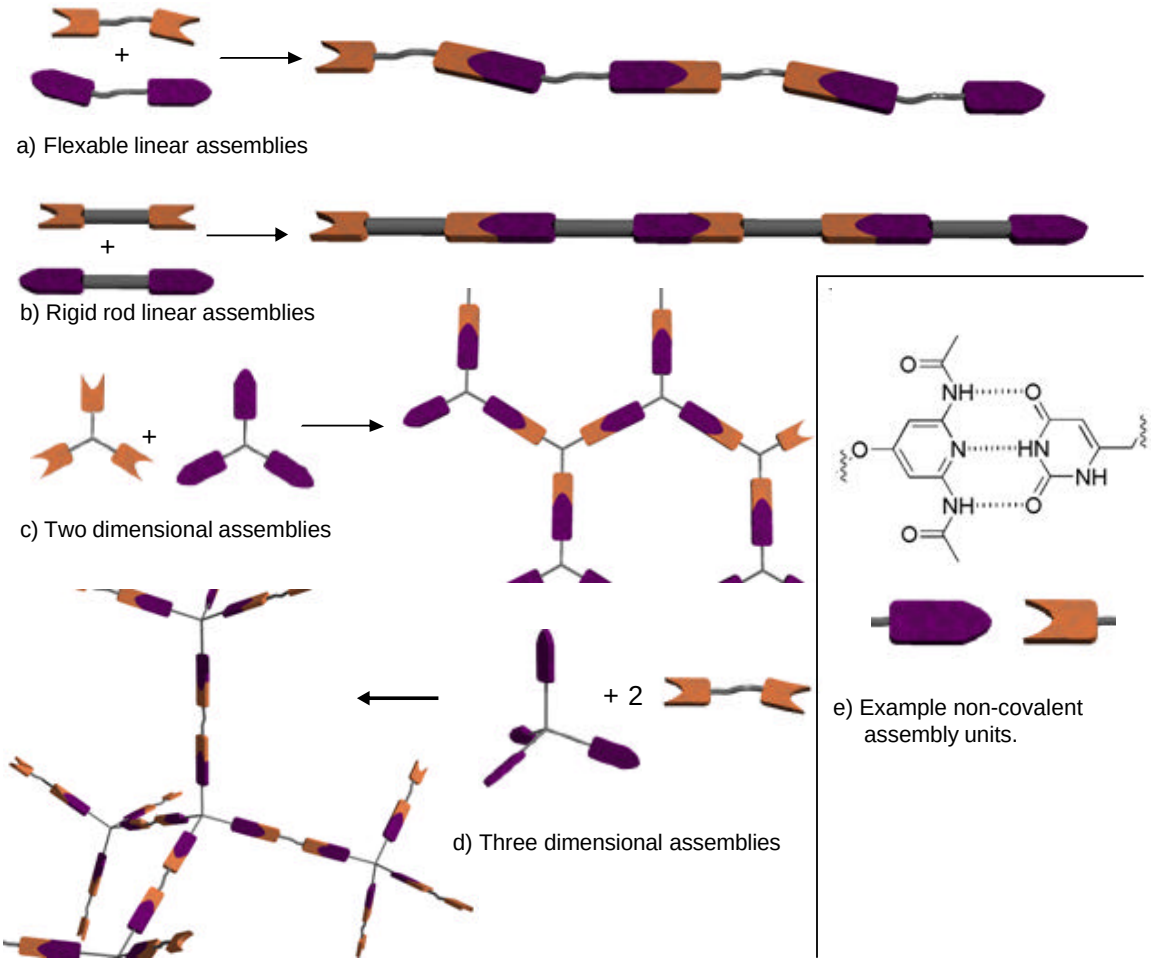

Figure 1.3 Representations of some supramolecular polymer chemistry architectures.

Supramolecular chemistry is also used to affect bulk phase structure and properties. New types and enhanced control of mesophases, often liquid crystalline

phases, have resulted from designed non-covalent interactions including hydrogen bonding and aromatic-aromatic interactions (Chapter 3) which give a thermodynamic driving force and directional bias for molecular order (Steed 2000). The directed interactions have also benefited the field of crystal engineering which has employed a number of hydrogen bonding, p-stacking, and metal coordination interactions in the creative design of novel packing structures used in many solid state devices (Braga 1998).

From its beginnings almost forty years ago, the field of supramolecular chemistry has exploded in hundreds of directions and is the foundation for innovation in many areas such as nanotechnology, sensor technology, material science, and drug delivery (Whitesides 2002). Such history and accomplishments are inspiring, and drive the exploration of new and different modes and applications of self-assembly, including those discussed in this work.

1.1.3 Foldamer Chemistry

Synthetic foldamer chemistry is relatively recent in its popularity among organic chemists, having been first recognized as a design motif in the late 1980's with ß-peptides (Seebach 1996, Gellman 1996, Appella 1997). ß-peptides, made up of non-natural ß-amino acids, are similar in form to the a-peptides prevalent in nature, and have been designed to exhibit extraordinary control of helix formation in various solvents, including water, via intramolecular hydrogen bonding (Appella 1997, 2000, Cheng 2001) (Figure 1.4). Other hydrogen bonding structures observed with a-peptides have also

been rationally designed into ß-peptides by altering the ß-amino acids used in their synthesis, including ß-sheet formation (Seebach 1999) and hairpin turns (Langenhan 2004). These synthetic foldamers are classified as biomimetic foldamers due to their close relation in form and covalent structure to naturally occurring molecules (Zych 2001). There are several other examples of biomimetic foldamers in the peptide family including ?- and d-peptides (Brenner 2001), and peptoids (Kishenbaum 1998).

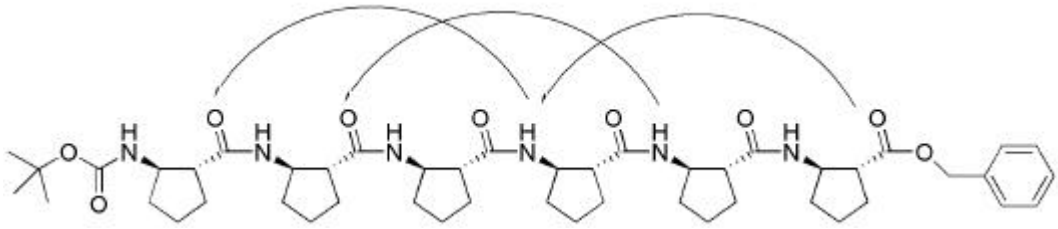

Figure 1.4 Synthetic ß-peptide that folds into a 12-helix via the implied H-bonds.

The field of foldamer chemistry has expanded quickly, and currently includes a great variety of exploited folding interactions and topologies, some of which are rendered in figure 1.5 (Hill 2001). The scope of designed intramolecular self-assembly has grown to include foldamers that are not similar in covalent structure to natural molecules. These molecules are termed “bio-inspired” as nature has given the inspiration to design self-assembled secondary structures, yet the compounds themselves are of unique synthetic design conceived from the imagination of the chemist (Zych 2001).

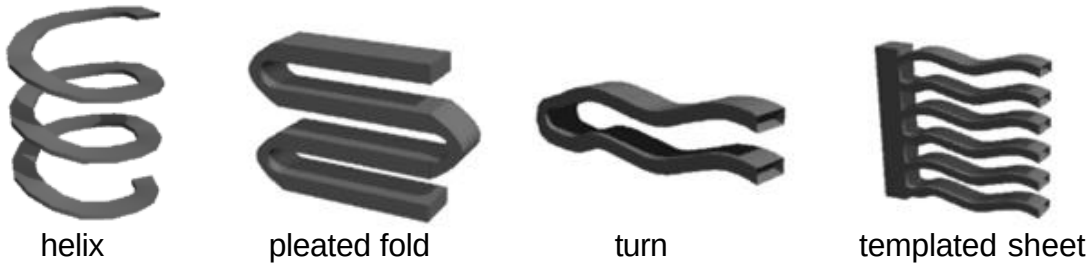

Figure 1.5 Renderings of common foldamer architectures.

Oligo(*meta*-phenylene ethynylene)s of Moore and co-workers, shown in figure 1.6a,b, are an example of a bio-inspired foldamer that forms stable helical conformations in solution through solvophobic driven aromatic-aromatic interactions promoted to fold by the geometric constraints along the backbone (Hill 2001). The folding of short oligomers was initially shown to be manipulated by temperature and organic solvent variations (Nelson 1997). In particular, double spin label studies showed a folded conformation in more polar solvents such as acetonitrile, and a completely random structure in less polar organics such as chloroform (Matsuda 2002). It was also shown that the twist-sense of the helixes could be affected by introducing chiral components into the side chains (Prince 2000a,b). These foldamers have been shown to participate in host-guest chemistry with rod-like guests of specific lengths (Figure 1.6d), exhibiting an emerging trend in the joining of foldamer and supramolecular chemistry (Tanatani 2001).

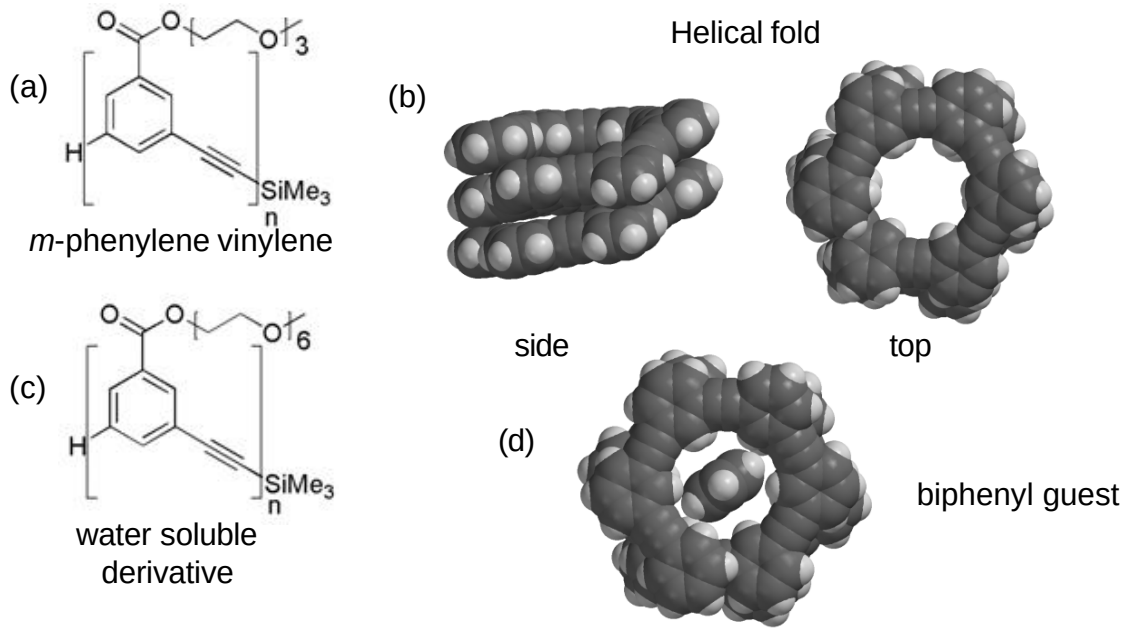

Figure 1.6 (a) Example of an oligo(*meta*-phenylene ethynylene) repeat unit. (b) Model of helical solution folding. (c) Repeat unit of water soluble foldamer. (d) Model of guest encapsulation by foldamer.

As increasing the polarity of the solvent generally increases the stability of aromatic-aromatic interactions, a water soluble version of the *m*-phenylene ethynylene was synthesized to enhance folding (Figure 1.6c) (Stone 2004). A percent water titration with methanol showed that the folded helix was stabilized as expected upon increasing water concentration up to 90%, but then surprisingly dropped at 100% water. The authors suggest that the inflexible conformation of the *m*-phenylene ethynylene molecule, while promoting folding in organic solvents, prevents complete water exclusion and requires a small amount of organic solvation for maximum stability. The first water soluble foldamer design, also of the bio-inspired class, is highly flexible, uses directing donor-acceptor components, and is most stable in 100% aqueous solution (Lokey 1995).

These foldamers, termed aedamers, were developed in the Iverson group and are discussed in detail below.

1.2 AEDAMERS

Aromatic electron donor-acceptor oligomers (aedamers) of the foldamer chemistry from this group (Lokey 1995) were the first synthetic molecules to adopt a designed secondary structure in aqueous solution due to directed aromatic interactions. These first generation aromatic donor-acceptor foldamers consist of relatively electron rich 1,5-dialkoxynaphthalene (Dan) units linked in an alternating fashion to electron poor 1,4,5,8-naphthalenetetracarboxylic diimide (Ndi) units (Figure 1.7). In water, the driving force of minimizing exposed aromatic surface area (hydrophobic affect), coupled with the face-to-face electrostatic compatibility of the Dan and Ndi units, leads to a stable secondary structure in which the molecule folds into a pleated form with a stacked aromatic core.

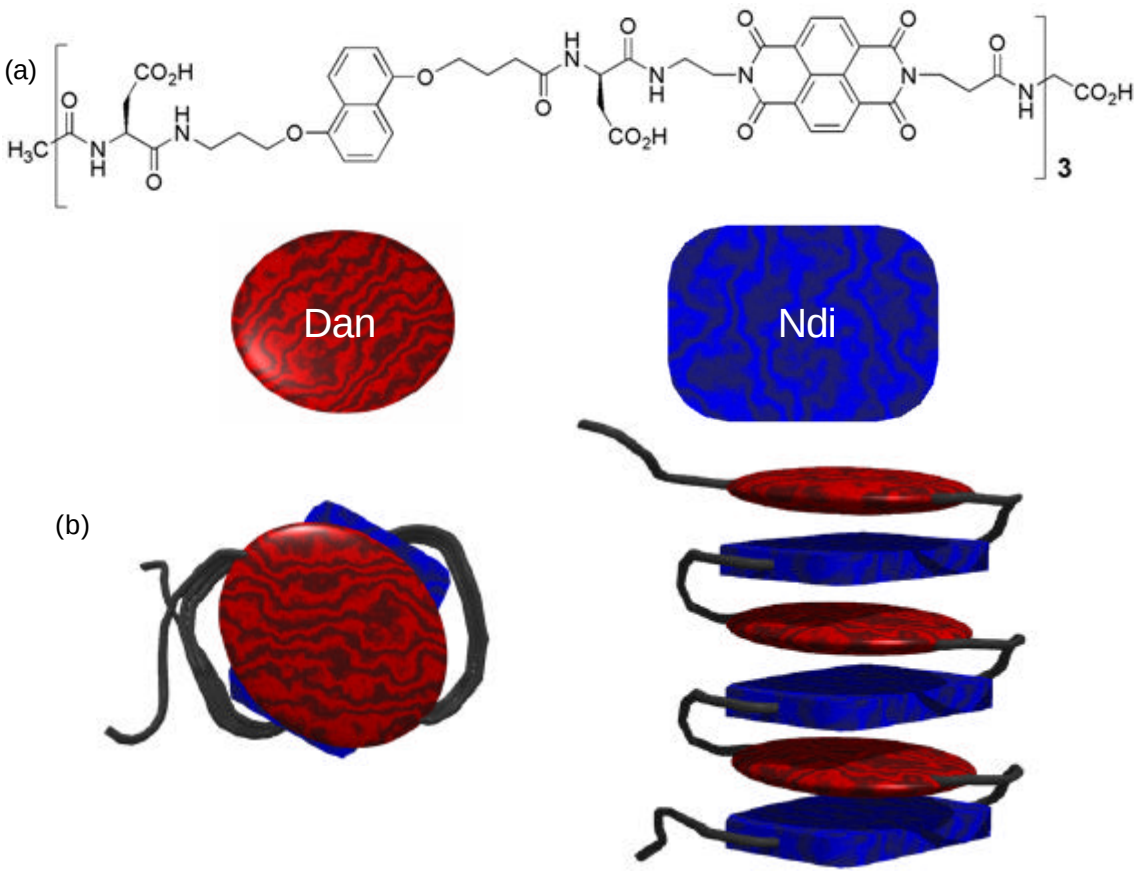

Figure 1.7 (a) Structure of the original aedamer. (b) Representations of the ideal aedamer folding.

A diagnostic spectroscopic feature of aedamers is the upfield shift of the aromatic proton signals in the ^{1}H-NMR spectra relative to independent Dan and Ndi monomers. Upfield shifting is caused by ringcurrent effects from the close proximity of the stacked aromatics (Zych 2000). This has been corroborated by weak intensity through-space coupling between the Dan and Ndi aromatic proton signals observed in NOESY spectra of model dimers. Another feature of aedamer folding is a significant hypochromism present in the UV-Vis spectrum for Dan and Ndi absorbance relative to the independent

monomers. This is similar in nature to the well characterized hypochromism of stacked DNA bases in the double helix. A visible region charge transfer band is also observed in the aedamer UV-Vis, a result of the orbital mixing of Dan and Ndi units, possible only with a close face-to-face orientation of the molecules (Lokey 1995, 1997, Cantor 1980).

1.2.1 Dan:Ndi association

To understand better the potential of the Dan:Ndi system to direct assembly, the Iverson group investigated the solvophobic driving force presumed to be at least partially responsible for the folding of the aedamer structure (Cubberley 2001). Neutral monomers of the Dan and Ndi components were synthesized, appending tetraethylene glycol side chains to the naphthyl cores, allowing for comparison of association constants (M^{-1}) between the Dan, Ndi, and 1:1 Dan:Ndi mixture in solvents of varying polarity (Figure 1.8). The data revealed a significant increase in aromatic-aromatic association as the organic nature of the solvent decreases, with a striking difference of almost 100x when comparing methanol to water to give an association of 2000 and a corresponding ? G value of -4.5 kcal/mol for Dan:Ndi complexation in water. The independent Dan and Ndi units exhibit similar behavior, to a lesser degree, with self-association constants of about 20 and 200 in water. This trend is classic solvophobics; when the naphthyl monomer faces are less likely to interact favorably with the solvent (water) they interact more favorably with each other.

Solvent	Dan:Dan	Ndi:Ndi	Dan:Ndi
$CDCl_3$	-	-	2
DMSO-d_6	1	2	3
CD_3CN	1	3	11
CD_3OD	1	8	30
D_2O	20	245	2045

(a) ↓

(b) →

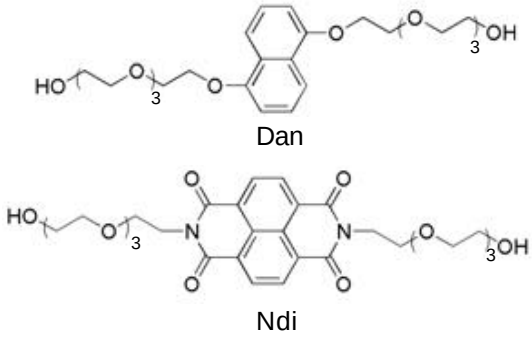

Figure 1.8 Solvent dependence on Dan and Ndi associations (a) Increased association upon increased solvent polarity. (b) Increase in association with better ability to participate in face-to-face stacking.

The naphthyl units similar in size and therefore should exclude a similar amount of water upon complexation by the hydrophobic effect. However, there is significant disparity in association constants for the Dan:Dan, Ndi:Ndi, and Dan:Ndi complexes in water, indicating that electrostatic compatibility of the monomers is important. The seminal work of Hunter and Sanders (Hunter 1990) predicts that electron rich aromatics, such as Dan, will prefer to stack in an edge-face conformation. This orientation does not entirely hide the aromatic faces from solvent, limiting the extent of water molecules that may be freed without paying an energetic cost to force the electron rich faces together. Electron poor aromatics such as Ndi are predicted to stack in a slipped face-to-face geometry, partially hiding the hydrophobic surface from solvent. This accounts for the increase in self-association of the Ndi monomers over Dan. It is with the combination of electron rich and electron poor aromatics that the predicted preferred stacking is a centered face-to-face orientation, with alternating naphthyl units. The electrostatic opportunity to completely cover the aromatic faces allows for the maximum benefit of

the hydrophobic interaction. Some stability may also be attributed to electrostatic forces and charge transfer interactions between the Dan and Ndi molecules. Crystal structures obtained for representative molecules of Dan, Ndi, and the Dan:Ndi mixture illustrate this interpretation (Figure 1.9). In short, the Dan molecules pack in a herringbone conformation, the Ndi in a off-centered face-to-face orientation, and the Dan:Ndi mixture in alternating columns of centered face-to-face complexation as predicted by aromatic-aromatic interaction theory of Hunter and Sanders (Hunter 1990).

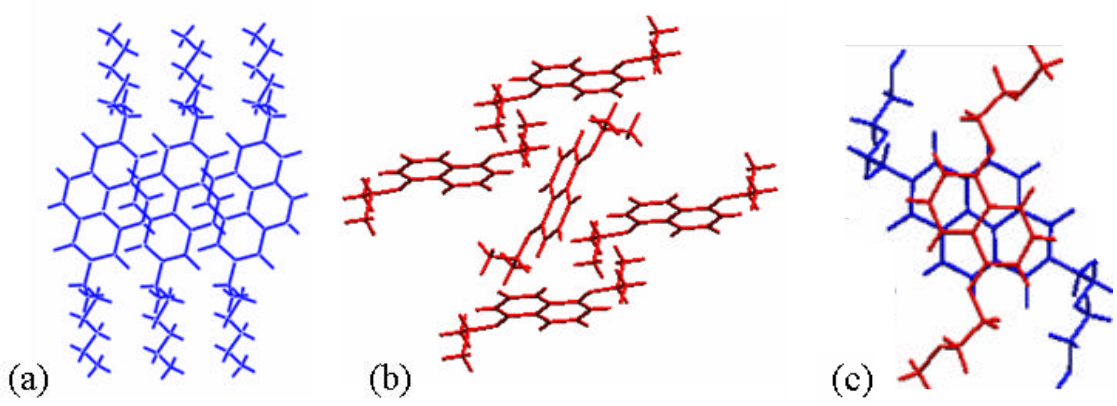

Figure 1.9 Single crystal structures: (a) Ndi packing, slipped face-to-face geometry. (b) Dan packing, edge face geometry. (c) Dan:Ndi packing, alternating face centered stacking.

1.2.2 Folding Robust in Linker

Unlike the sensitivity of many protein structure to the substitution of amino acids (LaBrenz 1995, Quinn 1994), the Iverson group has shown in dimer studies that aedamer folding is tolerant to subtle changes in the linkers between aromatic groups (Zych 2000). An algorithm was used for determination of the relative position of aromatic protons on the Dan and Ndi units based on NMR spectral analysis, and multiple computer model

conformations were obtained consistent with the algorithm. In the case of 10 dimers of varying linker length and structure, all were found to stack in a face-to-face geometry.

While all linkers designed to test the robustness of the donor-acceptor system allowed for face-to-face folding, the modeling implied a variety of slightly different low-energy structures for each system, rather than one most stable Dan/Ndi conformation. This implies a somewhat dynamic association, and may be the reason for the generality of the aromatic stacking interaction.

In further work this modeling system has proved useful in predicting the aromatic proton shifting, and therefore to some degree folding, in some more complicated aedamer systems (Zych 2001, 2002). In particular, Dan-Ndi-Dan trimers consisting of two different linkers closely resembled predictions for proton shifts made from the individual components. This predictability did not hold true with all expanded systems, but did offer insight into possible steric clashes between ligands that could cause the deviation from dimer generated predictions.

1.2.3 Altering Linear Covalent Order to Affect Secondary Structure

Inspired by Nature's ability to attain a multitude of secondary structures simply by altering the linear covalent attachment of a limited number of basic building blocks, for example a-helix vs. ß-sheet formation, the Iverson group synthesized non-altering naphthyl oligomers which alter the folding topology of the pleated aedamer to a hairpin type structure in water (Gabriel 2005). It was predicted that a non-alternating aedamer, Dan-Dan-Ndi, would fold back on itself, intercalating the Ndi units between the two Dan

components. In contrast to the pleated fold secondary structure of the alternating aedamer, this new folding motif would be analogous to a turn or hairpin structure.

Trimers of both alternating Dan-Ndi-Dan and non-alternating Dan-Dan-Ndi connectivity were synthesized, along with dimers and control trimers which were designed so that trimeric folding is not possible, and are illustrated in figure 1.10a-d. Extent of folding was compared using the percent hypochromism and CT band intensity in the UV-Vis spectra (Figure 1.10e). All four compounds qualitatively show interacting p systems. The dimer and control trimer show very similar UV-Vis characteristics, indicating that having a second Dan unit that is unable to participate in folding will not affect the Ndi hypochromism or CT band intensity. The alternating aedamer and the non-alternating aedamer exhibited almost identical features, indicating that they were folded to the same extent.

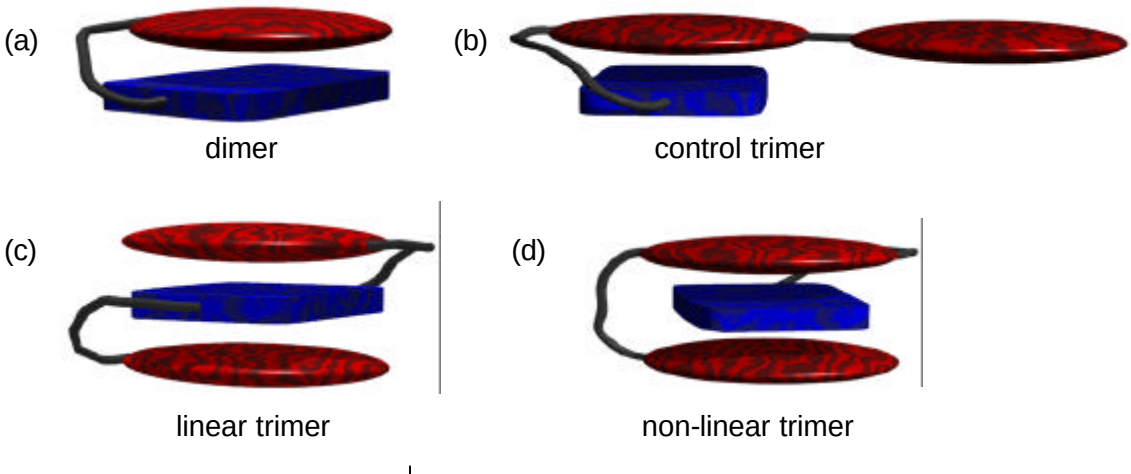

(e)

Compound	e_{CT}	% Hypochromism
	380	45
	490	48
	700	57
	670	60

Figure 1.10 Compounds and UV-vis data for alternative folding motif study.

Consistent with the UV-Vis experiments, 2D ^{1}H-NMR analysis of the non-alternating aedamer showed explicit contacts between the Ndi and both Dan units, indicating that both the adjacent and exterior Dan residue are in close proximity to the Ndi component. Further, the NOEs supported a structure in which the Ndi was intercalated between the two Dans. The NOESY for the control trimer showed Ndi contact with the adjacent Dan, but there were no cross peaks involving the exterior Dan.

The NOESY data was complemented by computer modeling of the folded turn in order to give a more complete structural model. It was noted above that with the

modeling of dimer structures several slightly different low energy conformations occurred, yet all of them exhibited face-centered stacking. Such was the case for the non-alternating aedamer, with which several conformations of relatively low energy were observed, all within 1 kcal/mol in calculated energy, and all with the folded intercalation of the Ndi between the two Dans. Models in which one or both of the Dan units were in the proximity of the Ndi but not face-center stacked gave significantly higher energy calculations, and were thus rejected as possible conformations of the non-alternating aedamer.

This study opens the way for new designs of secondary structure based on the Dan and Ndi directed aromatic interactions. By creative adjustment of the linear covalent connectivity of aromatics a host of topologies may be reached. This concept, perhaps with the inclusion of other orthogonal non-covalent directing interactions, could greatly extend the possibilities of designed secondary and higher order structures.

1.2.4 Intermolecular Assembly

As a natural extension of using directed aromatic interactions of aedamers as a driving force for foldamer chemistry, complementary molecules which participate in supramolecular chemistry via aromatic donor-acceptor interactions were investigated. In 2002 the Iverson group showed that donor-acceptor interactions could direct the association of independent Dan and Ndi oligomers into discrete hetero duplexes in water (Gabriel 2002).

Short oligomers consisting of only Dan or only Ndi aromatic units were prepared with up to four repeat units (Figure 1.11a). The binding characteristics of these molecules were measured using isothermal titration caloremetry (ITC) and NMR and are shown in figure 1.11d. The mixing of the independent Dan and Ndi strands is highly energetically favorable, with association constants that steadily increase as additional aromatic units are added to the oligomers. The combination of tetramers yielded a K_a of 3.5×10^5 M^{-1}, three orders of magnitude higher than the NMR measured association constant of the charged monomer of ~200 M^{-1}. It is important to point out that as these strands are brought together, the negative charges on each chain are brought into proximity, and so the association constants shown are in spite of any charge repulsion. This repulsion is proposed as the reason for a K_a of the charged monomers that is so much less than that measured for the neutral monomers (Figure 1.8) and is further discussed in chapter 4.

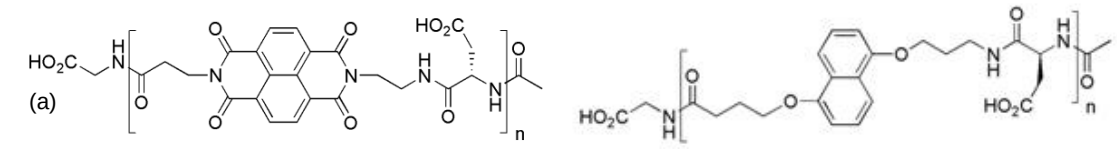

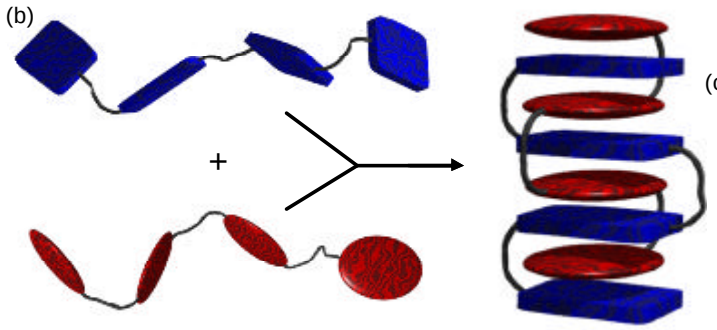

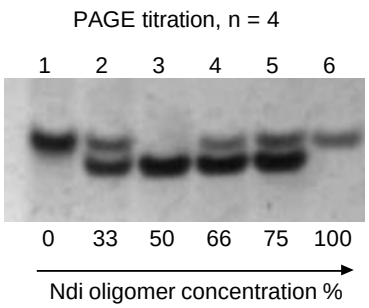

(d)

Duplex	K_a	$?G°$	$?H°$	$?S°$
n = 2	2.7 x 10^3	-5.0	-12.3	-23.0
n = 3	4.5 x 10^4	-6.8	-17.7	-34.2
n = 4	3.5 x 10^5	-8.1	-19.3	-35.3

Figure 1.11 Duplex formation from complementary Dan and Ndi oligomers. (a) Structure of monomers – tetramers. (b) Representation of ideal duplex. (c) PAGE titration indicating new, discrete complex formation. (d) Energy parameters for 1:1 oligomer association by ITC at 318K.

The binding curves obtained via ITC were best fit by a model with 1:1 binding stoichiometry. This was corroborated with an NMR based Job plot for dimer association that showed 1:1 binding, and NMR studies also indicated an association constant very similar to the ITC results. Polyacrylamide gel (PAGE) experiments were used to provide conclusive evidence for discrete 1:1 oligomer binding. As seen in Figure 1.11c, 1:1 mixing of the Dan and Ndi oligomers (column 3) produces a single discrete complex, no

streaking or multiple bonding, that behaves significantly different down the gel than either of the two individual components. Further, when the two components were titrated, the complex is formed to the full extent of the limiting component leaving the excess oligomer free, exhibited by columns 2, 4, and 5. These intriguing results not only confirm discrete complex formation, but also speak to the strength of the association since the complex travels as one unit even under the applied potential of the gel.

This work lays the foundation for opportunities of the directed Dan/Ndi aromatic interaction to be used in supramolecular chemistry designs. The significant association constants obtained, *in water*, imply the possibility for the design of self-assembled systems, templates, molecular machines, and materials processed from an environmentally benign solvent. Incorporation of this intermolecular motif with various intramolecular design possibilities, could lead to synthetic design of tertiary and quaternary structures with the ability to mimic and perhaps better understand some of Nature's more intriguing and complex systems. Still further directions are possible by employing the now well understood and well characterized Dan and Ndi molecules in entirely new covalent geometries.

1.3 DIRECTED AROMATIC-AROMATIC INTERACTIONS IN RELATED WORK

It has long been know that the shape of aromatic units, generally termed discotic, relays a natural propensity for order, such as that displayed by a pile of poker chips, and therefore mesophase and liquid crystal phase induction (Demus 1998). Thirty years ago it was discovered that mixing electron-poor species with some discotic mesophases could

alter and enhance phase properties (Park 1975). It was fifteen years later that Ringsdorf and co-workers started designing aromatic donor-acceptor mesophases in polymer and small molecules (Ringsdorf 1989). The discotic shape in combination with a driving force for face-to-face stacking is ideal for supramolecular formation of columnar systems. This initial work and its descendents have served as the model for Dan:Ndi mesophase exploration and is discussed in greater detail in the background of chapter 3.

Several systems have been developed that take advantage of directed aromatic interactions of the original aedamer since its report in 1995. Using Dan and pyromellitic diimide (Pdi), the Li group has developed systems with the aromatic units appended in comb geometries. In analogous work to that described above with aedamers these designs have been shown to fold into turns (Zhao 2004) and associate as duplexes (Zhou 2003) in organic solvent (Figure 1.12a,b). The same pleated fold design of the original aedamer was mimicked in the first published polymeric foldamers by Ramakrishnan and co-workers, with a combination of donor-acceptor aromatic interactions and ion complexation. Also using Dan and Pdi donor-acceptor units, alternating copolymers were synthesized with tetraethylene glycol linkers between the aromatics. The polymers were soluble in organic solvents, and with the addition of metal cations shown to adopt a pleated fold conformation (Ghosh 2004) (Figure 1.12c). Homo Pdi polymers were also synthesized and shown to fold in a similar pleated fashion upon addition of specific Dan small molecules with positively charged amine side chains, independent addition of neutral Dan or cation did not promote folding illustrating the need for both aromatic interactions and ion complexation (Ghosh 2005) (Figure 1.12d). Hydrogen bonding has

also recently been used to affect solution phase assembly of small molecules in concert with aromatic donor-acceptor interactions (Li 2005).

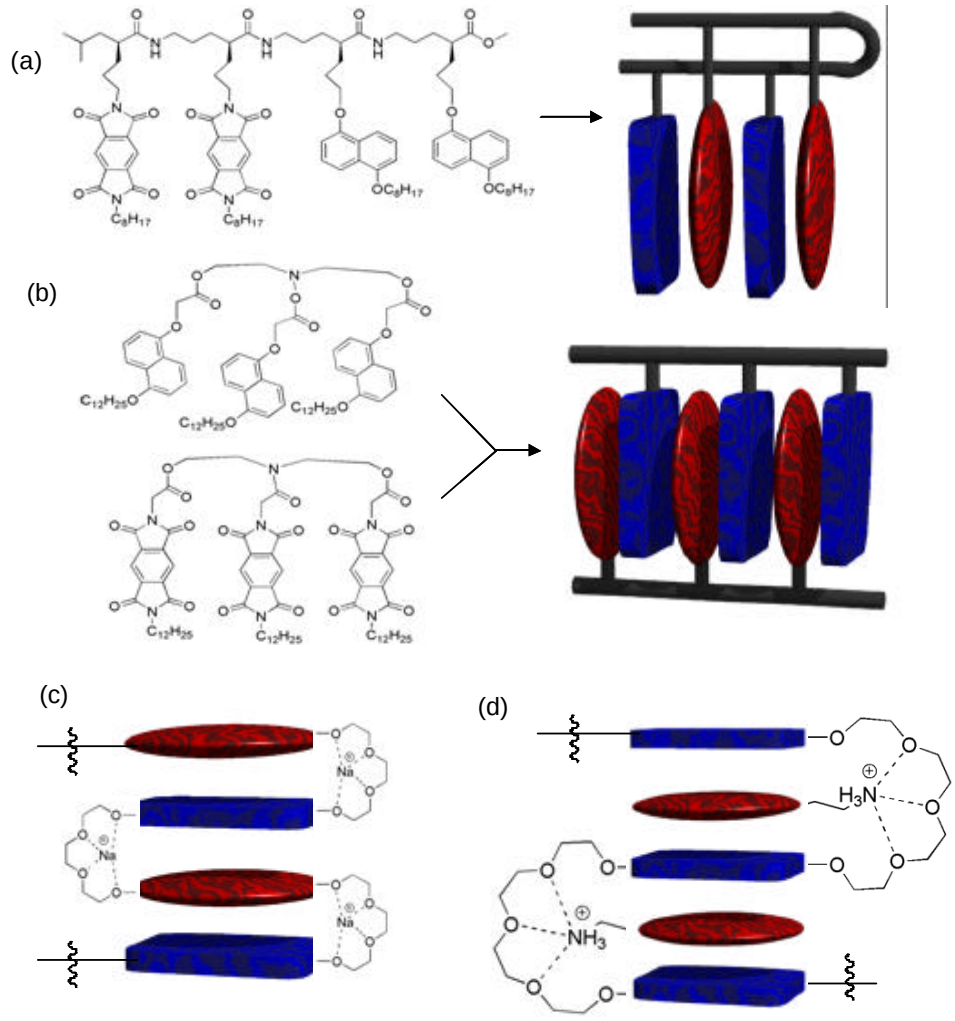

Figure 1.12 Aedamer-like assemblies (a) Turn architecture from branched oligomer in organic solvents. (b) Duplex of branched architecture in organic solvents. (c) Alternating Dan/Pdi polymer that folds upon cation complexation (red=Dan, blue=Pdi). (d) Poly Pdi that folds with introduction of amino-Dan molecule(red=Dan, blue=Pdi).

Catenanes and rotaxanes are supramolecular structures that include interlocking ring systems or threaded assemblies, respectively (Figure 1.13). The designs of Stoddart and co-workers to create these systems based on templation of electron rich aromatics with bipyridinium cations are a landmark of this field and discussed in several reviews (Anelli 1992, Amabilino 1994, Arico 2005). Sanders and co-workers created the first neutral donor-acceptor catenane based on Dan/Ndi and also Dan/Pdi units which exhibited benefits over the charged system in synthetic route and ability to be functionalized (Hamilton 1997). This new structural motif for the aedamer system, highlighting the advantage of the preferred orientation of the Dan:Ndi to complex with the linkers in orthogonal directions, provided some inspiration for the directional component of work in chapter 3.

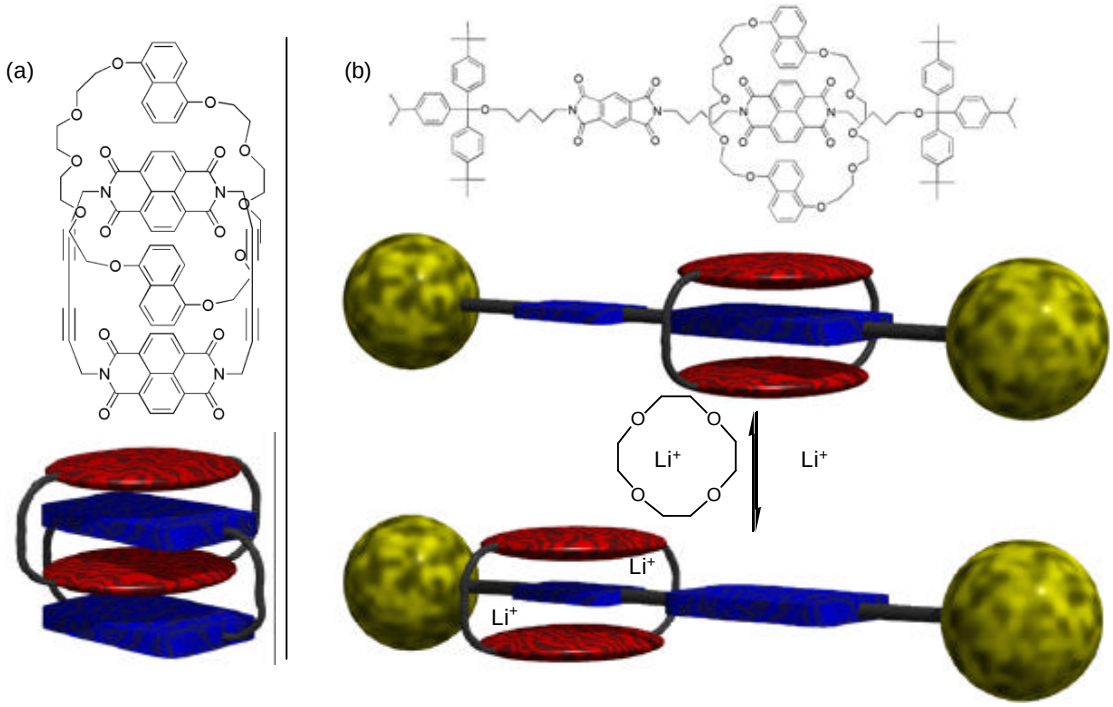

Figure 1.13 (a) Structure of Dan and Ndi catenane. (b) Dan encircled Ndi/Pdi rotaxane switch.

The recent partnership of Sanders and Stoddart has produced molecular machines based on neutral donor-acceptor rotaxanes (Iijima 2004). Linear molecules containing both Ndi and Pdi were "capped" at each end by a tetraphenyl group, and then a bi-Dan ring assembled around them to give the rotaxane shown in figure 1.12b. In solution the Dan ring selectively encircles the Ndi unit, characterized by UV-Vis and NMR spectroscopy. Upon addition of Li^+ ions to the solution the Dan ring shifts positions to the smaller Pdi unit, accommodating complexation of the cations by the polyether linker. The Dan ring switches back to the Ndi unit upon addition of [12]crown-4 to sequester the Li^+ ions. Switching has also been initially characterized in films made from these

rotaxanes. This beautiful work is surely the precursor, at least in concept, to practical responsive materials based on aromatic donor-acceptor interactions. It exemplifies the spirit of the work herein, to extend the aedamer interactions in directions, namely polymers, liquid crystals and alternate connectivity, that may one day lead to next generation controllable functional materials.

1.4 Overview of Directed Aromatic Electron Donor-Acceptor Projects

The original aedamer established the Iverson group in the field of synthetic molecular self-assembly, specifically foldamer chemistry. Immediately subsequent studies characterized the Dan:Ndi interaction in water in terms of the solvent effects, the association geometry, and the robustness of the folding interaction. Recently the group has shown the ability of the aedamer system to create both altered folding patterns and intermolecular complexes. The work of this dissertation extends the supramolecular chemistry of the aedamer system to supermolecular polymers, mesophase formation and control, and alternative linkage geometries (Figure 1.14).

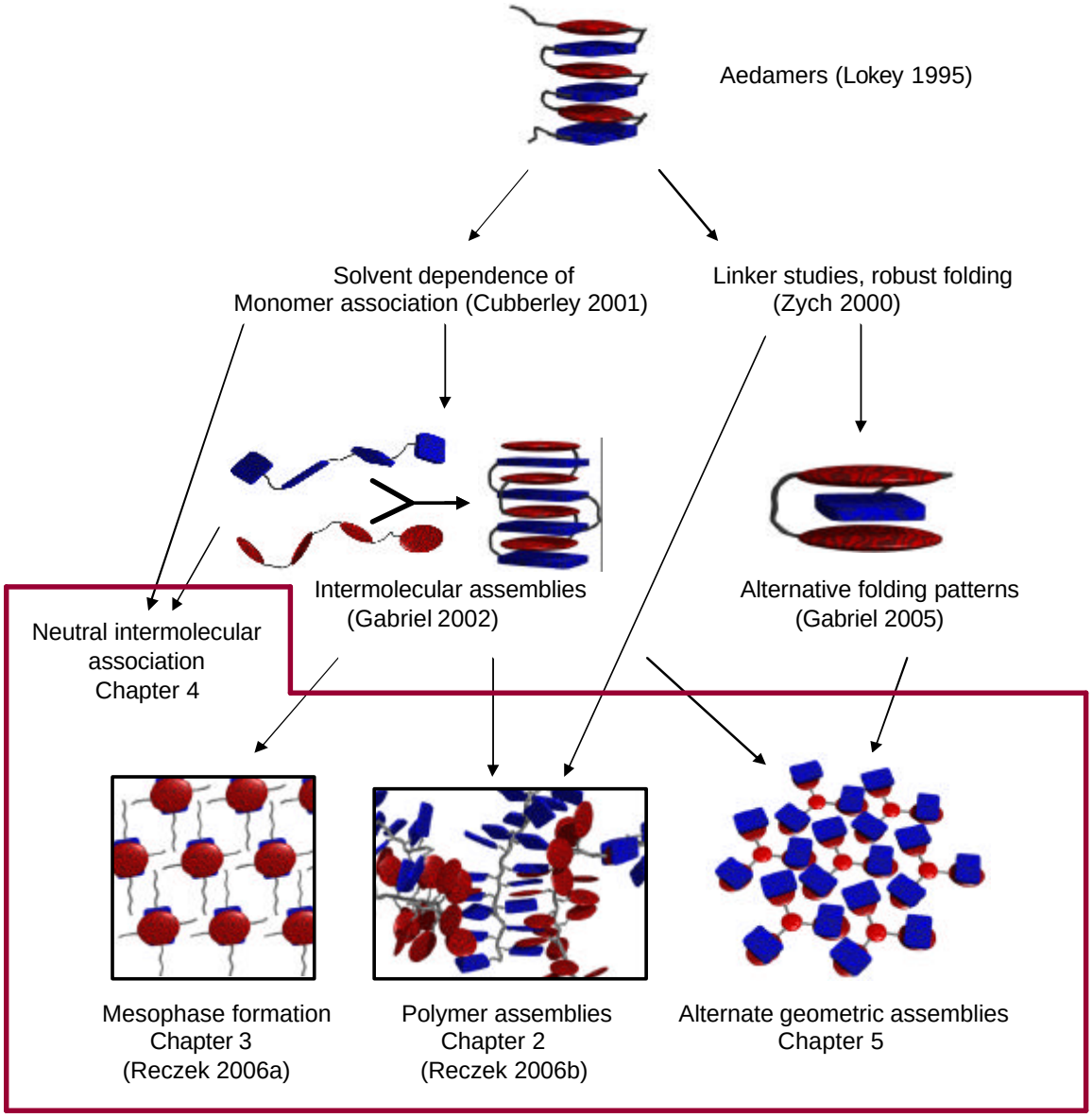

Figure 1.14 Aromatic donor-acceptor molecular self-assembly in the Iverson group

CHAPTER 2

Assembly of Complementary Ndi and Dan Polymer Strands

2.1 CHAPTER SUMMARY

Introduction. In water, the intermolecular association constant measured for the association of independent Dan and Ndi oligomers steadily increases as the number of aromatic units increases (Gabriel 2004). It is proposed that incorporating these aromatic units into independent polymer strands would offer extremely high intermolecular associations and possible control of solution phase and material properties. By synthesizing independent Dan and Ndi polymers, association and material processing could be controlled in the process of polymer mixing, much like the natural processing of spider silk. This Chapter describes the design, synthesis, and characterization of polymer chains consisting of Dan or Ndi repeat units, and the characterization of macrostructures resulting from their mixture.

Goals. The possibility of polymers with hundreds of designed intermolecular Dan/Ndi interactions in water, and therefore incredibly strong associations, is intriguing. Experiments in this chapter are designed to answer the question: *Can water soluble Dan and Ndi polymers be synthesized, and their combination affect macromolecular assembly?* It was the short term goal of this research to synthesize independent Dan and Ndi polymer chains that are soluble in aqueous solution and study their properties. These

initial studies could then be used to design and synthesize more efficient polymer chains in the long-term for the creation of new functional self-assembled materials.

Approach. Several linear and branched polymer architectures were investigated for water solubility and CT interactions. Solutions of polyDan, polyNdi and an equimolar mixture of the two were analyzed using UV-vis spectroscopy and rheometry. Films of the same polymers and their mixtures were analyzed by AFM and SEM. Short fibers were made of the polymer mixture and analyzed using SEM.

Results. Overall, the work described in this chapter demonstrates the assembly of macromolecular structures driven by donor-acceptor aromatic interactions. A variety of linear and comb polymer designs were explored before slightly water soluble Dan and Ndi polymers which exhibited aromatic-aromatic interactions were obtained via the functionalization of Polyethylene(alt maleic anhydride). All other polymers were insoluble in aqueous media. The Ndi polymer was soluble up to 3% by weight in basic solution, and an equimolar mixture of Dan and Ndi polymers was also soluble up to 3% weight. Independently the Dan polymer required the addition of a surfactant such as SDS to have any aqueous solubility. The polymer mixture showed a significant difference in solution and solid state properties from the independent polymers. UV-vis data confirmed the presence of a charge transfer band, indicative of Dan/Ndi interactions being present in the mixture of Ndi and Dan polymers. The viscosity of the polymer mixture was significantly higher than the independent polymers, even at low

concentrations. When the polyDan/Ndi mixture was made into a film it formed relatively large macrostructures of that were entirely different than the smooth film formed by the PolyNdi and the micelles observed in films of the PolyDan with SDS surfactant or Ndi monomer. Even at low concentration, the polymer mixture can be drawn into fibers by precipitating through a high gauge syringe needle (Reczek 2006b).

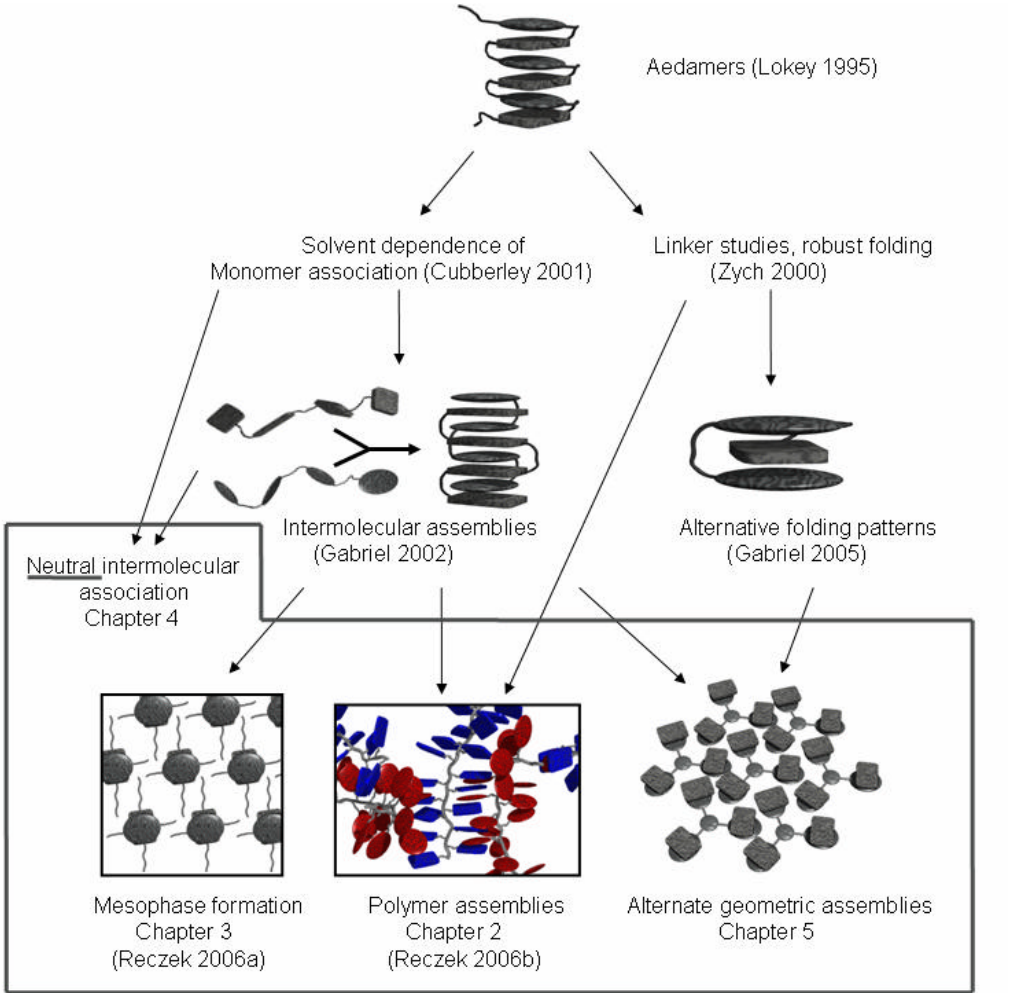

Chart 2.1 Aromatic donor-acceptor molecular assembly in the Iverson group.

2.2 BACKGROUND

The molecular structure and unique physical properties of many natural and synthetic polymers result from extensive directed non-covalent interactions between chains. The amazing tensile strength of spider silk is a result of interpolymer ß-sheet crystalline regions within the silk fiber (Gührs 2000). These regions serve as rigid locks holding the fiber together and giving it a per weight strength that is greater than that of even steel. What makes spider silk even more remarkable is that there are also amorphous regions that allow the polymer to stretch and give its responsive elasticity (Figure 2.1a). The crystalline regions are alanine and glycine rich portions of adjacent protein polymers, which associate tightly due to hydrogen bonding and the relatively unhindered nature of these amino acids (Winkler 2000). One key to the functions of this incredible organic polymer is in the processing of the polymer chains. The amino acid materials are kept in a liquid crystalline state in aqueous solution within the abdomen of the spider. Independent polymer strands are synthesized in one of several glands and kept unassociated until the spider combines them in specific ratios through its spigots, tailoring the interchain association, to create a web, dragline, or other fiber type (Vollrath 2001) (Figure 2.1b,c).

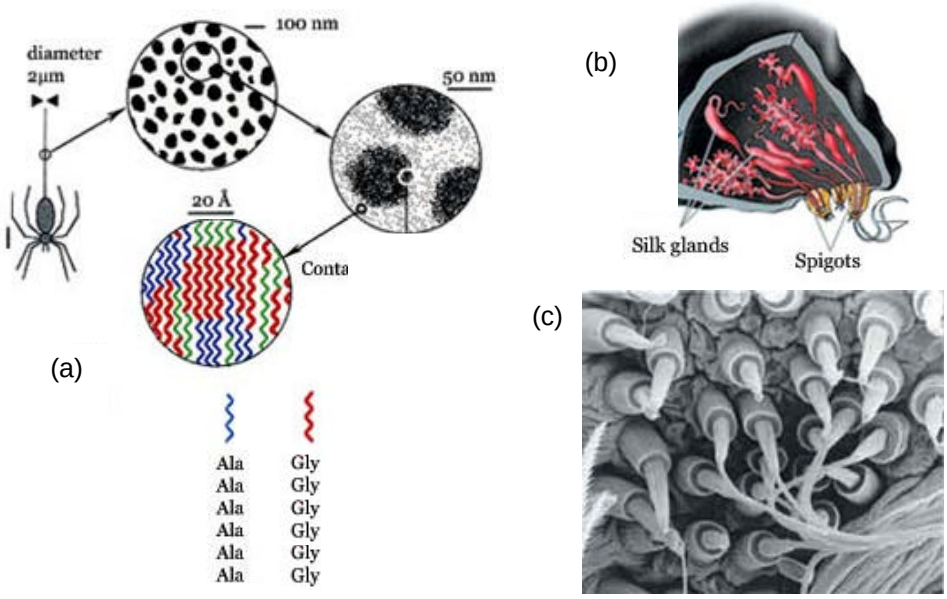

Figure 2.1 Illustration of the spider silk process and fiber. (a) Spider silk at various scales, consists of both amorphous and highly crystalline regions. (b) Multiple glands holding liquid crystal precursors, connecting to spigots. (c) Spigots combining strands to form a silk fiber. (adapted from: http://www.harunyahya.com/books/science/biomimetics/biomimetics01.php Copyright © Harun Yahya International © 2006).

Kevlar, and other aramides, also derive their amazing properties from directed non-covalent interactions between polymer chains. Inspired by Nylon, which has impressive properties in its own right based on inter-chain hydrogen bonding, Kevlar consists of aromatic amide linkages, creating very rigid individual polymer strands. Like aliphatic Nylon, the poly aramides take part in inter-chain hydrogen bonding as shown in figure 2.2a. The crystal structure of Kevlar indicates that along with inter chain H-bonding, there is aromatic stacking between chains, and perhaps even aromatic-aromatic interactions between the relatively electron rich N-bound and electron poor C-bound

aromatics on adjacent polymer strands (Figure 2.2b). Interestingly, the tensile strength of Kevlar increases over five times under water, perhaps the result of increased hydrophobic effect for the aromatic interactions (Fukuda 1988).

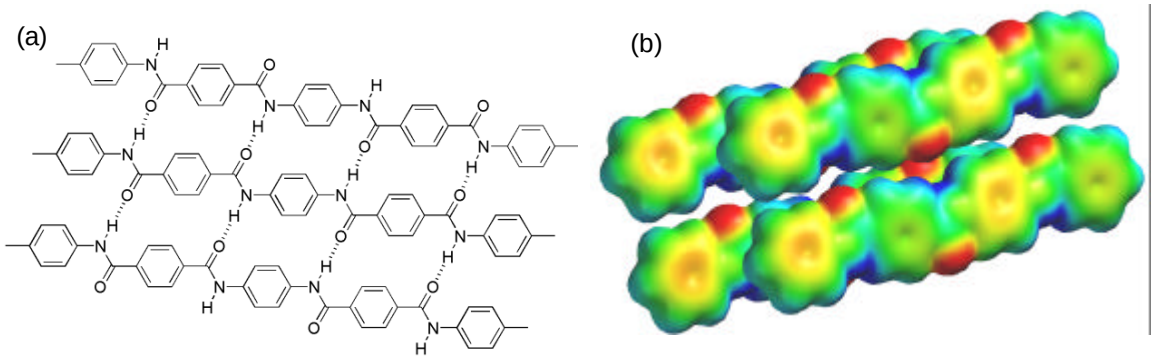

Figure 2.2 (a) Structure and hydrogen bonding of Kevlar. (b) Spartan electrostatic surface potential illustrating the hydrogen bonding and alternating electron-rich and electron-deficient aromatics.

Recent advances in supramolecular chemistry have yielded a variety of tools for the rational design and utilization of directed non-covalent interactions in the association of synthetic polymer chains. Extensive work by Rotello and co-workers has explored hydrogen bonding directed self-assembly in various polymer systems including their "plug and play" polymers. One example includes random copolymers incorporated with diaminopyridine (DAP) units, and then a *bis*-thymine small molecule was added to the polymer in solution to crosslink the chains and create temperature responsive microspheres (Figure 2.3a) (Thibault 2003). A second major class of non-covalent interactions utilized in the assembly and interaction of polymer chains is metal-coordination with polymer bound ligands (Albrecht 2001). Solution properties of

dissolved poly(methyl methacrylate) based copolymers, including terpyridine units, were altered through inter-chain cross-linking with Fe^{II} and Zn^{II} (Figure 2.3b) (Hofmeier 2003). Weck and co-workers have exploited the orthogonal assembly modes of metal-coordination and hydrogen bonding by using both simultaneously in recent work (Pollino 2005).

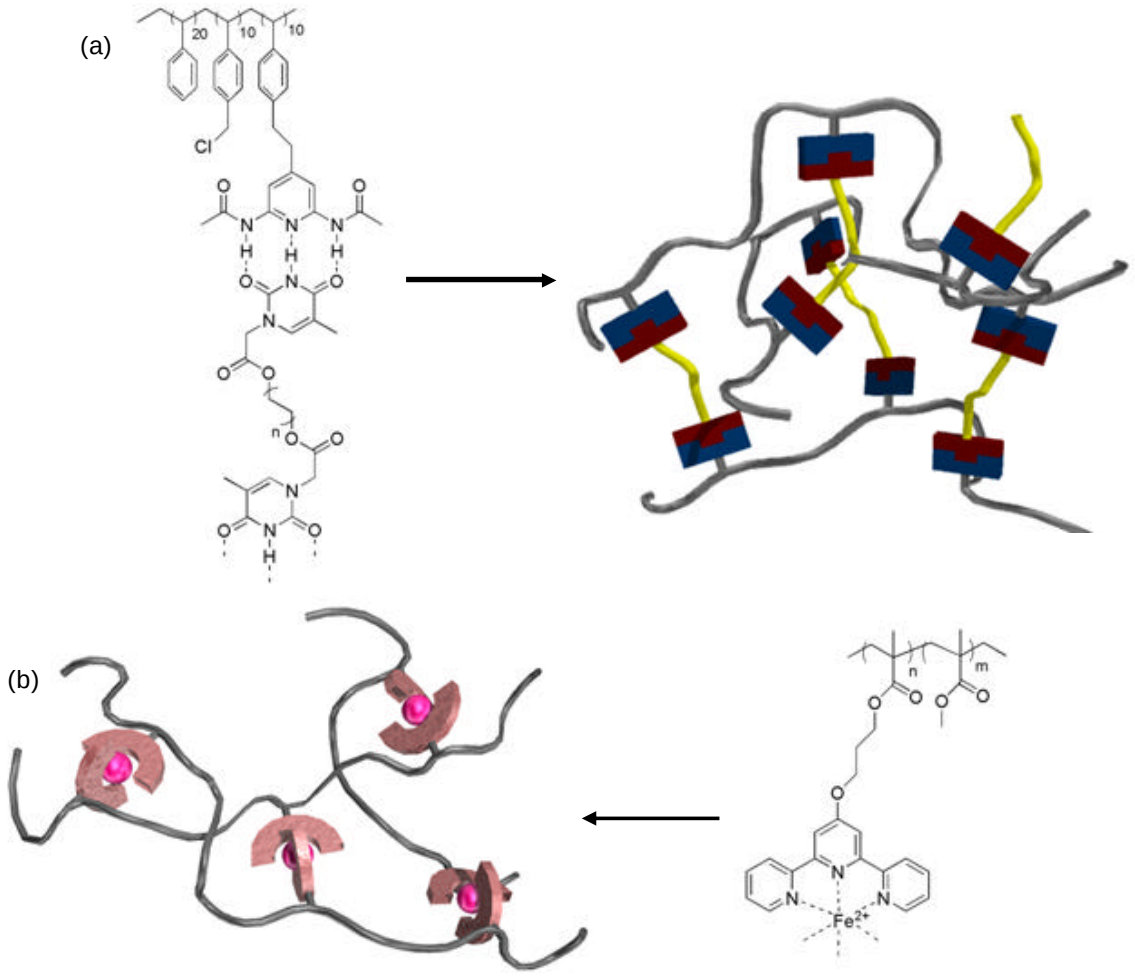

Figure 2.3 (a) Interstrand cross-linking by ditopic small molecule. (b) Interstrand cross-linking by transition metal ion.

Polymer association through directed non-covalent interactions involving only the polymer chains, as in the case with the protein polymers of spider silk, has recently been achieved. Coates and co-workers synthesized co-polymers incorporating 2-ureido-4[1*H*]-pyrimidinone (UPy) units have been shown to self associate and form interesting elastomeric gels and films (Figure 2.4a) (Rieth 2001). Zimmerman and co-workers synthesized two different co-polymers each incorporating one half of the complementary hydrogen bonding pair of a urea and 2,7-diamido-1,8-naphthyridine. They were mixed to give polymer blends with properties unique from the independent polymers (Figure 2.4b) (Park 2005).

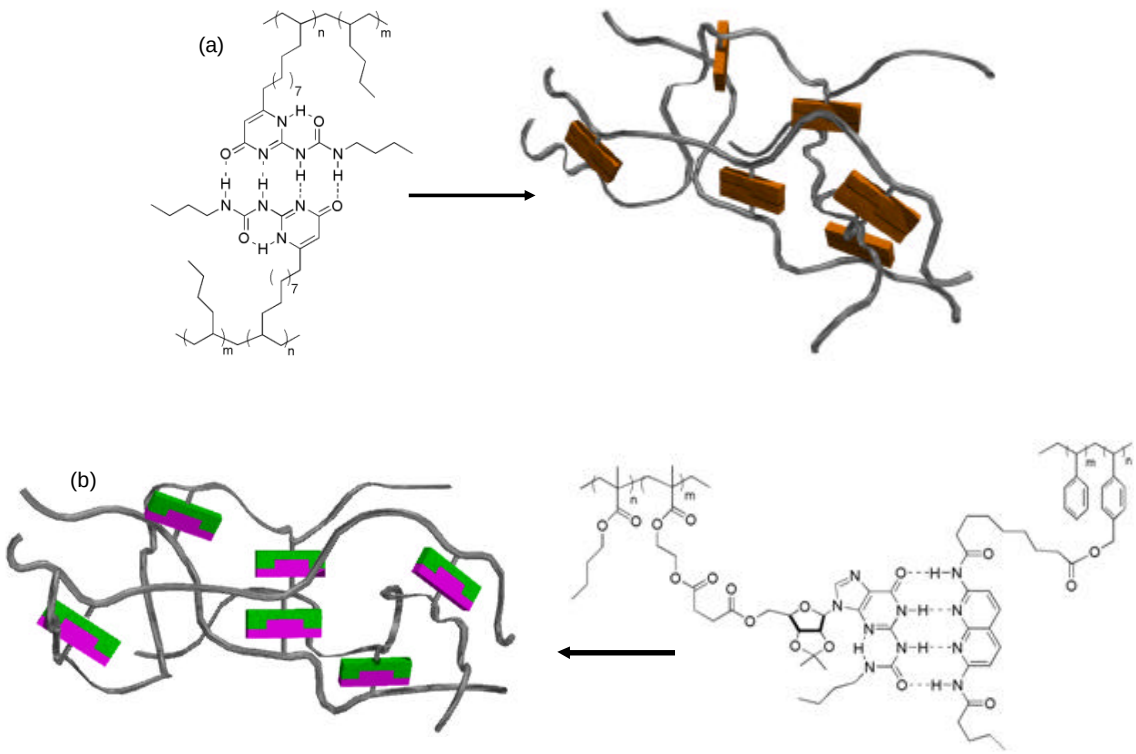

Figure 2.4 (a) Self-association of homopolymer. (b) Complementary polymer strand association.

Aromatic interactions have seen little use in supramolecular polymer assembly, previously used only to slightly alter solution conformations (Ghosh 2004, Ilhan 1999). Recent work in the Iverson group highlighted the ability to form hetero duplexes utilizing complementary Dan and Ndi donor-acceptor oligomers (Figure 1.11) (Gabriel 2002). This intermolecular complexation suggests that a similar design in polymeric systems could lead to extensive inter-chain assembly. Once an optimum design is reached, the columnar stacking of the Dan and Ndi units could provide highly crystalline regions of inter-chain association separated by amorphous un-stacked domains, mimicking the microstructure of natural spider silk (Figure 2.5). The poly-Dan and poly-Ndi molecules should be water soluble to drive the aromatic stacking, so that upon mixing, extended polymer networks are formed. The work described in this chapter details the design and characterization of the first polymer systems consisting of associating poly-Dan and poly-Ndi chains that interact in water. This approach offers an additional and orthogonal design element to the hydrogen bonding and metal complexation assemblies of previously designed non-covalent polymer networks, and is the first step towards realizing the potential of designing aromatic-aromatic interactions to affect polymer structure and material properties.

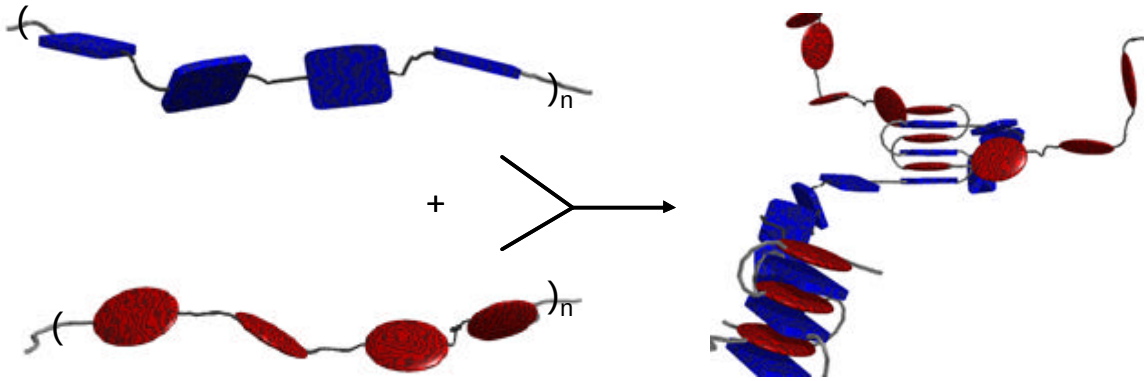

Figure 2.5 Representation of polyDan and polyNdi strands associating with stacked columnar regions.

2.3 POLYMER DESIGN AND SYNTHESIS

2.3.1 Design Options and Requirements

To maximize the hydrophobic driving force of aromatic-aromatic interactions requires that the polymers be soluble in aqueous solution. This is a significant challenge for a polymer with a high number of naphthyl units, and requires designs to include hydrophilic components either as part of the polymer backbone or appended off the aromatic units themselves. Specifically, incorporating functional groups that will carry a formal charge in solution is a likely requirement of polymer design to obtain aqueous solubility.

The connectivity of the aromatic repeat units in the polymer requires use of the functional handles on the Dan and Ndi components, and the aromatics can either be incorporated as part of a linear backbone, (as illustrated in figure 2.5) or as branches off of the polymer backbone (such as the branched duplexes shown in figure 1.12a). A linear

polymer design has the significant advantage of resembling the naphthyl oligomer intermolecular association system (Gabriel 2002) and the well understood pleated fold structure of the original aedamer (Lokey 1995). Previous work with those systems has also indicated there will be a tolerance of various polymer backbones/linkers to designs with respect to their ability to stack (Zych 2000). For this reason, a number of linear architectures were systematically explored. It is only upon encountering solubility difficulties that polymer designs with a branched geometry were investigated. Figure 2.6 shows the variety of linkers explored looking for water soluble Dan and Ndi polymers.

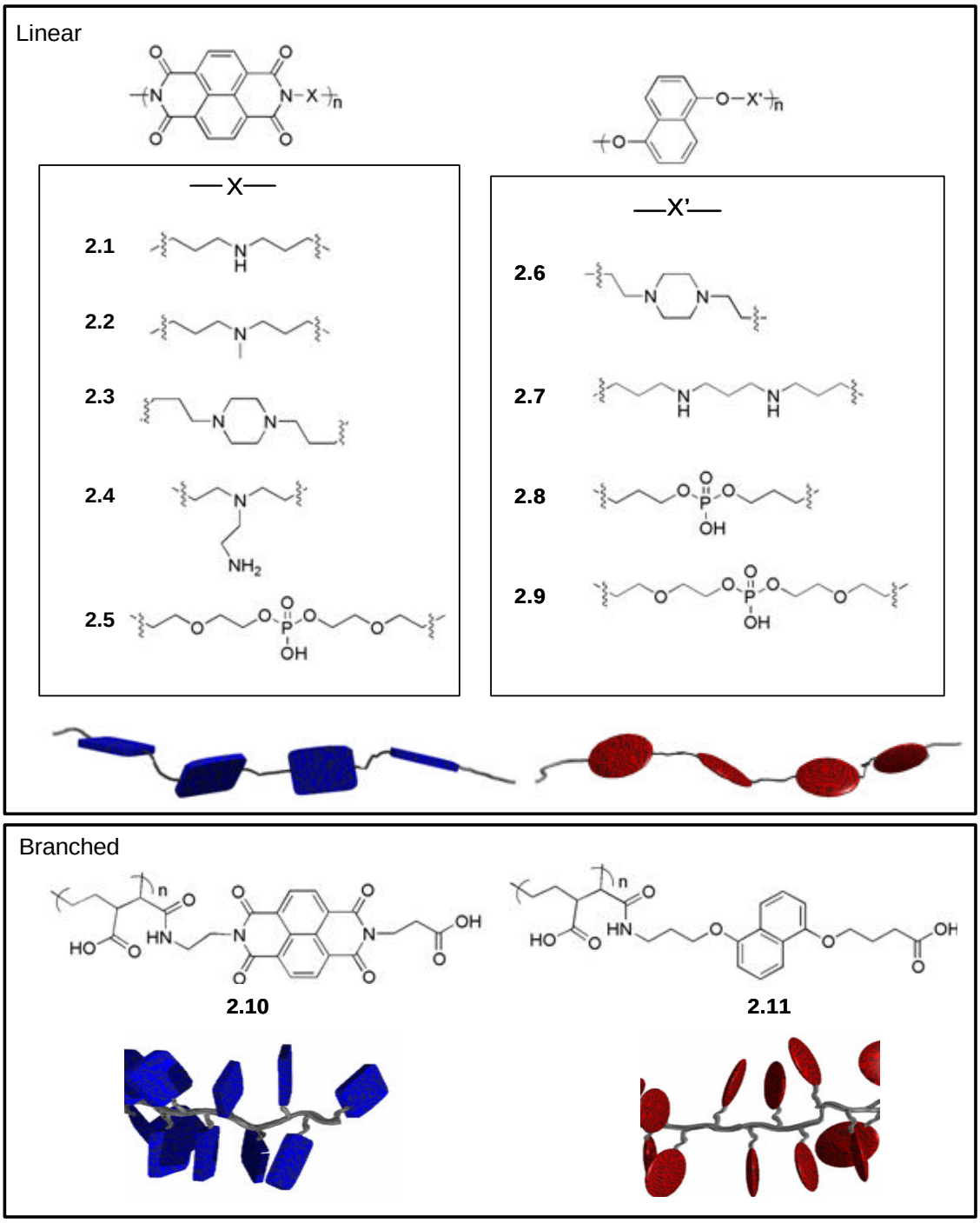

Figure 2.6 Various backbones/linkers used in designs for water soluble Dan and Ndi polymers. Linear architectures are included in the boxes and branched at the bottom.

2.3.2 Amine Based Linear Condensation Polymers 2.1-2.4, 2.6, 2.7

Ndi polymers **2.1-2.3** were synthesized via step growth polymerization according to scheme 2.1 by reacting naphthalene dianhydride (Nda) with the corresponding commercially available polyamines. Monomer **2.12** was synthesized via the mono Boc protection of *tris*-aminoethyl amine, and then condensed with Nda to yield polymer **2.13** which was deprotected to give polymer **2.4** (Scheme 2.1b). Scheme 2.1a to produce polymer **2.1** yielded a completely insoluble precipitate. It was hypothesized that the secondary amine in the linker competed with closing of the imide, and perhaps even caused some cross-linking of polymer chains. The tertiary amine linker in **2.2** again yielded an insoluble precipitate which did not dissolve even upon direct addition to 1M HCl.

Polymer bearing only one positive charge for every Ndi component are not sufficiently hydrophilic to allow for solubility, so polymer **2.3** was synthesized with two tertiary amines in the linker. This polymer precipitated out of the reaction solution, and was again not soluble in acidic aqueous solution. The steric rigidity of the cyclic linker was thought to perhaps be interfering with the solubility, so polymer **2.4** was designed with a flexible diamine backbone unit. The tetra amine was mono-boc protected, to yield monomer **2.12**, which was then condensed with Nda. The polymer remained in solution, and was deprotected without isolation. Unfortunately, upon deprotection polymer **2.4** precipitated out of solution and was insoluble in DMF, DMSO, and aqueous solution.

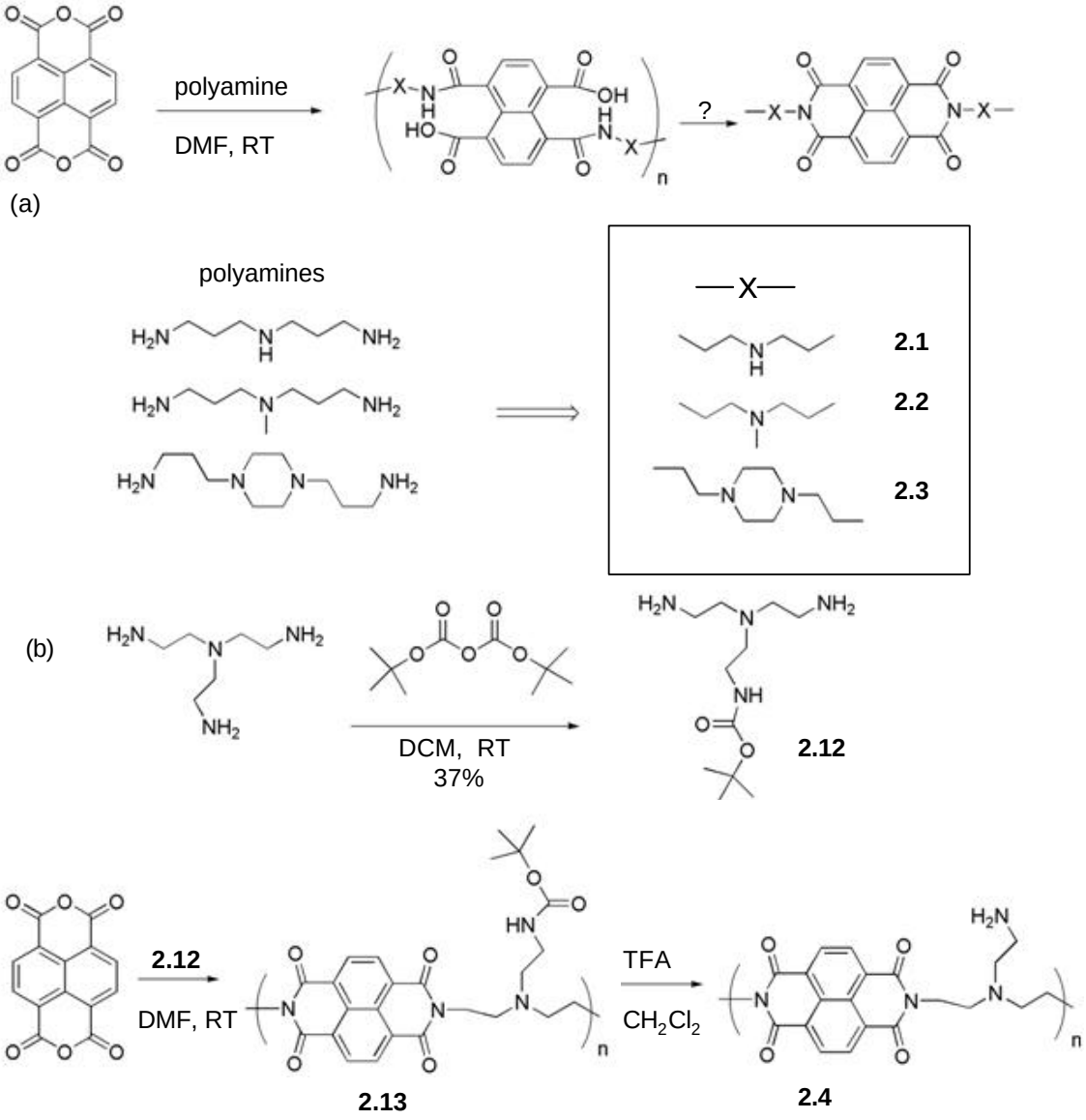

Scheme 2.1 Synthesis of Ndi polyamines

Dan polymer **2.6** was synthesized via the step growth polymerization of 1,5-dihydroxy naphthalene (Dhn) with the corresponding dibromide (Scheme 2.2a), and polymer **2.7** by condensation of Dan diamine **2.16** with a dialdehyde according to scheme

2.2b. Similar to the linear amine Ndi polymers, the Dan polyamines were completely insoluble in pure water and 2M HCl solutions.

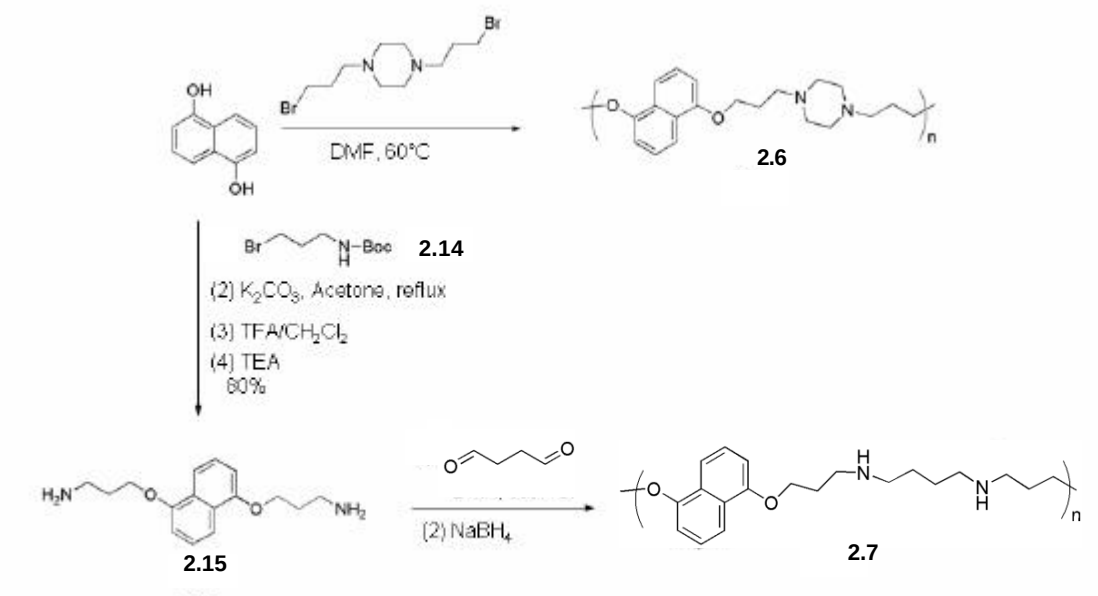

Scheme 2.2 Synthesis of Dan polyamines.

2.3.3 Phosphate Based Linear Polymers 2.5, 2.8, 2.9

Polymers **2.5**, **2.8**, and **2.9** were designed with phosphate repeat units in the backbone in order to investigate whether a negative formal charge would better promote aqueous solubility. Dhn was functionalized with the corresponding bromoalcohols to form the Dan diols **2.16** and **2.17**. After purification via column chromatography and then sublimation, the Dan monomers were condensed with dimethyl phosphonate,

followed by oxidation to the phosphate according to scheme 2.3 to yield polymers **2.8** and **2.9**. Initial attempts at this polymerization yielded only short oligomers of the polyphosphonate, possibly due to methylation of the Dan alcohols in the course of the reaction (Branham 2000). Significant molecular weights for the polymerization were achieved, according to scheme 2.4, by adding an excess of the phosphonate and allowing it to cap the Dan diol and letting the evolved methanol to escape the reaction. A light vacuum was then applied to drive the formation of short oligomers, still capped by phosphonates, by removal of excess dimethyl phosphonate. High molecular weight was then achieved by applying a high vacuum for several days. The reaction was monitored by ^{31}P NMR and the molecular weights determined via GPC prior to oxidation.

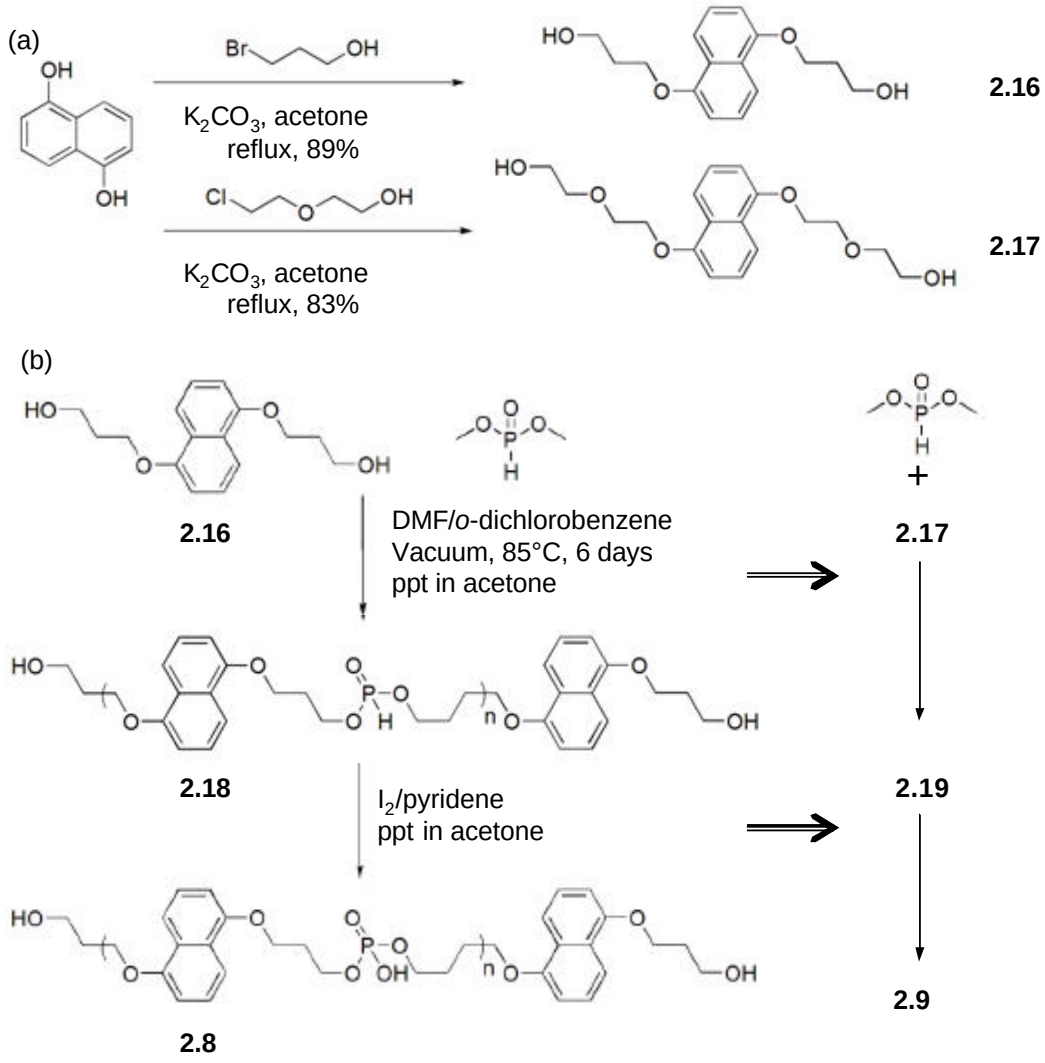

Scheme 2.3 Synthesis of phosphate Dan polymers.

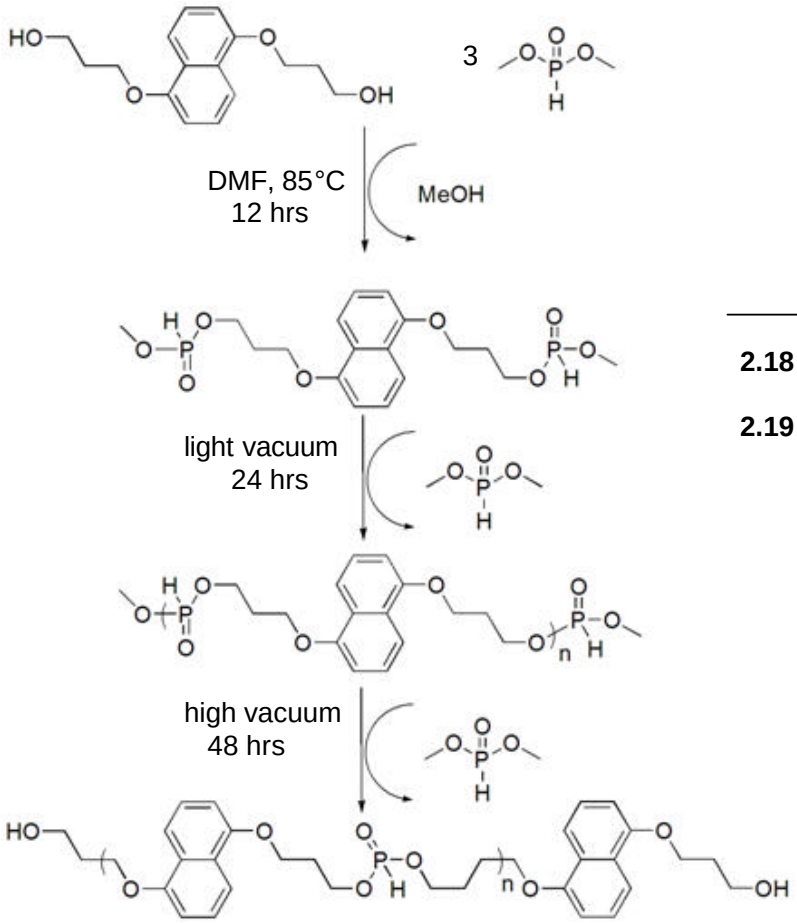

	M_w(kD)	pdi
2.18	32,312	2.2
2.19	27,595	2.3

Scheme 2.4 Route to higher molecular weight.

This synthetic route gave reasonable molecular weights ~(30,000 kD) for the Dan polymers, however when attempted with Ndi diols only short oligomers were obtained. This may be due to slight impurities in the Ndi monomer, as suitable sublimation conditions could not be found for any Ndi diols. An alternative approach was used to synthesize Ndi polyphosphates, in which the phosphate piece was synthesized as a diamine and then condensed with Nda, shown in scheme 2.5. Ethyl(ethoxy amine) was first mono-boc protected, and then reacted with dimethyl phosphonate to yield compound

2.21. Attempts to deprotect the boc groups at this point with TFA were unsuccessful, and so **2.21** was oxidized to the phosphate and then deprotected prior to condensation with Nda to form polymer **2.6**.

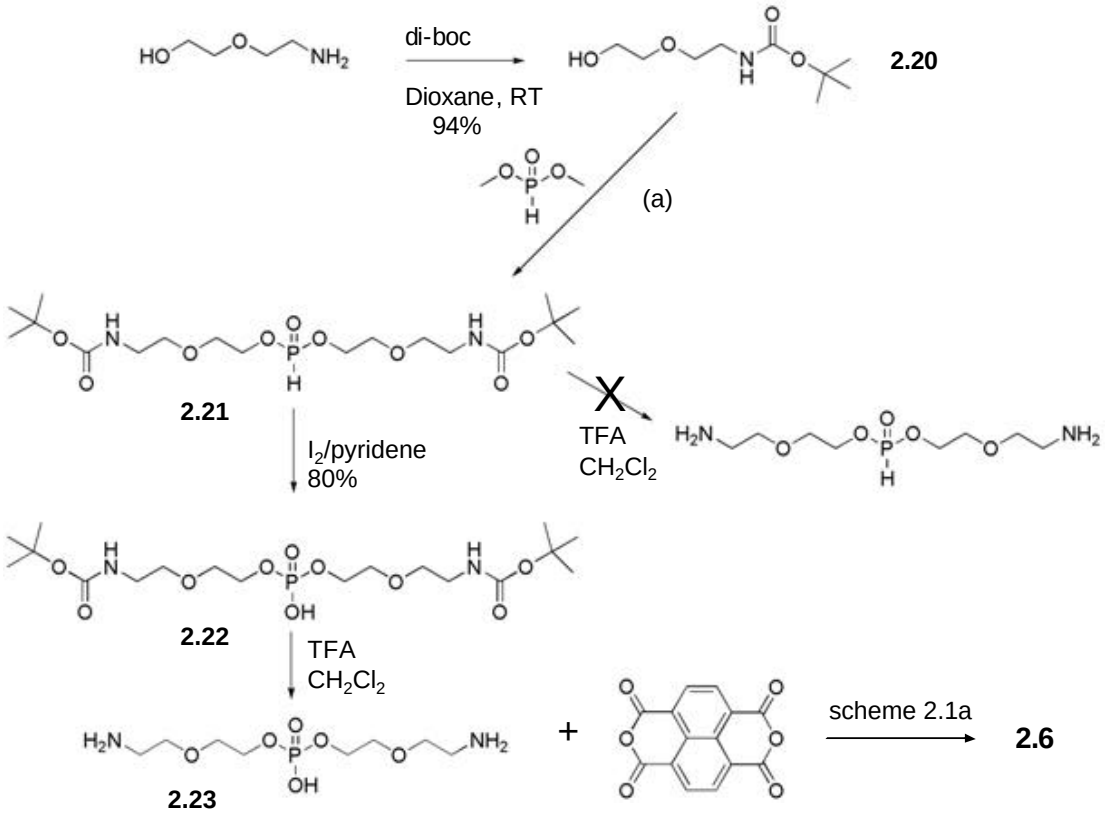

Scheme 2.5 Synthesis of phosphate Ndi polymers.

Ndi polymer **2.6** precipitated in solution during the condensation and upon isolation would not re-dissolve in any solvent, including aqueous base. There was no monomer left in the reaction. The Dan polyphosphonates were soluble in most organic solvents, including THF, and the polymer remained soluble through the oxidation. However, neither polymers **2.8** or **2.9** were soluble in basic solution, even when dropwise

added directly from the I_2/pyridine oxidation into 1M NaOH, in which case a precipitate immediately formed.

The inability of either positive or negative formal charge to promote the aqueous solubility of Dan and Ndi polymers was initially surprising. It was thought that having hundreds of charges incorporated into a polymer chain would allow it to be sufficiently solvated. However, the naphthyl units are apparently too hydrophobic in the linear polymer geometry even with the addition of surfactants such as SDS and CTAB. It was thought that by adding the complementary aromatic monomer the hydrophobic surface area could by minimized and solubility promoted, but adding water soluble monomers of Dan or Ndi to the complementary polymer had no affect on the solubility. By switching to a branched polymer architecture it was thought that soluble polymers could be synthesized with charges both along the backbone, and appended to the opposite end of the aromatic unit.

2.3.4 Functionalize backbone

Polyethylene-alt-maleic anhydride, supplied by Zeeland chemicals, was functionalized with Dan and Ndi monomers **2.24** and **2.25** to yield polymers **2.11** and **2.10** respectively according to scheme 2.6. The reactions were monitored by TLC to determine completion by disappearance of the starting material. Molecular weights for the functionalized polymers were calculated from the characterization data provided by the supplier of the starting co-polymer with 95% Dan or Ndi monomer incorporated. Ndi polymer **2.10** was soluble in 0.02 M aqueous base, up to 3% by weight. Dan polymer

2.11 was not soluble in aqueous media independently, but did dissolve up to 3% weight upon addition of sodium dodecyl sulfate surfactant (SDS), Ndi monomer, or polymer **2.10**. The Ndi polymer completely dissolved over about two hours of constant shaking, and the Dan over six hours with SDS or Ndi monomer, and fourteen hours with Ndi polymer **2.10**. The negative charge on both the backbone and the appended aromatic unit appear to be a minimum requirement for aqueous solubility, yielding the first water soluble Ndi and Dan polymers and allowing for initial studies on the association and structure of aromatic donor-acceptor polymers.

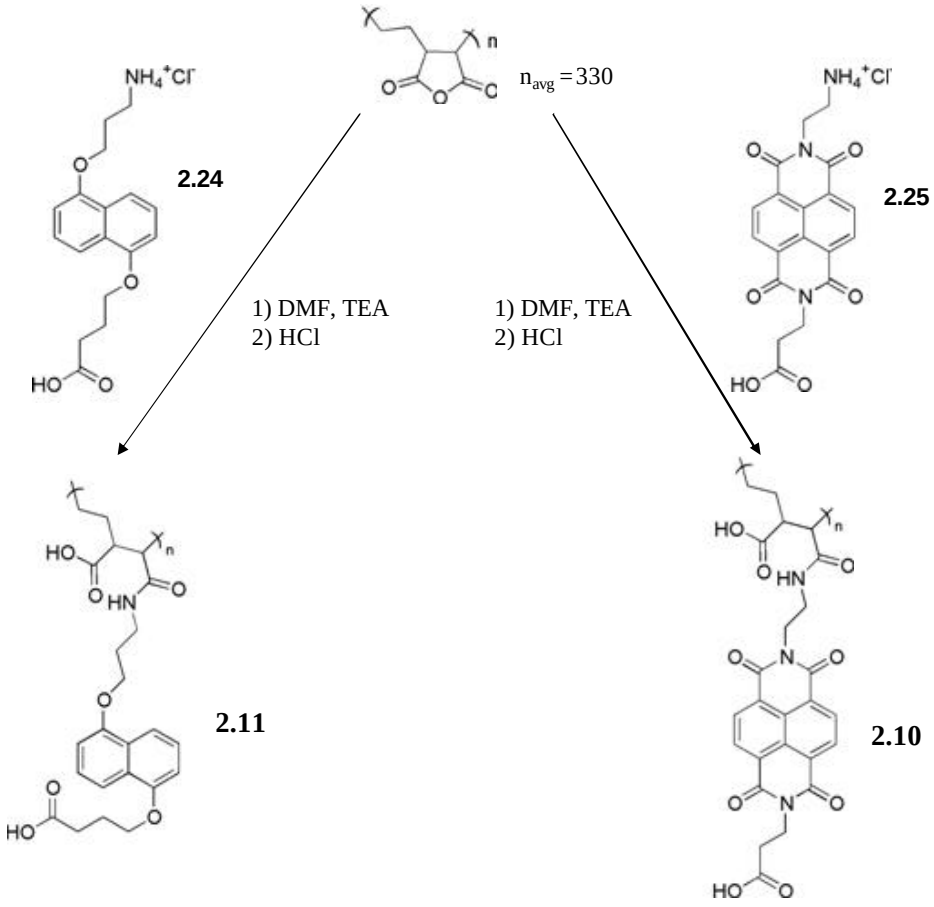

Scheme 2.6 Synthesis of branched polyDan and polyNdi.

Due to the dependence on the supplier for the polymer backbone, the molecular weight and polydispersity of the branched polymer chains cannot be controlled or altered. In future experiments next generation polymers can be designed with greater solubility and synthetic control.

2.4 RESULTS

2.4.1 UV-vis Analysis of Solutions

UV-vis spectroscopy was used to compare dilute aqueous solutions that were 0.2M in NaOH, of **2.11** + 0.01M SDS, **2.10** and an equal molar mixture of **2.11** + **2.10**. Figure 2.7a and 2.7b show the UV-vis spectrum for the Dan + SDS and Ndi polymers respectively at 0.6 mM of the aromatic unit. The spectra of a solution 0.6 mM in both the Dan and Ndi polymer is shown in figure 2.7c. The spectra of the independent polymers show absorbance in the region of 300 nm and 360 nm for the Dan and Ndi unit respectively. As would be expected of supramolecular polymers, the absorption bands are broad and lack definition, particularly in the case of polymer **2.10**. In the case of the mixture, the UV-vis absorbance bands decrease slightly in intensity, the Dan absorbance become visibly less sharp, and the Ndi absorbance red shifts by 3nm. All of these are indicative of a slight hypochromism in the mixture.

Upon increasing the concentration of the mixture to 6 mM in the aromatic units on both polymers, a charge transfer band becomes evident at ~550 nm (Figure 2.7d). This CT band is not present at this concentration for either of the two independent polymers, and is responsible for the purple color observed for the mixture.

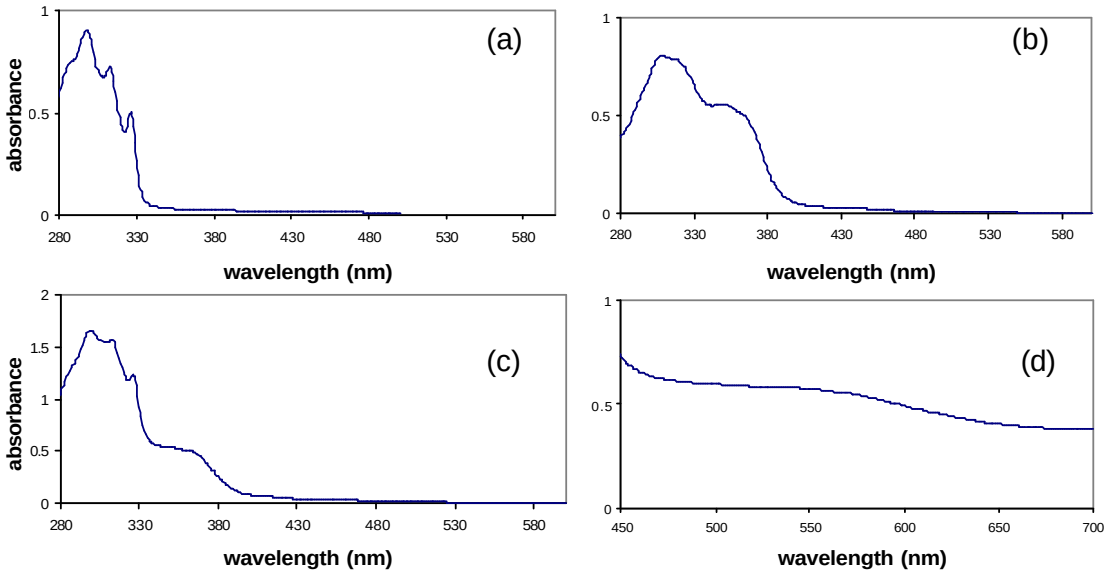

Figure 2.7 UV-vis absorption in 0.2M NaOH of (a) 0.6 mM in aromatic unit of **2.11** + 0.01M SDS detergent. (b) 0.6 mM in aromatic unit of **2.10** (c) 0.6 mM in aromatic unit of **2.11** + 0.6 mM in aromatic unit of **2.10**. (d) 6.0 mM in aromatic unit of **2.11** + 6.0 mM in aromatic unit of **2.10**.

2.4.2 Solution Viscosity

The viscosities of solutions containing polymers **2.11** + SDS, **2.10** and an equal molar mixture of **2.11** and **2.10** were measured at various concentrations under constant shear rate using cone and plate geometry, the results are shown in figure 2.8. Ndi polymer **2.10** exhibited a slight, linear increase in viscosity on increasing concentration form 0.6% to 3% by weight of the polymer (Figure 2.8c). The relative viscosity of Dan polymer **2.11** + SDS was slightly higher than that observed of **2.10** at all concentrations, but also linear up to 3% solids. The viscosity of the polymer mixture was significantly

higher than that of either polymer solution independently, and increases in a non-linear fashion from 0.6% to 3% in total polymer weight. 0.01M SDS was added to the mixture at 3% solids and the viscosity measured was 11.3 cp, essentially equal to that of the mixture without SDS.

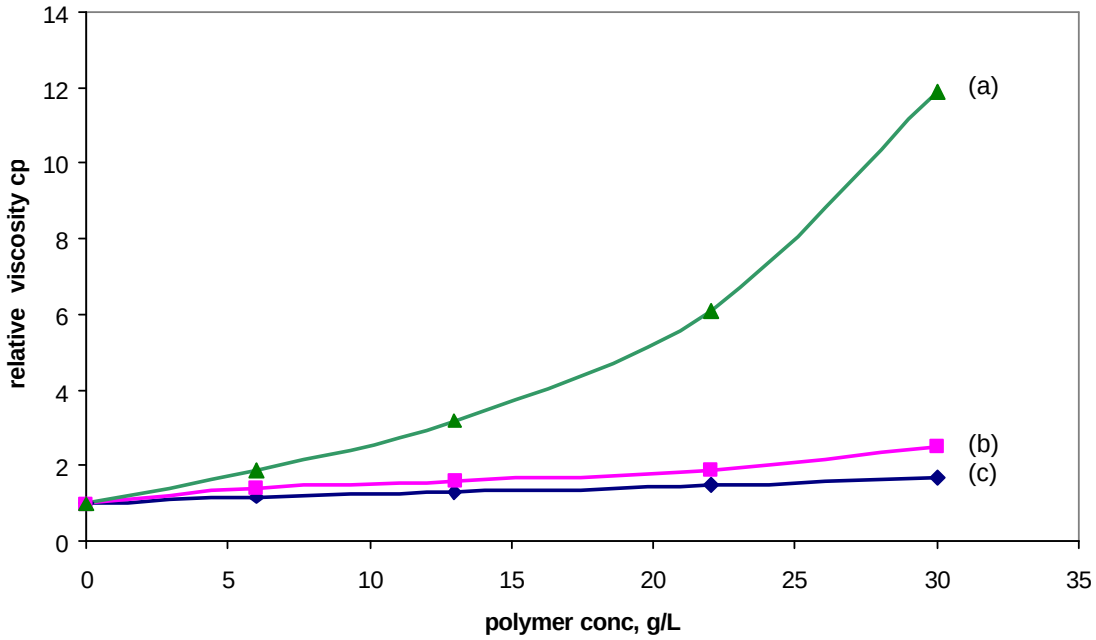

Figure 2.8 Cone and plate viscosity measurements at a constant shear rate for (a) 3% total weight of **2.10** + **2.11**, (b) **2.11** + SDS, (c) **2.10**.

2.4.3 TGA and DSC Analysis

Polymers **2.11** + SDS, **2.10**, and their mixture were analyzed by TGA and DSC. The polymers were dried in a vacuum oven over night at 70°C prior to the measurements. TGA results show that the polymers are stable up to 300°C both independently and as a mixture. The thermal decomposition of **2.11** + SDS plateaus at 60% weight

decomposition and is then stable up to 700°C. DSC of the same samples showed no phase transitions up to 300°C.

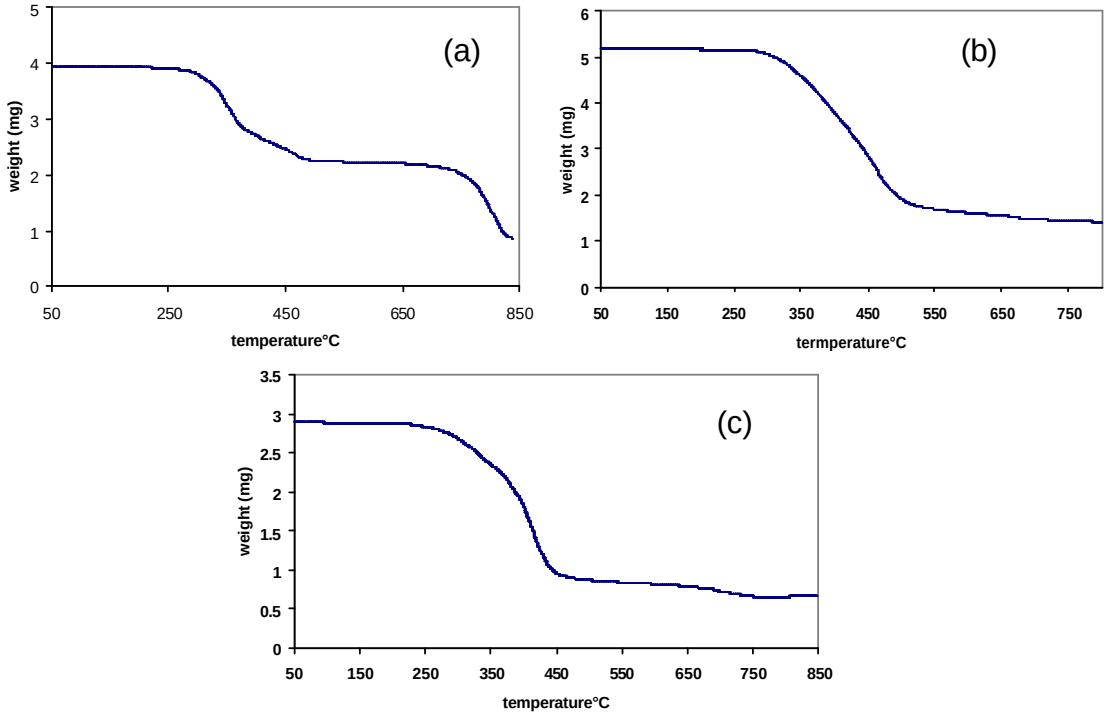

Figure 2.9 TGA decomposition of (a) **2.11** + SDS, (b) **2.10**, (c) **2.11** + **2.10**.

2.4.4 AFM of Polymer Films

AFM was used to evaluate the solid state structures of films made from the polymers and their mixture. Thin films were spun from 0.2 mM NaOH solutions of **2.11** solubilized with SDS, **2.10**, and a mixture of **2.11** and **2.10**. All solutions were 3% weight of total polymer. The solutions were spun onto glass supports and allowed to dry.

Films were then washed with 0.5 M HCl followed by water to remove salts, and annealed at 180°C for 24 hours. AFM imaging carried out in tapping mode verified that films formed from the solution of **2.11** + SDS yielded roughly circular deposits with average widths and heights of 500 nm and 75 nm, respectively (Figure 2.10a). This texture is characteristic of micelles deposited on a surface (Carmichael 2004, Hamley 2004). Films made from solutions of **2.10** were smooth and uniform, displaying a thickness of about 100 nm (Figure 2.10b). The viscous, purple mixture of polymers **2.10** and **2.11** yielded structures approximately 700 nm high, 1.6 μm across and averaging 14 μm in length (Figure 2.10c). Optical microscopy shows these features uniformly over the film (Figure 2.10d). Using polarized NSOM on the surface revealed that there is no anisotropy in the macrostructures.

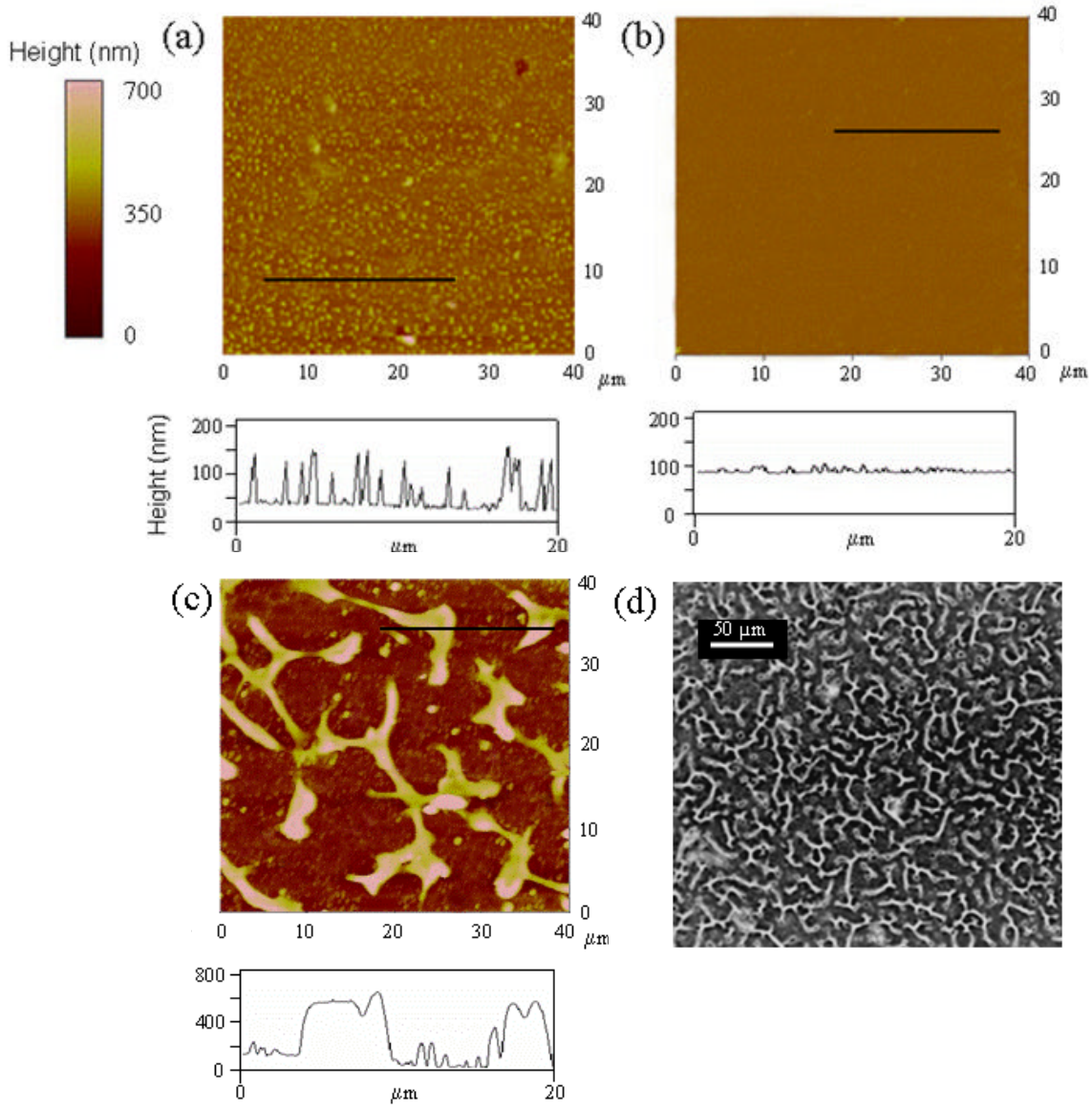

Figure 2.10 Tapping mode AFM, (a, b, c) and optical microscopy (d) of polymer films made from 0.2 M NaOH solutions (3% total weight polymer). (a) **2.11** + 0.01 M (SDS), (b) **2.10** (c) equal aromatic equivalents of **2.10** and **2.11**, (d) view of network of structures from equal aromatic equivalents of **2.10** and **2.11**.

2.4.5 Fiber Formation

Preliminary attempts at forming fibers from combined Dan and Ndi polymer strands were made by precipitating the mixture after quickly passing through a small aperture. An aqueous solution of **2.10** + **2.11** (0.2 M NaOH, 3% total weight polymer) was injected via a 30 gauge needle into 1 M HCl yielding long, delicate fibers up to several centimeters in length (Figure 2.11a). Similar solutions of either **2.11** solubilized with SDS, or **2.10** formed no fiber, but rather very fine precipitates in the case of **2.10** and slowly dispersing dilute clumps in **2.11** + SDS (Figures 2.11b,c).

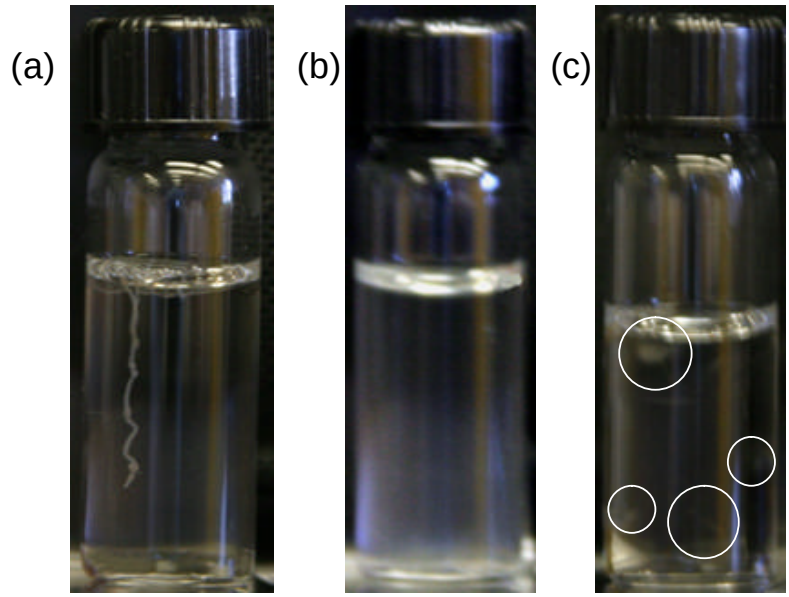

Figure 2.11 3% by weight polymer 0.2 M NaOH solutions quickly injected into 1 M HCL. (a) **2.10** + **2.11**, (b) **2.10**, (c) **2.11** + 0.01 M SDS.

2.4.6 SEM of Polymer Blend Film and Fiber

SEM was performed on the **2.10** + **2.11** film to further analyze the surface morphology. The film structures are made of small densely packed domains, averaging 300nm in diameter (Figure 2.12a). The surface image shows a rough amorphous morphology for these domains. Closer inspection of the disperse regions between domains reveals the presence of discrete polymer threads traversing the gaps between dense domains (Figure 2.12b). These threads have an average width of 30 nm, lengths of up to 200 nm, and appear to be connecting densely packed regions.

The **2.10** + **2.11** fiber was removed from aqueous solution and placed on an aluminum strip and dried in a vacuum oven for SEM analysis. The fibers were uniform in thickness with what looked like bubbles created by escaping solution along the surface (Figure 2.12c). Higher magnification of the fiber showed a smooth surface with long thin rivets along the length of the fiber. Similar to the interpretation of the **2.10** + **2.11** films, the fiber seems to be made up of densely packed threads. However, the threads are now oriented in a uniform direction to form an elongated fiber (Figure 2.12d).

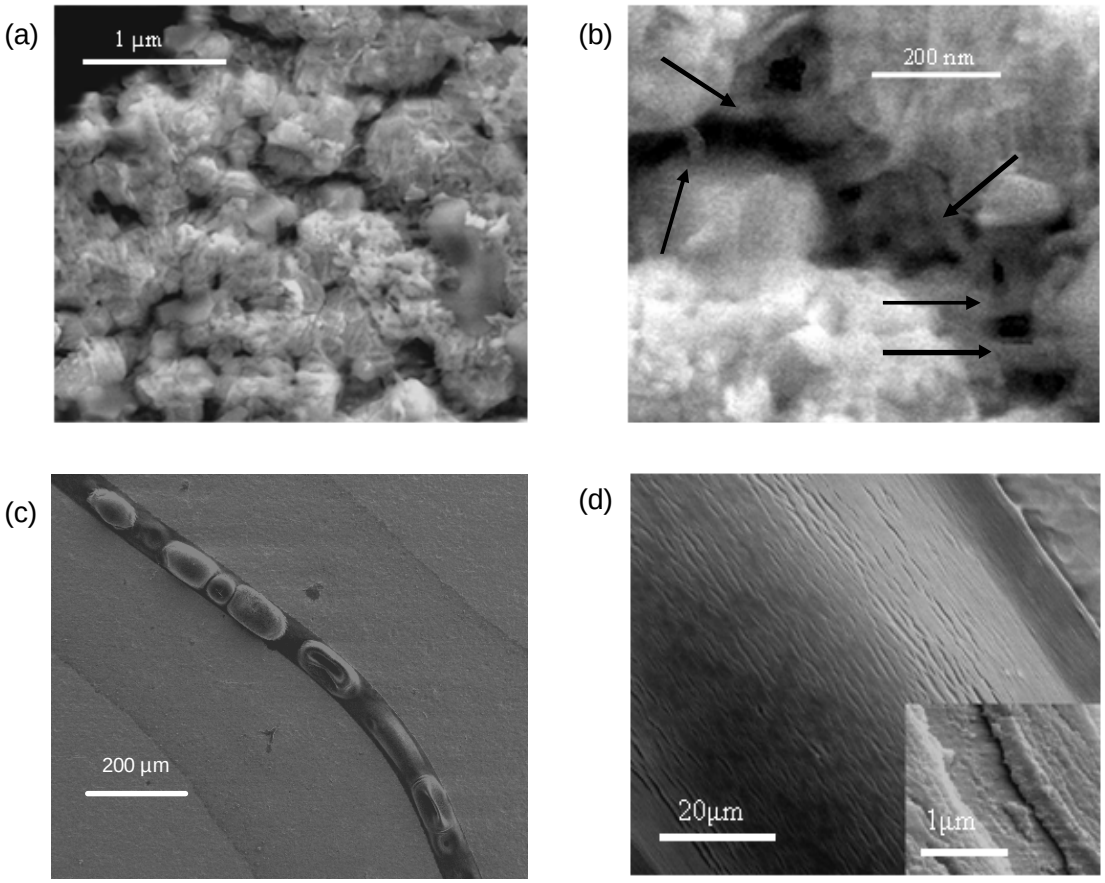

Figure 2.12 SEM images of polymer film and fiber generated from a 0.2M NaOH solution 3% total weight in **2.10** + **2.11**. (a) Amorphous surface of the macrostructures seen in the AFM (Figure 2.11c). (b) Close up of the regions between amorphous domains. Arrows point to the small threads that span the gaps and appear to be connecting domains. (c) Fiber on aluminum support. Bubbles can be seen where solvent escaped upon drying. (d) Close up of fiber showing the orientation of small threads along the fiber axis.

2.5 DISCUSSION

2.5.1 Linear vs. Branched

The connectivity, either linear or branched, of the Dan and Ndi polymers has a profound affect on their solubility. None of the linear polymer designs produced a polymer that could be brought into aqueous solution. Solubilizing a segment of the linear chain requires solvation of the charges in the backbone, and the exposure of all local aromatic groups. This could be an energetic barrier that prevents the linear chain from being brought into solution. With the branched architecture, charges along the backbone and individual aromatic units can be solubilized without immediately disturbing neighboring units. It is speculated that this allows for the polymer chains to be slowly coaxed into solution, and is an explanation for the difference in the observed solubility of the Ndi polymer, and the ability of the Dan polymer to be brought into solution.

2.5.2 Solution Characterization: Evaluation of UV-vis and Viscosity Data

Both the hypochromism and the charge transfer band observed by UV-vis for the **2.10** + **2.11** solution are diagnostic features of Dan:Ndi face-to-face association. There can be no doubt that the Dan and Ndi units on independent polymer chains are interacting, and that there is therefore directed non-covalent interactions between chains. However, both of these observed UV-vis phenomenon are small in magnitude, and so the extent of association is either much smaller than anticipated, or the effect washed out in the supramolecular polymer environment. The fact that the UV-vis peaks for the aromatic units lack definition when the polymers are observed independently may mean that the chains are tightly coiled and self stacking in solution. This would cause a large

kinetic barrier to inter-polymer association, and may contribute to there being relatively few Dan:Ndi interactions.

The viscosity measurements clearly show that the **2.10** + **2.11** mixture has interacting polymer strands in solution. The fact that the viscosity of the mixture is significantly higher than the independent polymers, and that its viscosity increases at a much higher rate upon increasing concentrating, indicates that there is non-covalent cross-linking of unlike chains in solution. Adding SDS to the polymer mixture has no affect on the viscosity increase, illustrating that it is not merely the Dan polymer without SDS that contributes to the high viscosity, and that the donor-acceptor interactions between chains is not broken up by addition of surfactant. The UV-vis and viscosity experiments both support association of independent Dan and Ndi polymer chains through aromatic donor-acceptor interactions. Figure 2.13 illustrates the model of the branched polymers interacting at a few aromatic sites to promote assembly in solution.

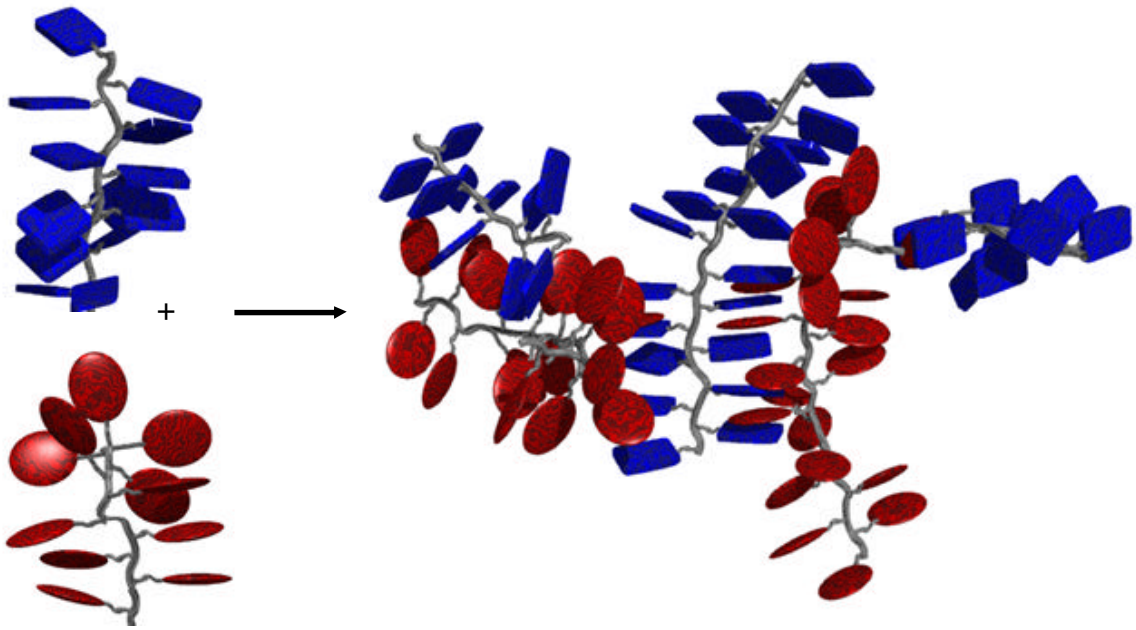

Figure 2.13 Illustration of independent Dan and Ndi polymer strands associating through a limited number of donor-acceptor interactions.

2.5.3 Solid State Characterization: Evaluation of Film and Fiber Data

The macrostructure of the film formed from the combined polymers, as observed by AFM, is quite distinct from either of the two films made with individual components, indicating that the structures in figure 2.10c are the result of interactions between the unlike polymer chains. The Dan-Ndi stacking interaction drives the association of **2.11** and **2.10** into an integrated polymer network that results in large elongated structures upon film formation. The film of **2.11** with SDS has small spherical micelle deposits as might be expected if the surfactant is solubilizing the hydrophobic polymer as the polymer wants to remain coiled up, possibly self-interacting, to avoid the aqueous

solution. The film from Ndi polymer **2.10** is quite smooth, perhaps due to the ability of the Ndi units to stack in the off-set geometry observed in the representative crystal structure (Figure 1.9a). This again supports that there may be some self-stacking of the polymer in solution.

The fact that polarized NSOM reveals no anisotropy in the structures of the polymer mixture may mean that there are not regions of extended donor-acceptor columns responsible for the elongation of the structures. This is supported by the relatively low amount of Dan:Ndi association observed in the UV-vis experiments. Yet, the inter-chain aromatic interactions that are present are apparently sufficient to cause formation of significantly sized structures, illustrating the use of donor-acceptor aromatic interactions as a means of promoting supramolecular polymer assembly.

The packing of amorphous domains displayed in the SEM images of the films from the **2.10** + **2.11** polymer mixture are consistent with a model in which several polymer chains, which are tightly folded and self-stacking, interact via a few Dan-Ndi interactions to form individual threads in solution, inducing the noted viscosity increase and UV-vis characteristics. These threads then aggregate together upon film formation to form the rough amorphous regions. Threads on the periphery of the domains interact with other regions, connecting them together and forming the structures of the film. This model of structure assembly is illustrated in figure 2.14.

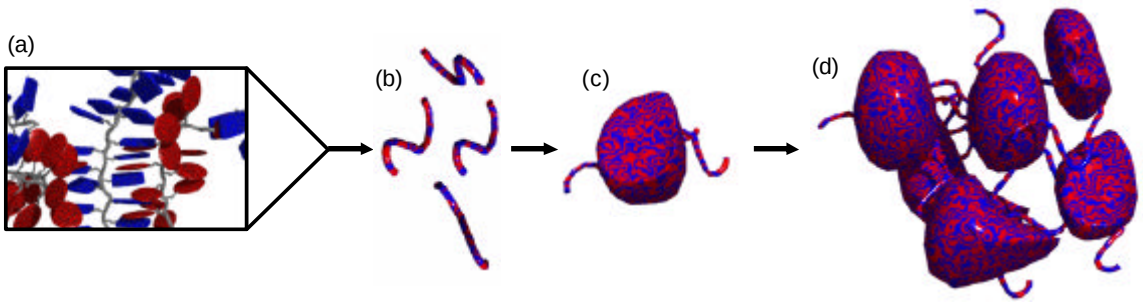

Figure 2.14 Model for film structure formation. The independent polymers associate via a few Dan:Ndi interactions in aqueous solution (a) and form co-polymer threads with domains of self-stacked polymers (b). These threads come together through the overlap of branched Dan and Ndi units to create the amorphous regions of the macrostructure (Figure 2.12a). These regions then conglomerate, held together via Dan:Ndi complexation with shared threads (Figure 2.12b) to form the film structure.

By forcing the polymer mixture quickly through a small aperture at the time of precipitation, small fibers were formed. The small threads could be aligned in one direction, interacting with each other to form extended fibers. Independently, solutions of the Dan and Ndi polymers precipitated into the acidic solution showing no fiber formation. This illustrates that the aligning and extended association of polymer chains is unique. The fiber is very easily broken, again consistent with a relatively small percentage of Dan/Ndi overlap. Nevertheless, the polymer fiber is remarkable in its assembly compared to the independent polymers, and further indicates the ability and potential of directed aromatic interactions to affect assembly of macrostructures.

2.6 CHAPTER CONCLUSIONS

The progression of linear Dan and Ndi polymer architectures explored in search of water soluble molecules highlights the extreme difficulty of solubilizing a large number of naphthyl repeat units. It may be that with linear connectivity a conformation cannot be found which lessens the exposure of aromatic surfaces to an extent that allows for solubility, or perhaps there is simply not enough room on the chain to solvate the charges sufficient to provide solubility. Whatever the reason, linear charged polymers with Dan or Ndi incorporated into the backbone is not a feasible design for water soluble polymers. Success in design of an aqueous soluble polymer was found with a branched geometry. Future generations of aqueous soluble naphthyl polymers should include branching of the aromatic unit, and perhaps extensive branching of solubilizing repeat units off of the backbone. Solubility needs to be the first priority in any polymer design. The ability of the Ndi polymer to promote solubility of the Dan polymer should be noted, and can perhaps be taken advantage of in future research.

This first generation of water soluble Dan and Ndi polymers has illustrated the ability of directed aromatic interactions to affect structural assembly in solution, films and fibers, for the first time adding Dan:Ndi association to the tool box of the supramolecular materials chemist. The most striking features in the experiments of this chapter are the significant difference in behavior of the polymer mixture from its components. A model in which chains interact to a small degree to form threads in dilute solution, and then inter-associate to form macrostructures is supported by observations in both solution and the solid state. Even with limited solubility and interaction, the structures formed are significant, and evidence of the ability to align solution threads into

fibers warrants future design of new polymers that can obtain a higher concentration in solution and make use of more aromatic donor-acceptor interactions, thereby associating more efficiently in the search for novel functional materials.

2.7 EXPERIMENTAL SECTION

General methods. All starting materials were obtained from Aldrich and used without further purification. NMR spectra were taken on a Varian Unity +300 spectrometer in solutions of DMSO or 0.2M NaOD. Tapping-mode atomic-force microscopy (AFM) measurements were made using a Digital Instruments Dimension 3100 microscope in combination with a Nanoscope IV Controller (Veeco Metrology, Santa Barbara, CA). Scanning electron micrograph (SEM) data was obtained from a LEO 1530 scanning electron microscope operating at an accelerating voltage of 3 KeV. TGA experiments were performed on a TA Instruments TGA Q500. UV-Vis spectra were taken with a Perkin-Elmer Lambda 35 spectrophotometer. ~50 kD M_w with a PDI of 2.2 polyethylene-alt-maleic anhydride was supplied by the Zeeland chemical company. Molecular weight of the branched polymers was estimated based on 95% aromatic unit incorporation. DSC experiments were performed on a TA Instruments DSC Q100; no transitions were observed in either of the polymers before degradation began at 250°C. Compounds **2.14, 2.15, 2.16, 2.17, 2.20, 2.24,** and **2.25** were synthesized as reported previously in the Iverson group (Lokey 1997, Cubberley 2000).

Film formation. Solutions 3% by weight of polymer **2.10**, **2.11** + SDS, and **2.10** + **2.11** were prepared in 0.2 M NaOH. Glass slides were washed in a base bath, rinsed, and allowed to air dry before being put on a spin coater and covered with the respective solutions. The slides were then spun until dry, rinsed with 1M HCl, then deionized water before annealing at 160° for 24 hours.

Linear Ndi polymers 2.1-2.3, 2.5. 1,4,5,8-Naphthalenetetracarboxylic dianhydride (1.0g, 3.7 mmol) was added to a round bottom flask with DMF (50 ml), TEA (1 ml) and a stir bar. The brown solution/suspension was degassed by bubbling Ar gas through it for fifteen minutes, and the corresponding amine (3.7 mmol) dissolved in DMF (20 ml) was added dropwise at room temperature via an addition funnel over 20 minutes, to give a clear brown solution. The solution was then heated to 90°C and allowed to stir under argon for 14 hours. All reactions formed a precipitate which was filtered off and found to be insoluble in THF, DMSO, NMP, DMA, 2M NaOH and 2M HCL.

***N,N*-bis(2-aminoethyl) ethane-2-amino-1-carbamic acid *tert*-butyl ester (2.12).** Di-*tert*-butyl dicarbonate (7.4 g, 34 mmol) in dioxane (50 ml) was added dropwise to *N,N*-bis(2-aminoethyl) ethane-1,2-diamine (15g, 0.1 mol) in dioxane (250 ml) over 19 h under an argon atmosphere. The solvent was removed under reduced pressure and H_2O (300 ml) was added. The aqueous solution was filtered and then extracted with CH_2Cl_2 (7 x 200 ml). The combined organic layers were dried over Na_2SO_4, and concentrated under reduced pressure to give a yellow oil. This was purified via column chromatography (75% CH_2Cl_2, 25% acetone) to yield the title compound as a viscous yellow oil (37%).

^{13}C NMR ($CDCl_3$) *d* 156.0, 79.5, 55.7, 52.9, 39.0, 38.9, 28.5; ^{1}H NMR ($CDCl_3$) *d* 3.00 (q, *J* = 5.4 Hz, 2H), 2.58 (t, *J* = 6.3 Hz, 4H), 2.33-2.41 (m, 6H), 1.27 (s, 9H), 1.17 (br, 4H) ppm; ESI –MS (positive-ion) 247 ($[M + H]^+$).

Linear Ndi polymers 2.13, 2.4. 1,4,5,8-Naphthalenetetracarboxylic dianhydride (1.0g, 3.7 mmol) was added to a round bottom flask with DMF (50 ml), TEA (1 ml) and a stir bar. The brown solution/suspension was degassed by bubbling Ar gas through it for fifteen minutes, and then **2.12** (0.91 g, 3.7 mmol) dissolved in DMF (20 ml) was added dropwise at room temperature via an addition funnel over 20 minutes, to give a clear brown solution. The solution was then heated to 90°C and allowed to stir under argon for 14 hours yielding polymer **2.13**. ^{1}H NMR ($CDCl_3$) *d* 8.82 (br, 4H), 3.45 (br, 4H), 2.98 (br, 4H), 2.23 (br, 4H), 1.32 (s, 9H) ppm. The solution was then concentrated under reduced pressure to 1/3 volume, and a 50:50 mixture of CH_2Cl_2:TFA was added (50 ml). After one hour polymer **2.4** precipitated out of solution, was filtered, and found to be insoluble in THF, DMSO, NMP, DMA, 2M NaOH and 2M HCL.

Linear Dan polymer (2.6). 1,5-Dihydroxy naphthalene (1.5 g, 9.3 mmol), 1,4-bis(3-bromopropyl)piperazine (3.07 g, 9.3 mmol), potassium carbonate (3 g) were all added to CH_3CN (100 ml). The solution was degassed by bubbling Ar gas through it for fifteen minutes, and then stirred under reflux for 24 h. The polymer precipitated out of solution, was filtered and then found to insoluble in THF, DMSO, NMP, DMA, 2M NaOH and 2M HCL.

Linear Dan polymer (2.7). **2.15** (0.5 g, 1.8 mmol) was dissolved in DMA (20 ml) and degassed. One drop of conc, HCl was added, and then succinalehyde (0.15 g, 1.8 mmol) in DMA (5 ml) was added dropwise via an addition funnel underargon over 20 minutes. The solution was allowed to stir at room temperature for one hour in which time a fine precipitate began to form. $NaBH_4$ (0.1 g, 2.5 mmol) was then added, and after two hours the polymer precipitated from solution, was filtered, and found to be insoluble in THF, DMSO, NMP, DMA, 2M NaOH and 2M HCL.

Polyphosphate 2.8. **2.21** (0.5g) was placed into a 50ml RB flask with a stir bar and dissolved in DMF (30ml). The solution was cooled to 0°C, and then 2ml of a 2M I_2 solution in pyridine (2% H_2O) was added. The solution was allowed to come to room temperature, and stir for 10 min. This process was repeated twice more, turning a dark brown and becoming thick. The solution was then allowed to stir at RT for 12 hours. The brown mixture was precipitated into acetone and dried in a vacuum oven at 50°C to yield **2.9** as a sticky brown solid (61%). ^{31}P NMR (DMSO) *d* -11.92 ppm; ^{1}H NMR (DMSO) *d* 9.63 (br, 1H), 7.61 (br, 2H), 7.05 (br, 2H), 6.90 (br, 2H), 4.60 (br, 4H), 4.20 (br, 4H), 3.81 (br, 4H); ppm.

Polyphosphate 2.9. According to the method used for **2.8**, **2.9** was obtained as a amorphous brown solid in 58% yield. ^{31}P NMR (DMSO) *d* -11.80 ppm; ^{1}H NMR (DMSO) *d* 9.59 (br, 1H), 7.60 (br, 2H), 7.15 (br, 2H), 6.88 (br, 2H), 4.64 (br, 4H), 4.42 (br, 4H), 4.21 (br, 4H), 4.16 (br, 4H); ppm.

PolyDan 2.11. Polyethylene-alt-maleic anhydride (0.6g) was dissolved in dry DMF (20ml) and TEA (1.44g, 14mmol) and placed under argon. **1** (1.59g, 4.69mmol) in dry DMF (20ml) was added to the solution via an addition funnel over 1 hr, and the reaction was allowed to stir at RT over night. Upon no evidence of reagent **1** by TLC in the reaction, the solution was precipitated in 1M HCl, filtered, and dried under vacuum at 30°C to yield **2.11** (1.2g, 60% recovered) as a light brown solid. ^{1}H NMR (0.5M NaOD + 0.01M SDS) *d* 7.37 (br, 2H), 6.85 (br, 2H), 6.36 (br, 2H), 4.04 (br, 2H), 3.27 (br, 2H) 2.16 (br, 4H), 1.82 (br, 4H), 1.25 (br, 4H) ppm.

PolyNdi 2.10. According to the method used for **2.11**, **2.10** was obtained as a light yellow solid in 59% yield. ^{1}H NMR (DMSO) *d* 12.39 (br, 2H), 8.68 (s, 4H), 4.29 (t, J = 7.3 Hz, 2H), 3.33 (br, 2H), 2.61 (t, J = 7.8 Hz, 2H), 2.52 (t, J = 9.3 Hz, 2H), 2.44 (br, 2H), 1.42 (br, 4H) ppm.

Polyphosphonate 2.18. Diol **2.16** (0.74g, 2.7mmol) was placed into a dry 50ml roundbottom flask fitted with a condenser and a stir bar and dissolved in a solution of DMF (15ml) and *o*-dichlorobenzene (15ml). The solution was heated under argon gas to 85°C. Dimethylphosphonate (0.84g, 7.6mmol) was slowly added over 15min and the solution was allowed to stir under argon for 14 hrs. A second refluxing condenser was then attached, and a slight vacuum applied for 24 hrs. The cold water in the condensers was then turned off, and the reaction was left under high vacuum for 48 hrs. This yielded **2.18** as a clear/yellowish transparent solid (0.97g, 90%). ^{31}P NMR (DMSO) *d* 10.22 ppm;

^{1}H NMR (DMSO) *d* 7.73 (br, 2H), 7.38 (br, 2H), 6.90 (br, 2H), 4.25 (br, 4H), 4.11 (br, 4H), 2.18 (br, 4H) ppm.

Polyphosphonate 2.19. According to the method used for **2.18**, **2.19** was obtained as a clear transparent solid in 84% yield. ^{31}P NMR (DMSO) *d* 10.24 ppm; ^{1}H NMR (DMSO) *d* 7.75 (br, 2H), 7.37 (br, 2H), 6.92 (br, 2H), 4.25 (br, 4H), 4.17 (br, 4H), 3.79 (br, 4H), 3.64 (br, 4H); ppm.

Bis-[(2-ethoxy-ethyl)carbamic acid *tert*-butyl ester]phosphonate 2.21. According to the method used for **2.18**, **2.21** was obtained as a viscous yellow oil in 77% yield. ^{31}P NMR ($CDCl_3$) *d* 10.10 ppm; ^{1}H NMR ($CDCl_3$) *d* 5.21 (br, 2H), 4.21 (m, 4H), 3.64 (t, *J* = 4.8 Hz, 4H), 3.53 (t, *J* = 5.4 Hz 4H), 3.30 (q, *J* = 5.1 Hz, 4H), 1.42 (s, 9H); ppm; ESI –MS (positive-ion) 457 ($[M + H]^+$).

Bis-[(2-ethoxy-ethyl)carbamic acid *tert*-butyl ester]phosphate 2.22. According to the method used for **2.8**, **2.22** was obtained as a brown oil in 62% yield. ^{31}P NMR (DMSO) *d* -12.04 ppm; ^{1}H NMR (DMSO) *d* 6.79 (br, 2H), 3.60 (m, 4H), 3.40 (t, *J* = 4.7 Hz, 4H), 3.32 (t, *J* = 5.4 Hz 4H), 3.10 (q, *J* = 5.2 Hz, 4H), 1.39 (br, 9H); ppm; ESI –MS (positive-ion) 473 ($[M + H]^+$)..

Bis-[(2-ethoxy-ethyl) amine]phosphate 2.23. TFA (10 ml) was added dropwise to a solution of **2.22** (0.5 g, 1.1 mmol) in CH_2Cl_2 (10 ml). After stiring for six hours, the solvent was evaporated under reduced pressure and then the remaining TFA was

azeotroped with three additions of EtOH (20 ml) to yield the TFA salt of the title compound as a dark brown solid (0.48 g, 96%). ^{31}P NMR (DMSO) *d* -11.84 ppm; ^{1}H NMR (DMSO) *d* 7.79 (br, 6H), 3.56 (m, 4H), 3.28 (t, *J* = 4.8 Hz, 4H), 3.12 (t, *J* = 5.2 Hz 4H), 2.61 (q, *J* = 5.1 Hz, 4H) ppm; ESI –MS (positive-ion) 273 ($[M + H]^+$).

CHAPTER 3

Mesophase Formation and Manipulation with C_2 symetric Donor-Acceptor Complexes

3.1 CHAPTER SUMMARY

Introduction. Previously in the Iverson group electron rich Dan and electron poor Ndi have been studied in aqueous solution as monomers, foldamers and short complementary naphthyl oligomers. Chapter 2 expanded the scope of aqueous driven aromatic interactions to polymers and provided initial insight into material assembly driven by the Dan/Ndi interaction. This chapter deals with supramolecular aromatic donor-acceptor interactions removing all solvent, to study the basic interactions and material properties of Dan and Ndi monomers in bulk. Here the side chains, rather than linkers as in previous self-assembly studies, become variable length spacers for the novel control and tunability of aromatic donor-acceptor mesophases. This work extends applications of the Dan:Ndi assembly into the realm of supramolecular phases, and illustrates unprecedented predictable control of mesophase properties.

Goals. The electrostatic and geometric complementarity of Dan and Ndi that allows for solution phase assembly may also be exploited in the melt and solid state by ordering molecules into a plastic or liquid crystalline columnar mesophase. The objective of work

described in this chapter is to answer the question: *Can Dan and Ndi monomers interact to form mesophases, and can we gain predictable control of mesophase structure and properties by "mixing and matching" Dan and Ndi components?* Long-term goals of this work include fine control over the molecular structure of mesophases and exploring applications in crystal engineering and organic electronic materials.

Approach. A series of Dan and Ndi monomers, which vary in the length and bulk of appended side chains, were synthesized and studied upon mixing and melting. Polarized optical microscopy was used to visualize the optical texture of mesophases, and DSC to determine phase transitions and energies. Powder x-ray diffraction was used to determine mesophase structure by comparisons to, and models from, single crystal x-ray data of individual monomers and example co-crystals. Additionally UV-Vis data was used to evaluate the CT band of donor-acceptor stacking and therefore the extent of face-to-face interactions in the liquid, measophase, and crystalline phase.

Results. Overall, the work described in this chapter demonstrated that the mixing of Dan and Ndi monomers in bulk can induce mesophases that have tunable properties, with unprecedented control. A variety of 1:1 Dan:Ndi mixtures produced mesophases that were found to be stable over temperature ranges starting from 25°C and extending up to 110°C. Analysis of these mesophases indicates that they are all composed of alternating donor-acceptor columns. A correspondence was found between the clearing and crystallization points of the mesophase mixtures and the melting/clearing points of the component Ndi and Dan units, respectively. This correspondence enables the predictable

tuning of mesophase phase transition temperatures. X-ray diffraction also shows that there is a predictable trend with the length and size of the side chain of the Dan or Ndi unit and unit cell dimensions of the mesophase. The study of sterically hindered derivatives led to a set of mixtures in which a dramatic and sudden color change (deep red to yellow) was observed upon crystallization of the mesophase due to a phase separation of the component donor and acceptor units.

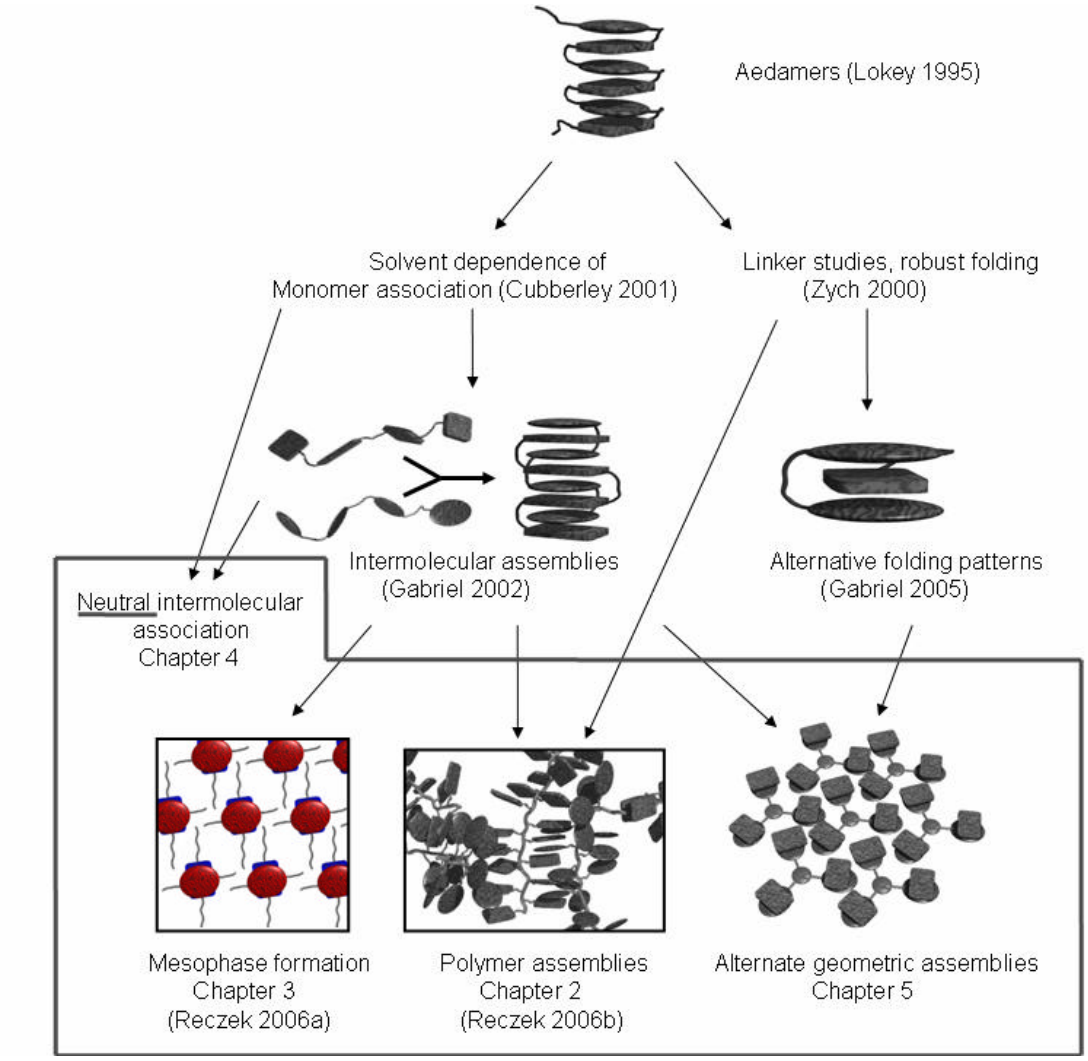

Chart 3.1 Aromatic donor-acceptor molecular assembly in the Iverson group.

3.2 BACKGROUND

The term mesophase refers to a state of matter that is "in between" the complete 3-D orientational and positional order of crystalline solids, and the complete isotropy of liquids. The familiar term liquid crystal is often used synonomously with mesophase, and in fact all liquid crystals are also mesphases, although there is some debate if the reverse is true, as the term liquid crystal carries with it the connotation of having physical properties of both a liquid and a crystal, rather than simply being defined by molecular order. Mesophase formation is governed by weak forces instigating some degree of molecular order from an isotropic state. In the case of enantiotropic mesophases (thermodynamically stable phases over some temperature range without outside influence), molecules usually interact via non-covalent interactions. The assembly of relatively flat aromatic molecules via aromatic-aromatic interactions is ideal for applications in mesophase formation. Over thirty years ago, aromatic donor-acceptor interactions were first observed to affect mesophase transitions in calamitic (rod like) systems when the electron poor aromatic 4-cyano-4'-pentylbiphenyl (CPB) was added to electron rich *N*-(4-methyl-oxybenzylidene)-4-butylaniline (MBBA) creating a mixture with a slightly higher clearing and crystallization temperature than either of the independent mesogens (Park 1975). There have been several examples in calamitic systems, some of which are shown in figure 3.1a. Most exhibit characteristics of nematic or smectic A phases, illustrated in figure 3.1b,c, with a few having indications of higher order smectic phases (Demus 1998).

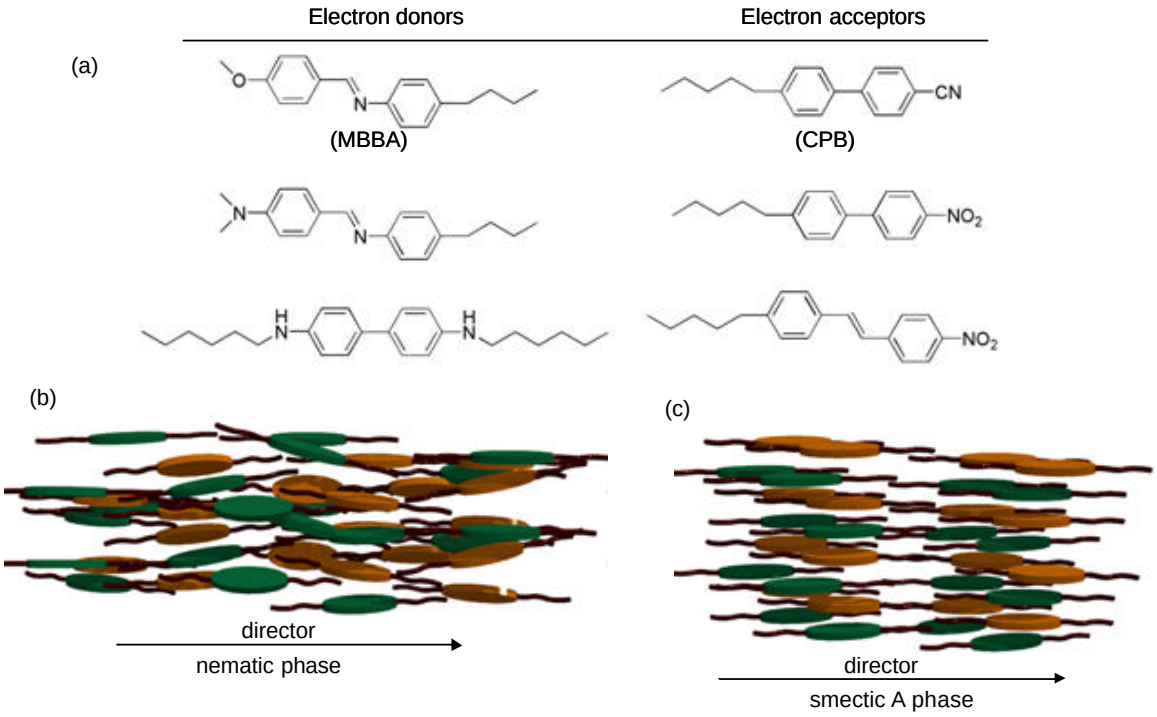

Figure 3.1 (a) Examples of calamitic donor and acceptor molecules. (b) Representation of a nematic calamitic donor-acceptor phase with orientational order along the director. (c) Representation of a smectic A calamitic donor-acceptor phase with orientational order along the director and some positional order.

It was soon realized that the affect of aromatic interactions on mesophase alteration and induction is much more pronounced in discotic (disk-like) mesomorphic complexes. The strong electron acceptor 7,7,8,8-tetracyano-1,4-quinodimethane (TCNQ) was shown to form columnar mesophases with tetra(4-dodecyloxyphenyl) dithiapyranylidene and other thiopyran derivatives (Gionis 1982). Although the structure is not absolutely defined for these mesophases, an extremly interesting result of the mixture is a slight ability to conduct in the liquid crystalline phase.

Ringsdorf and co-workers were the first to implement aromatic donor-acceptor interactions as a design element for mesophase induction, bringing it into the field of supramolecular chemistry, with the creation of columnar mesophases in polymeric systems (Ringsdorf 1989). Polymers incorporating side chains appended with 2,3,6,7,10,11-hexasubstituted triphenylene (HAT) derivatives were doped with electron deficient 2,4,7-trinitro-9-flourenone (TNF), inducing columnar hexagonal (Col_{ho}) mesophases. The natural step to low molecular weight compounds was made with monomeric HAT derivatives and TNF (Figure 3.2a) (Bengs 1990). The mesomorphic temperature range of the HAT mesophase increased with addition of TNF to a maximum at 40 mole percent of the acceptor. At this 6:4 HTP:TNF ratio the mixture behaves as a single complex, with clear crystallization and clearing transitions from the Col_{ho} phase. Interestingly, even HAT derivatives that do not exhibit an independent mesophase upon the addition of TNF usually display columnar mesophase behavior.

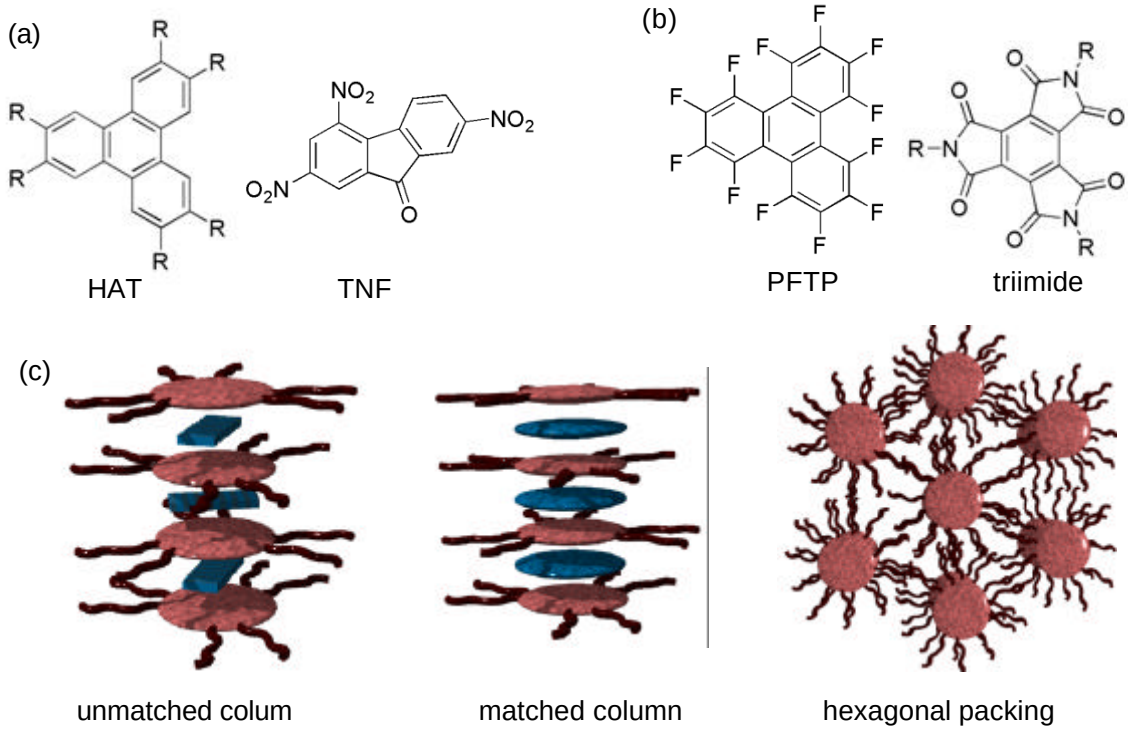

Figure 3.2 (a) Orignial discotic HAT and TNF donor-acceptor pair. (b) Example of geomectrically matched discotic acceptors. (c) Representations of columnar stacking and hexagonal packing.

While TCNQ, TNF, and a few other electron deficient molecules have proven effective in altering and inducing mesophase behavior of discotic molecules, they are poorly matched geometrically with their donor counterparts to create well ordered and predictable columnar structures. This makes their resulting complexes, while empirically interesting, difficult to characterize, at least without heavy assumption and amgiuity Demus 1996). Joint work by the groups of Grubbs and Coates used a perfluorotriphenylene (PFTP) electron acceptor to interact with HATs (Figure 3.2b) (Weck 1999). The geometrically similar PFTP enhances the mesophase temperature

range by 70°C and the alternating face-centered columnar structure of the mesophase is assigned based on the obtained crystal structure of a 1:1 mixture of triphenylene with PFTP.

Another structurally similar donor-acceptor pair was designed by Park and Hamilton (Park 2003). Again HAT derivatives were used as the donor molecule, this time coupled with mellitic triimides. Unlike previously discussed acceptor molecules, the triimides can be synthesized with various side chain functionality, therefore adding the novel design element of mesophase formation through the mixing and matching of slightly different donor and acceptor components. Indeed, by varying the length of alkyl chains on the HAT or triimide independently a wide range of mesophases transition temperatures were obtained, although there does not appear to be any predictable trend to altering one or both components. The structure of the mesophases was reported to be columnar hexagonal (Col_{ho}), and it was assumed the there was complete face-centered alternating stacking in the mesophase, even though the crystal structure shows trimers of acceptor-donor-acceptor molecules in the crystalline state.

With the "geometrically matched" acceptors discussed above there remains the desire for better complementary donor-acceptor pairs, with the goal of obtaining structural and predictable control over mesophase properties. While the geometry may be well matched in the HAT:PFTP and HAT:triimide structure (ie. the cores are of comparable size and shape), the overall compatability leaves much to be desiered. The electrostatic complementarity, in the absence of a solvophobic affect, provides the greatest driving force for stacking of the aromatic units. This parameter is far from optimized in the preceding complexes, with electronegative atoms placed in close

proximity (Figure 3.3). In addition, the C_3 symmetry of the components, while promoting a Col_h geometry in the mesophase, prevents independent structural control. This is due to the dependency of packing on the side chains of both components simultaneously in the x and y plane.

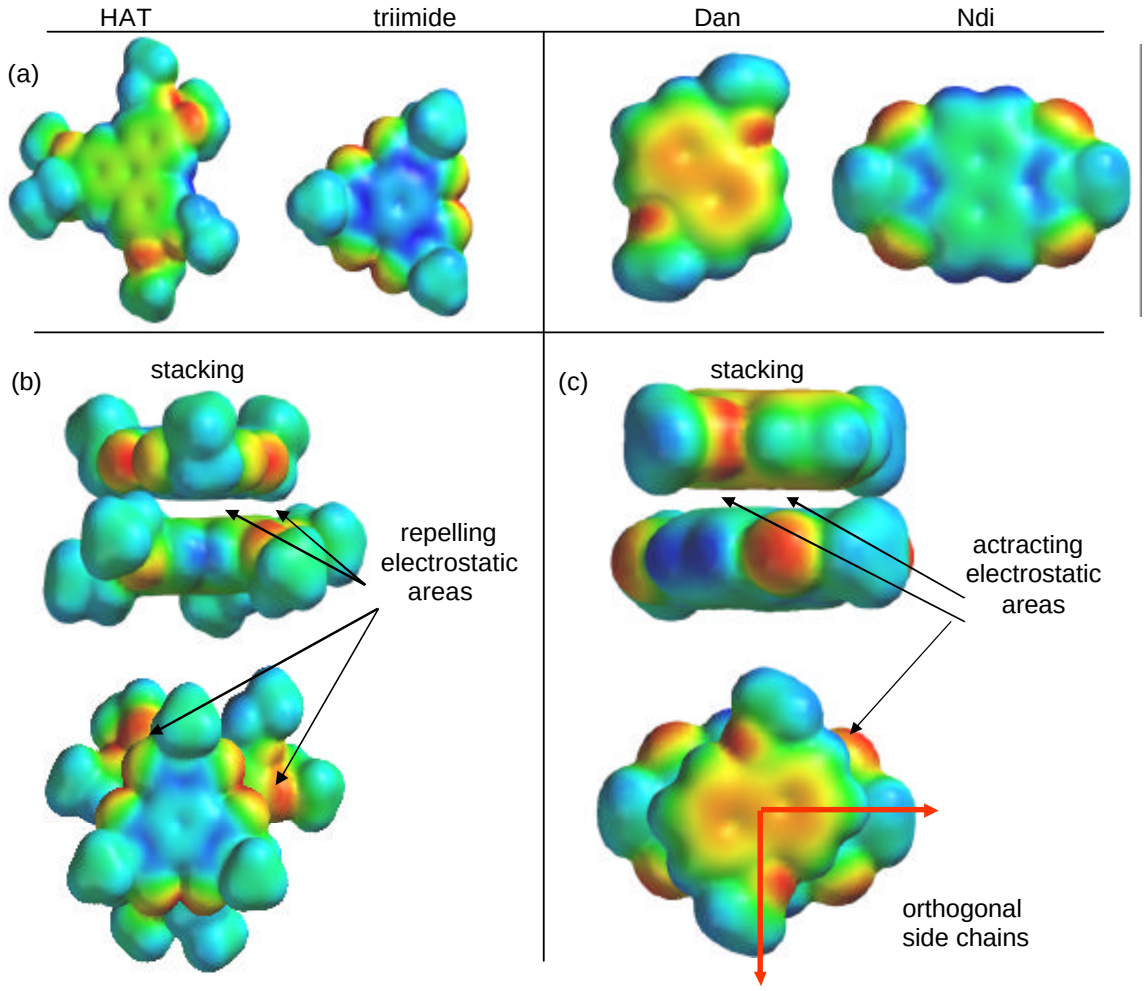

Figure 3.3 (a) Electrostatic potential surface maps the HAT:triimide and Dan:Ndi cores. (b) Stacking geometry from the reported co-crystal structure of HAT:triimide with arrows pointing towards poorly matched electrostatics. (c) Stacking geometry from Dan:Ndi co-crystal with black arrows pointing toward well matched electrostatics, and red arrows highlighting the orthogonal side chain direction.

The Dan and Ndi units of this group have been well characterized and their optimal stacking geometry observed for the folded geometries discussed in chapter 1. Figure 3.3c shows the optimal overlap of the two C_2 symmetric components. It is noteworthy that the side chains of the Ndi are almost orthogonal to those of the Dan. It is predicted that the complementary size, shape, and electrostatic compatibility of the Dan and Ndi aromatic units will lead to the formation of alternating face-centered columnar ordering from an isotropic melt. Unlike the previously discussed C_3 symmetric molecules, the C_2 symmetry and orthogonal optimal stacking of the Dan and Ndi cores may give unprecedented mesophase tunability and property control by mixing and matching various derivatives. The reason being that side chains from the Dan and Ndi units will be locked along orthogonal axes, so columnar packs can be achieved in a controllable fashion. This work could offer new insight into the design and control of liquid crystalline substances, in particular the control and tunability of properties and structure. These concepts could then by applied to other design elements, such as ferromagnetic response columnar phases or electronic materials, in particular as a charge carrying component for photovoltaics (Schmidt-Mende 2001).

3.3 RESULTS

3.3.1 Design and Synthesis of Dan and Ndi components

The Dan and Ndi molecules used in the experiments discussed in this chapter are shown in figure 3.4. The Dan derivatives **3.1**-**3.6** were synthesized by the reaction of

dihydroxynaphthalene (Dhn) with various alkyl bromides. Ndi derivatives **3.7**-**3.11** were synthesized from 1,4,5,8-naphthalenetetracarboxylic dianhydride (Nda) and the corresponding alkyl amines. Compounds **3.6** and **3.11** were synthesized to obtain a Dan/Ndi co-crystal for single crystal x-ray analysis. Purity is of the utmost importance for accurate mesophase determinations, so all compounds were rigorously purified via several column chromatography iterations, recrystalization, and/or sublimation. The location and extent of branching was varied in the alkyl derivitives to evaluate steric and dimensional constraints on face-centered stacking and mesophase formation. Phenyl Ndi derivative **3.12** was designed as a negative control to sterically block the aromatic stacking interaction.

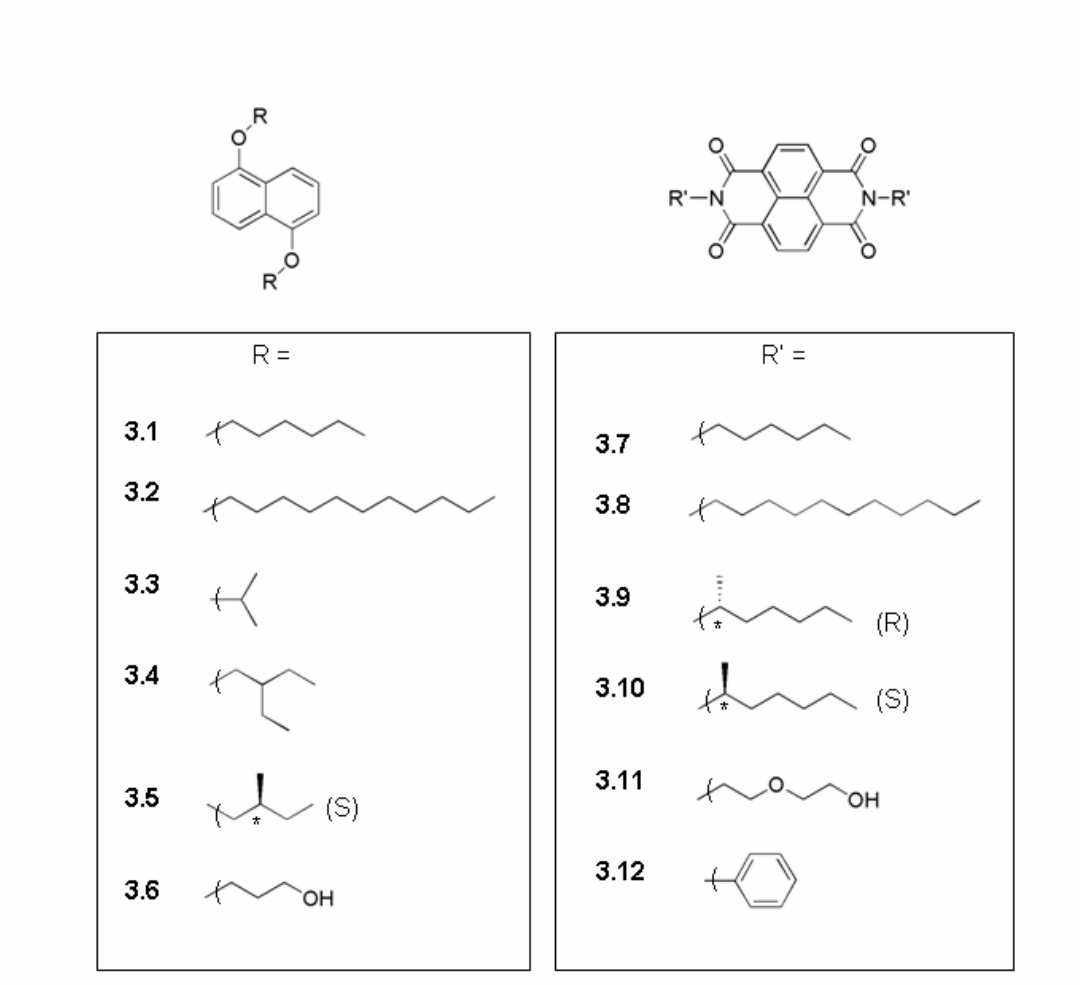

Figure 3.4 Dan and Ndi derivatives

3.3.2 Forming Dan/Ndi Mixtures

The mixtures of Dan and Ndi components with the desired molar equivalents were weighed and then crushed together in a ½ dram vial. The solid mixture was then heated to melting and stirred, the mixture allowed to cool, and then the process repeated several times. Upon close inspection of the initial melting, the crushed crystals of the Dan derivatives in general melted first into a liquid that then appeared to dissolve the Ndi

component. During the dissolution of the Ndi derivative, there was usually a rapid change in color from off-white or light yellow to a deep red characteristic of the Dan-Ndi charge transfer (CT) band (Figure 3.5). The one exception includes mixtures with Ndi **3.12** in which no CT band is ever observed upon mixing and heating with a Dan component. Subsequent meltings exhibited smooth phase changes with a persistent dark red color with the notable exception of mixtures involving Dan **3.3** which turns red upon heating, but back to yellow on cooling.

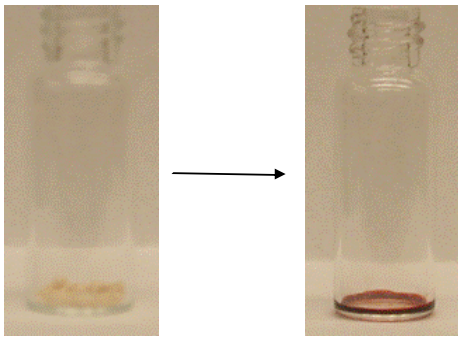

Figure 3.5 Dramatic color change upon heating a mixture

3.3.3 Differential Scanning Calorimetry

Differential scanning calorimetry (DSC) was used to characterize the phase transitions of the individual Dan (compounds **3.1**-**3.5**) and Ndi (compounds **3.7**-**3.10**) derivatives and their mixtures. The phase transition temperatures and enthalpies measured upon cooling are reported in table 3.1. All values are reported after several iterations, when a reproducible curve had been confirmed to ensure equilibrium.

3.3.3.1 Individual Naphthyl Components

Upon heating and cooling, all Dan derivatives undergo a single transition to the isotropic phase. Two of the pure Ndi derivatives (**3.9** and **3.10**) also undergo a single transition to an isotropic phase. Ndi derivatives with the longest unbranched alkyl chains, **3.7** and **3.8**, exhibit a mesophase over modest temperature ranges (20-30°C range). Compound **3.12** exhibited no phase transition up to 250°C.

3.3.3.2 1:1 Dan:Ndi mixtures

The 1:1 mixtures of all Dan:Ndi combinations for which evaporation of the Dan component was not a problem produced at least two transitions, indicating mesophase formation over a sometimes relatively large temperature range (i.e. **3.5**:**3.9**). Figure 3. shows representative DSC data measured for compounds **3.2**, **3.8**, and a 1:1 molar mixture of the two cooling at 5°C/min. The mixture exhibits two phase transitions, one of lower energy at 135°C, and one at 70°C. Closer inspection of the phase transition at 135°C reveals several overlapping small peaks. 1:1 mixtures of **3.2** with **3.9** and **3.10** exhibited transition enthalpies indicative of a liquid crystal phase along with a third phase transition, the nature of which is not clear at this time. The phase transitions of many Dan:Ndi mixtures follow an interesting trend in that the clearing point transition is generally similar to the melting point of the Ndi component (or the clearing points in the cases of Ndi **3.7** and **3.8**), while the crystallization temperature of the mixture is generally very similar to the Dan component melting points. When Ndi **3.12** was mixed with the Dan components they behaived identically to their independent experiments, exhibiting no interaction with **3.12**.

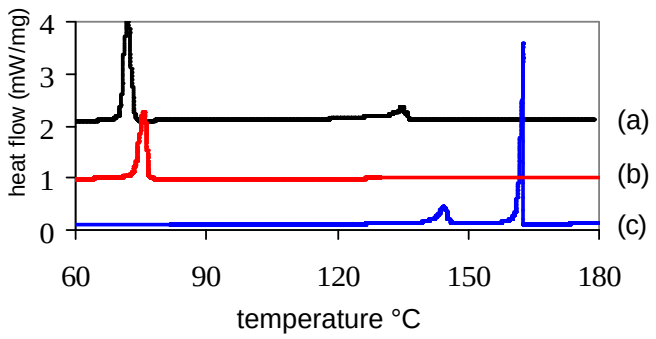

Figure 3.5 DSC upon cooling at 5°C/min of (a) Dan:Ndi mixture **3.2**:**3.8**, (b) Dan **3.2**, (c) Ndi **3.8**.

Table 3.1[a]

	Ndi →	**3.7**	**3.8**	**3.9**	**3.10**
Dan ↓		204° → 150° 92.2 61.9	162° → 144° 72.7 19.1	159° 134.6	159° 134.6
3.1	86° 460.8	146° → 78° 6.1 54.5	1a evaporated	1a evaporated	
3.2	75° 175.3	143° → 68° 5.4 101.7	134° → 71° 21.4 60.0	127° → 96° → 72° 2.5 22.5 32.4	127° → 96° → 72° 2.5 22.5 32.4
3.3	101° 452.7	1c evaporated	140° → 79° 4.1 16.2	129° → 81° 11.3 100.3	129° → 81° 11.3 100.3
3.4	31° 212.1	1d evaporated	136° → 26° 12.5 18.7	123° → 27° 15.3 38.7	123° → 27° 15.3 38.7
3.5	45° 221.6	1e evaporated	131° → 49° 10.7 39.9	115° → 17° 10.6 37.2	125° → 38° 6.8 58.1

[a]Temperatures (°C) and enthalpies (kJ/mol) for phase transitions upon cooling from the isotropic phase to the mesophase (left), and from the mesophase to the crystalline phase (right) determined by DSC (5 °C/min).

3.3.3.2.1 Diastereomeric Mixtures

The transition temperatures of Ndi enantiomers **3.9** and **3.10** with chiral derivative Dan **3.5** are of particular interest. While **3.9** and **3.10** have identical phase behavior individually and when mixed with other non-chiral Dan derivatives, the **3.5**:**3.9** mixture has phase transitions that are ~20°C higher than those of the **3.5**:**3.10** mixture. In other words, the diastereomeric relationship of the side chains has an affect on both the crystallization and clearing temperatures. Further, combining a racemic mixture of Ndi **3.9** and **3.10** with Dan **3.5** in a ½:½:1 ratio results in no mesophase transition at all, only an isotropic to crystalline phase transition upon cooling at 25°C.

3.3.3.2.2 Two Different Dan Units

Mixing two Dan components, **3.3** and **3.4**, with Ndi **3.9** in a 1:1:2 ratio resulted in three phase transitions, shown in figure 3.6a. The clearing point is consistent with other 1:1 mixtures involving Ndi 2c. The middle temperature transition is 15°C lower than the crystallization transition of 1:1 **3.3**:**3.9**, and the lower temperature transition is correspondingly 15°C higher in temperature than the crystallization temperature of a 1:1 mixture of **3.4**:**3.9**. Similar results were seen with a 1:1:2 mixture of **3.2**:**3.4**:**3.9**.

3.3.3.2.3 Titrations

Both the clearing and crystallization points were monitored as titrations were carried out with mixtures of **3.2**:**3.8** and **3.3**:**3.9**. For both titrations, a relatively slow

linear increase was seen in the clearing point with increasing concentration of the Ndi component until the mixture was 33% in the Ndi derivative. The titration curve then took on a much steeper increase in clearing point until 66% in Ndi was reached, after which there was a return to the slower linear increase. For the crystallization point, only a relatively slow decrease in temperature with increasing amounts of the Ndi derivative was seen. Data are shown for the molar titration of **3.2** with **3.8** (Figure 3.6b). Note the two phase transition at molar ratios of 66% in **3.9** and higher, no doubt due to the fact that this Ndi derivative has its own mesophase in the pure state.

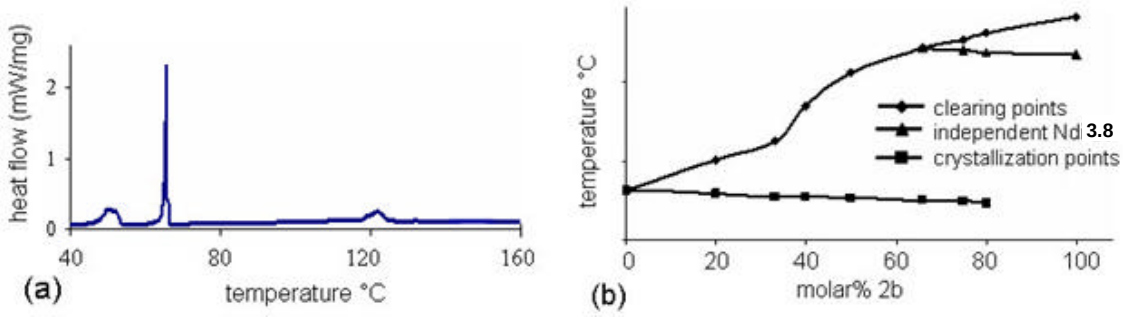

Figure 3.6 (a) Two Dan, **3.3**, **3.4**, and one Ndi, **3.9**, in a 1:1:2 ratio. (b) Titration of **3.2** with **3.8**.

3.3.6 Thermochromic Behavior

Most mixtures of Dan and Ndi derivitives exhibit the characteristic deep red color of the Dan:Ndi CT absorbance throughout the isotropic liquid phase, the mesophase, and the crystalline solid phase during cooling. Figure 3.7a-c shows representative colors of all three phases, in this case for the 1:1 **3.2**:**3.8** mixture. A noted exception to this constant color is observed in mixtures involving Dan derivative **3.3**. In these cases, the isotropic

phase and mesophase exhibited the characteristic deep red color of the Dan:Ndi CT absorbance. However, upon cooling to the crystallization point, a color change to a light yellow was observed. This change is particularly prominent in the 1:1 mixture of **3.3** with **3.9** where the mixture changes color from a deep red to yellow instantly upon reaching the crystallization point, shown in figure 3.7d-f. This dramatic color change is not accompanied by any significant distortions of the texture at low magnification (i.e. 10X), but inspection under greater magnification (100X) revealed that the transition to the yellow color was accompanied by extensive small fractures and blurring of once sharp boundaries.

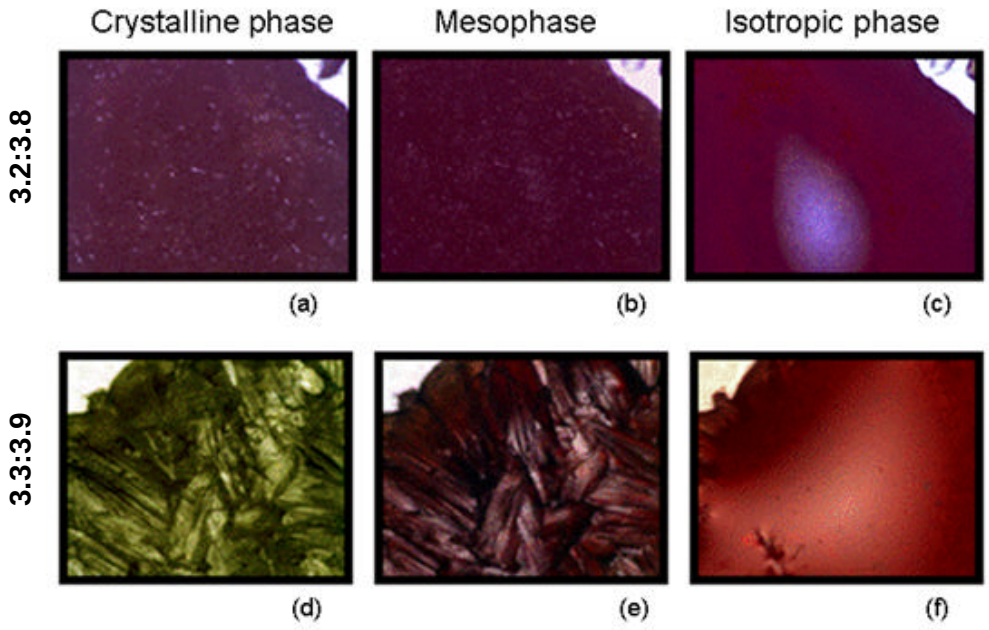

Figure 3.7 Color of bulk samples of 1:1 mixtures. (a) deep red **3.2**:**3.8** crystalline phase (60°C). (b) deep red **3.2**:**3.8** mesophase (110°C). (c) deep red **3.2**:**3.8** liquid phase (160°C). (d) light yellow **3.3**:**3.9** crystalline phase (60°C). (e) deep red **3.3**:**3.9** mesophase (110°C). (f) deep red **3.3**:**3.9** liquid phase (160°C).

3.3.4 Polarized Optical Microscopy

The bulk optical characteristics of the Dan:Ndi mixtures were observed by melting small amounts of sample between glass cover slips, then cooling slowly (5°C/min) under a polarizing microscope. Cooling from the isotropic liquid, dendritic or sheet-like domains were seen to grow over about a 10°C temperature range for all mixtures. Onset of domain growth occurred at a temperature corresponding to the clearing point measured by DSC. Polarizing microscope images showing textures of the different mixtures in their respective mesophase temperature regions are shown in figure 3.8. Complexes involving chiral Ndi **3.9** (or **3.10**) exhibit long, thin, sheet-like patterns of various size and order with all of the Dan derivatives, (panels a-c in Figure 3.8) characteristic of a columnar molecular order. Complexes involving Ndi **3.8** in general gave a mosaic of small or elongated rectangles also representative of a columnar mesophase (panels d-f in Figure 3.8).

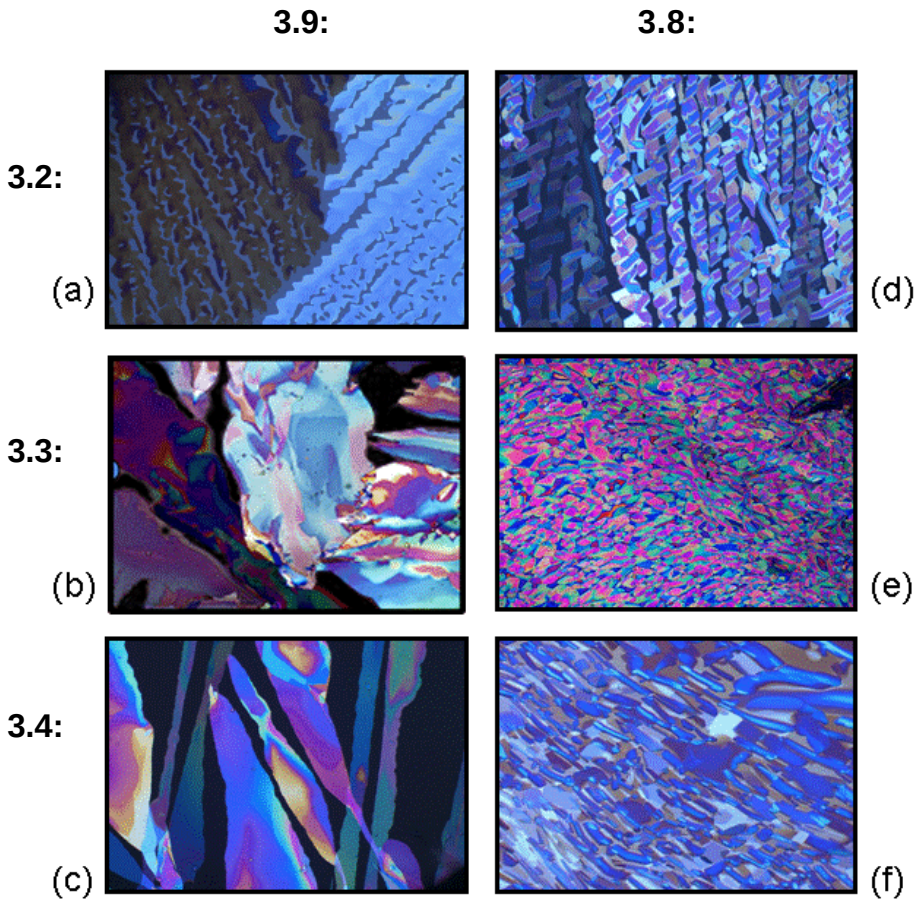

Figure 3.8 Optical texture of 1:1 mixtures at 110°C of (a) **3.2**:**3.9**, (b) **3.3**:**3.9**, (c)**3.4**:**3.9**, (d) **3.2**:**3.8**, (e) **3.3**:**3.8**, (f) **3.5**:**3.8**.

3.3.5 Shear Tests

Shearing pressure was applied to the slides in the mesophase temperature region by pushing the cover slips in opposite directions. The cover slips slid past each other with little resistance. The domains shift relative to each other, but otherwise remain

unchanged. Upon reaching the crystallization point the cover slips could no longer move relative to each other with applied pressure.

3.3.8 Single Crystal X-ray Crystallography

Single crystal data was obtained for the homo-crystals of compounds **3.3**, **3.4**, and **3.9** (Figure 3.9a-c). Compounds **3.3** and **3.4** were crystallized via gradual evaporation of a 70:30 CH_2Cl_2:hexanes solution, and **3.9** from evaporation of a CH_2Cl_2 solution. In these homo-crystals the electron rich Dan molecules **3.3** and **3.4** adopt a herringbone structure, the stacking directed by edge-face interactions. With the electron poor Ndi molecule **3.9** there is an offset face-to-face packing, similar to crystal structures previously reported by this group (Cubberly 2000). Both of these solid state arrangements are as expected based on modeling of the electrostatic considerations.

A co-crystal of suitable quality for single crystal determination could not be grown from solution using any combination of Dan:Ndi derivatives with hydrocarbon side chains. Likewise, when slowly cooled from melts, no suitable crystal could be isolated. However, using compounds **3.6** and **3.11** with slightly hydrophilic side chains a single crystal of suitable quality for analysis was grown from vapor absorbtion of water into a 30% DMF:water mixture. The resulting structure reveals complete face-face centered stacking in columns of alternating Dan and Ndi units in a monoclinic cell (Figure 3.9d-f). This result complements the previously reported co-crystal structure from this lab (Lokey 1995).

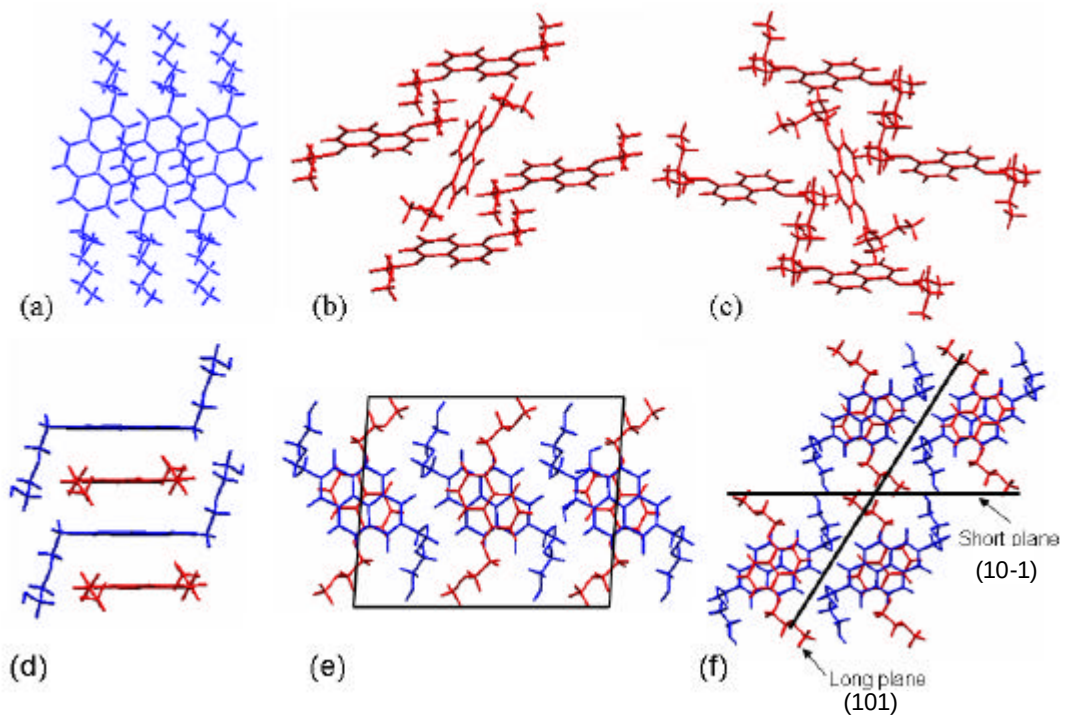

Figure 3.9 X-ray single crystal structure of (a) **3.9**, (b) **3.3**, (c) **3.4**, (d) **3.6**:**3.11** co-crystal, alternating face-centered columns (e) **3.6**:**3.11** co-crystal, oblique monoclinic cell (f) **3.6**:**3.11** co-crystal, planes between columns and their Miller indices

3.3.7 UV-Vis Spectroscopy

The Dan:Ndi CT band of the mixtures was further investigated using UV-Vis spectroscopy in quantitative comparisons of the liquid, meso, and crystalline phase of the mixtures. Data was acquired by sandwiching pre-melted samples of the 1:1 mixtures between glass cover slips. The samples were then subjected to several melting and cooling cycles while taking spectra continuously and monitoring temperature with a thermocouple. Representative spectra from the isotropic liquid phase, mesophase, and

crystalline phase of mixtures **3.2**:**3.8** and **3.3**:**3.9** are shown in Figure 3.10a-f. For comparison purposes, UV-Vis spectra were taken of a 1:1 mixture of the slightly hydrophilic **3.6**:**3.11** in both the isotropic and crystalline phases (Figure 3.10g, h), since the co-crystal structure had been determined.

The absorbance of the CT band at the λ_{max} was compared to the Ndi absorbance in the various phases. In all cases, the 1:1 Dan:Ndi isotropic phases exhibited Ndi:CT absorbance ratio close to 3:1, regardless of the side chains on either component. Upon cooling to the mesophase, these ratios shifted to an average of 1.7:1 in all cases, again regardless of the particular mesogens involved. Upon crystallization, the Ndi:CT absorption ratios did not change significantly, remaining at about 1.7:1. These measurements are particularly significant in that the **3.6**:**3.11** mixture is essentially identical in the CT band ratio and single crystal X-ray analysis has confirmed essentially complete alternating Ndi-Dan, face-centered stacking in this crystalline phase. The noted exception is mixtures including Dan **3.3** in which, as illustrated by the **3.3**:**3.9** mixture in figure 3.10d, evidence of the CT band disappears completely upon crystallization consistent with the instantaneous red to yellow color change previously noted.

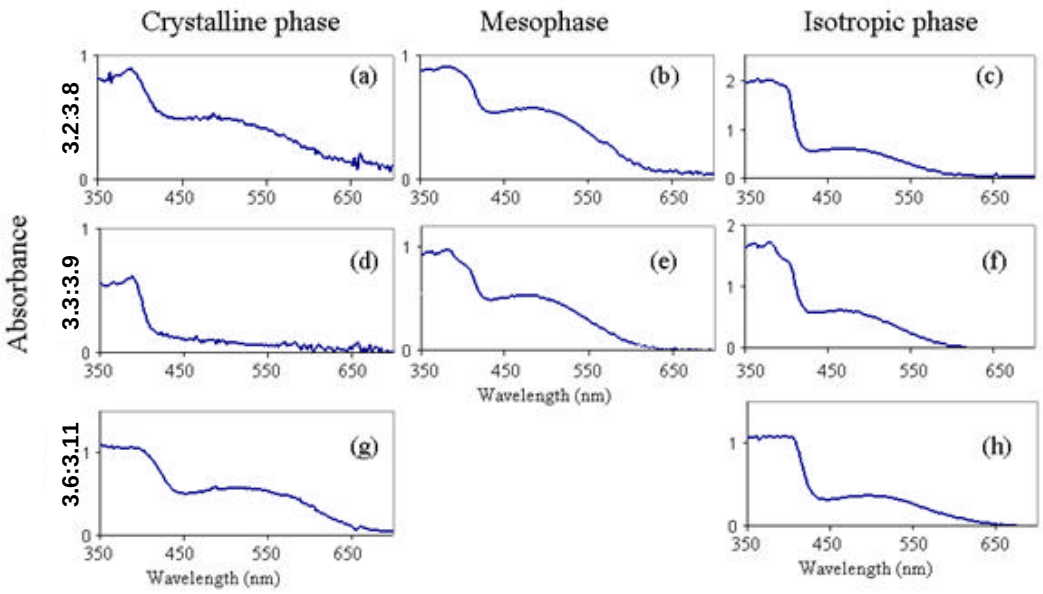

Figure 3.10 UV-Vis Spectra comparing Ndi adsorbtion (380nm) to CT band adsorbtion (475nm) of 1:1 mixtures. (a) (a) **3.2**:**3.8** crystalline phase (60°C). (b) **3.2**:**3.8** mesophase (110°C). (c) **3.2**:**3.8** liquid phase (160°C). (d) **3.3**:**3.9** crystalline phase (60°C). (e) **3.3**:**3.9** mesophase (110°C). (f) **3.3**:**3.9** liquid phase (160°C). (g) **3.6**:**3.11** crystalline phase (60°C). (h) **3.6**:**3.11** liquid phase (180°C).

3.3.9 X-Ray Powder Diffraction

X-ray powder diffraction studies were carried out on compounds **3.3**, **3.4**, **3.9**, and the **3.6**:**3.11** co-crystal for which the structure was known from single crystal data. In addition, x-ray powder diffraction was used to investigate the mesophase and crystalline phases for two different mixtures (**3.3**:**3.9** and **3.4**:**3.9**) for which the single crystal data are not available (Figure 3.11). For the **3.6**:**3.11** sample, the two most intense peaks in the X-ray powder pattern, (10-1) and (101), correspond to the planes between columns.

Mapping these reflections to the single crystal structure, they are seen to represent the short plane (smaller distance between side chains within a column) and the long plane (greater distance between side chains within a column) as shown in Figure 7f. Importantly, the short plane corresponds closely with the (001) of Ndi **3.11**, which is essentially the length of the Ndi molecule, while the long plane similarly corresponds to the length of Dan **3.6**. This result implies that the spacing between intercolumn planes (10-1 and 101) of the co-crystal is indeed dictated by the lengths of the Ndi and Dan units, respectively.

The X-ray powder pattern of the mesophases of 1:1 mixtures of **3.3**:**3.9** and **3.4**:**3.9** (Figure 3.11a,b) both show at least two-dimensional order. Additionally, the mesophase of the **3.4**:**3.9** mixture produced sharp reflections at wide angles possibly indicating three-dimensional ordering. Strong 100 reflections are seen for both mesophases that are very similar to the 200 reflection seen in the x-ray powder pattern of the Ndi component **3.9** (Figure 3.11g), corresponding to essentially the length of the Ndi molecule. In addition, less intense 010 reflections are seen in both mesophases corresponding to the 100 reflections of the component Dan molecules **3.3** and **3.4**, respectively (Figure 3.11e,f), which in turn reflect the length of the Dan component. Beyond these two prominent reflections, neither mesophase contains the remaining diffraction patterns of the individual components, and therefore do not contain crystalline domains of the individual mesogens.

In the **3.4**:**3.9** crystalline phase (Figure 3.11d), the low angle 100 and 010 reflections seen in the mesophase remain. Again, these correspond to essentially the lengths of the Ndi and Dan components, respectively. However, the remaining reflections

measured for the **3.4**:**3.9** crystalline phase are distinct from either component indicating the new crystalline form is unique from its parts.

For the **3.3**:**3.9** crystalline phase (Figure 3.11c), the positions of reflections closely resemble the sum of the two components, the only independent peak being the broad one at ~ $2q = 6$. In particular, the reflections corresponding to the Ndi **3.9** mesogen are all present, albeit less intense and broader in the mixture. The exception is the reflection corresponding to the 200 reflection of **3.9**, which is of similar intensity and sharpness in the mixture. Reflections in the mixture corresponding to the Dan 1c pattern are present and sharp, although the 100 reflection is significantly higher in relative intensity in the mixture. Recall that crystalline **3.3**:**3.9** is yellow with no charge transfer band even though the mesophase of the same mixture is deep red.

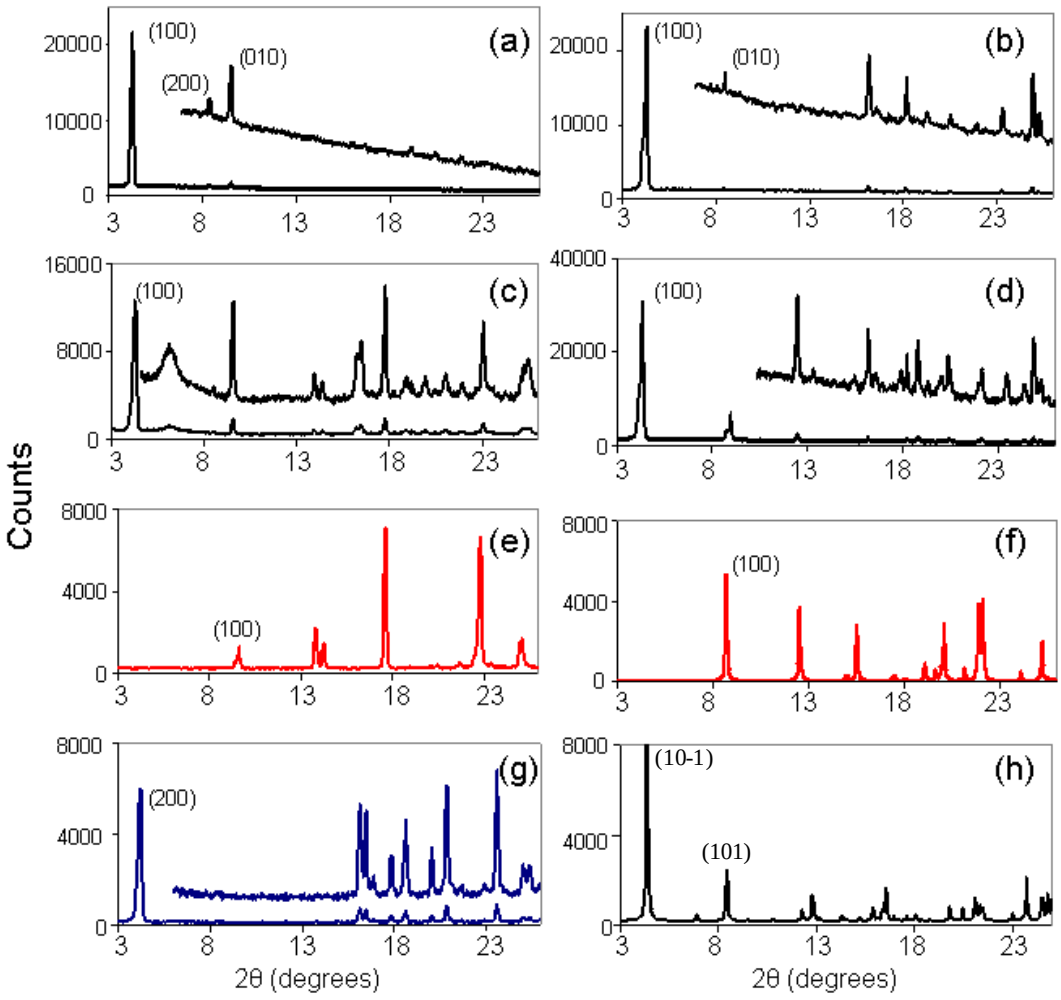

Figure 3.11 X-ray Powder Diffraction data including expansions over the same degree range (top spectra) where informative for (a) **3.3**:**3.9** mesophase (110°C) (b) **3.4**:**3.9** mesophase (100°C) (c) **3.3**:**3.9** crystalline phase (35°C) (d) **3.4**:**3.9** crystalline phase (27°C) (e) **3.3** crystalline phase (35°C) (f) **3.4** crystalline phase (27°C) (g) **3.9** crystalline phase (35°C) (h) **3.6**:**3.11** crystalline phase (27°C).

3.3.10 Preliminary Electrical Properties

Initial measurements were preformed on thin films of Dan:Ndi mixtures to determine if any current could traverse through the material. A sample of the **3.3**:**3.9** mixture was melted between two overlapping pieces of indium tin oxide (ITO) covered glass, separated by thin spacers of 5µm, and attached to a multimeter as shown in figure 3.12. Upon melting to a liquid, the multimeter gave reading up to 65 mV. The reading decreased upon the visible transformation to the mesophase to average at about 16 mV. Immediately upon crystallization, no voltage reading was observed. Similar tests with compounds **3.3** and **3.9** individually, as well as an empty cell, showed no reading upon heating. These results were reproduced over several heating and cooling cycles, and also with a mixture of compounds **3.2** and **3.8**.

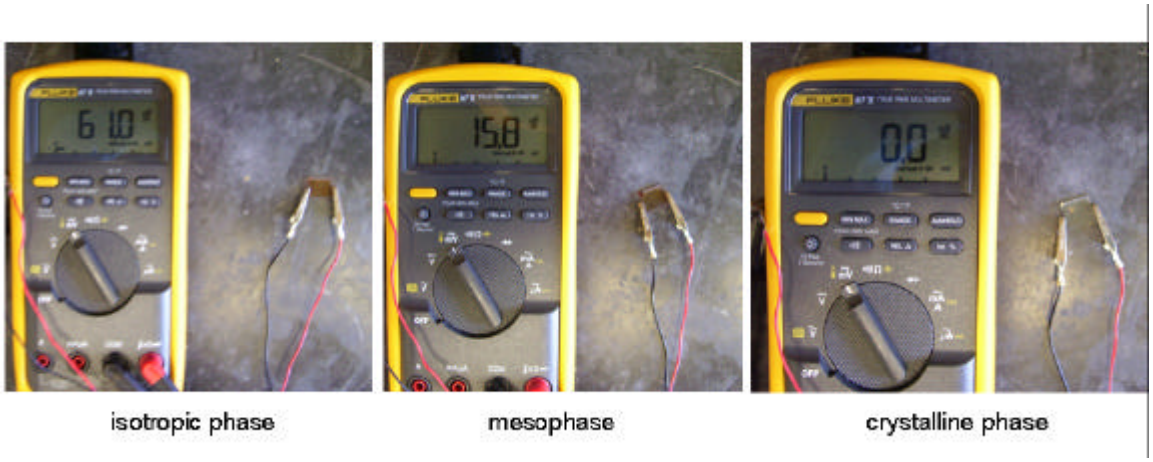

Figure 3.12 Pictures showing that there is some qualitative electron flow in the Dan:Ndi liquid and mesophase.

3.4 DISCUSSION

3.4.1 Dan:Ndi Mesophase

The majority of the DSC data for the 1:1 Dan:Ndi mixtures indicates two phase transitions. Analysis of the UV-Vis and x-ray powder diffraction data make it clear that the DSC peaks represent a uniform phase transition and not simply two independent transitions, one for each component. This powder diffraction data along with the shearing tests and optical microscopy are evidence that these transitions involve a mesophase, and are not crystal-crystal transitions.

3.4.1.1 Not the Sum of the Parts

The deep red color seen upon melting of the Dan:Ndi mixtures, interpreted as an aromatic donor-acceptor CT band, is qualitative evidence that the Dan and Ndi molecules are stacking in an alternating, face-centered geometry. The UV-Vis spectrum of a 1:1 mixture of **3.6**:**3.11** (figure 3.10h), for which single crystal X-ray data reveals a co-crystal structure consisting of alternating Dan:Ndi face-centered stacks (figure 3.9d), showed an Ndi:CT? absorbance ratio of 1.7:1 in the crystalline phase. We therefore associate complete face-centered stacking of an Dan:Ndi mixture in the crystalline phase as having this 1.7:1 absorbance ratio. This value is identical to the value observed for all of the Dan:Ndi complexes investigated below the first phase transition and almost all (the exception being **3.3**:**3.9**) below the second. It is therefore impossible that the Ndi component is crystallizing out of the melt by itself at the higher temperature phase

transition, followed be the Dan component, as they must be together in a face-centered geometry similar to that of the **3.6**:**3.11** co-crystal.

The powder x-ray diffraction of both the **3.3**:**3.9** and **3.4**:**3.9** mixtures below the first observed phase transition each have one peak corresponding to the Ndi component, but no others. This is also true with respect to Dan component. A spectrum identical to one of the pure components is not present as would be necessary if a single independent crystallization event was taking place. This is further evidence that the transitions are not simply the crystallization of one component followed by the other, but rather are uniform and unique bulk transitions involving both the Dan and Ndi components.

3.4.1.2 True Mesophase

The simple shear tests preformed on the prepared mixtures are direct evidence that the phase transitions observed are not transitions between two crystalline states. The prepared coverslips with the mixtures in between were able to slide across each other with little resistance, while largely maintaining the optical texture of the sample, indicating that these mixtures are not crystalline between the phase transition temperatures. Below the second transition, the coverslips could no longer move relative to one another, as expected for crystallization from the mesophase.

The small amount of order indicated by the powder diffraction data for the Dan/Ndi mixtures in the temperature region between the clearing and crystallization points is also indicative of a true mesophase formation and not crystal-crystal transitions. The lack of peaks in the fingerprint region of the powder diffraction spectra indicates that

there is no rigid three-dimensional order, i.e. the samples are not crystalline at that temperature.

3.4.2 Mesophase Structure

Significantly, the Ndi:CT absorbance ratio of 1.7:1 that is diagnostic of complete face-centered stacking as seen in the **3.6:3.11** co-crystal structure is observed in the mesophases of all the 1:1 Dan:Ndi mixtures. It is therefore reasonable to propose that the structure of these mesophases includes at least moderately sized domains of columnar, alternating face-centered stacked Dan and Ndi molecules. Further, it appears that the mesophase to crystalline transition for most of the mixtures does not involve a significant reorganization of columnar stacked aromatic donor and acceptor cores, the exception being mixtures with Dan **3.3** in which the CT band disapears.

As noted above, two of the major peaks in the powder diffraction pattern of mixture **3.6**:**3.11** correspond to the lengths of the component Dan and Ndi molecules in their independent single crystal structure. The diffraction pattern observed from the mesophase of mixtures **3.3**:**3.9** and **3.4**:**3.9** both have major peaks that correspond to the single crystal lengths of their component molecules as well. It is therefore reasonable to create a model of the two mesophases in which there are two planes between the face-centered Dan/Ndi columns, a long plane and a short plane, whose distances are dictated by the single crystal length of the Dan and Ndi component respectively, as modeled and predicted by the **3.6**:**3.11** co-crystal. According to this interpretation, both complexes show the short plane reflection corresponding to the length of the Ndi **3.9**, which has a d

spacing calculated to be 20.5 Å. The calculated d spacing for the long plane of complex **3.3**:**3.9** (with isopropyl side chains on the Dan) is 9.1 Å, corresponding to the length of Dan **3.3**, while the longer side chains on the Dan in the **3.4**:**3.9** complex give a somewhat longer distance of 10.5 Å, corresponding to the length of Dan **3.4**. Figure 3.13 illustrates packing structures for the two mixtures that are consistent with all the spectroscopic data, the obtained co-crystal structure and the conclusions drawn here.

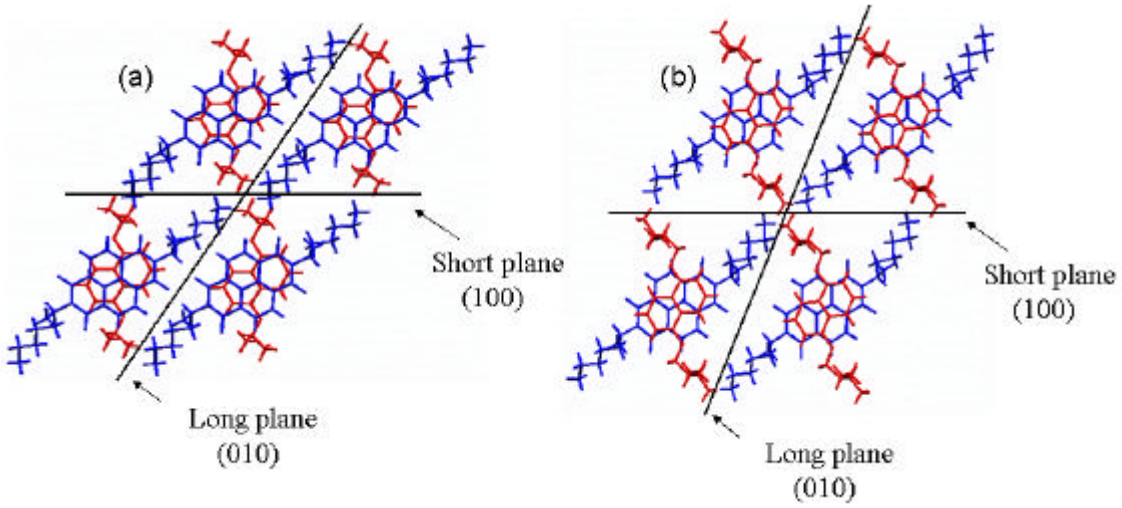

Figure 3.13 Computer models of the proposed oblique rectangular packing for the mesophase of (a) **3.3**:**3.9**, (b) **3.4**:**3.9** (Hyperchem, Hypercube, Inc.).

This structural analysis also indicates that the mesophase of Dan:Ndi mixtures should be classified as columnar oblique rectangular (Col_{Ob}). This conclusion is supported by the optical textures (See Figure 4d-f) in which rectangular domains are observed (Kouwer 2002). This is a rather rare form of packing for columnar phases, due mostly to the higher symmetry of most studied discotic mesogens. The complementary C_2 symetry of the Dan and Ndi association allows for this rectangular packing.

The implications of this are significant in the context of self-assembly. The general ability of directed aromatic-aromatic interactions to assemble into face-to-face columnar stacks is expanded by the directionality of the Dan:Ndi stacking interaction. As proposed in the background of this chapter (Figure 3.3c) the orthogonal side chain direction observed in the crystal structure is present in the mesophase, and allows for the Dan and Ndi side chains to affect predictably the two-dimensional structure of the one dimensional aromatic stack, illustrated in figure 3.14.

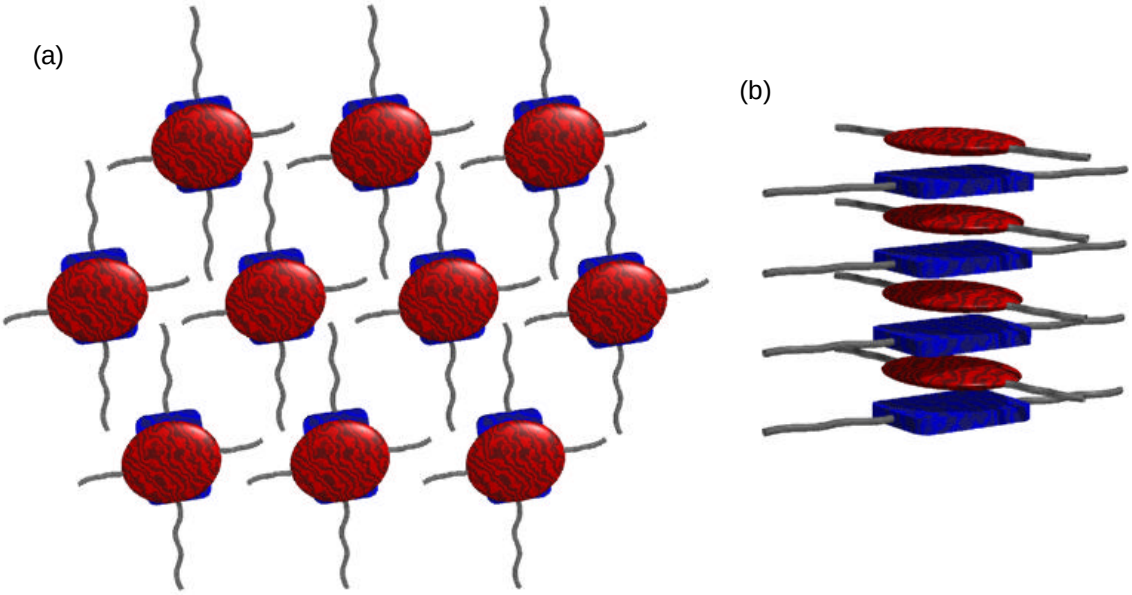

Figure 3.14 (a) Representation of the mesogen packing directed by orthogonal side chains. (b) Representation of a face-centered aromatic stack.

3.4.3 Steric Inhibition of Face-centered Stacking

Upon melting of any Dan derivative with Ndi **3.12** no color change or interaction of any kind was observed. The two possibilities for a lack of interaction are (1) that the

phenyl side chains of Ndi **3.12** change the electronic surface of the Ndi and reduce the aromatic donor-acceptor driving force, and (2) the phenyl groups prevent stacking due to steric interactions. Models of **3.12** show that there is no or little electronic affect to having the phenyl side chains (Figure 3.15a), but that the conformation of the phenyl groups is perpendicular to the Ndi face, and should interfere sterically with Dan association (figure 3.15b).

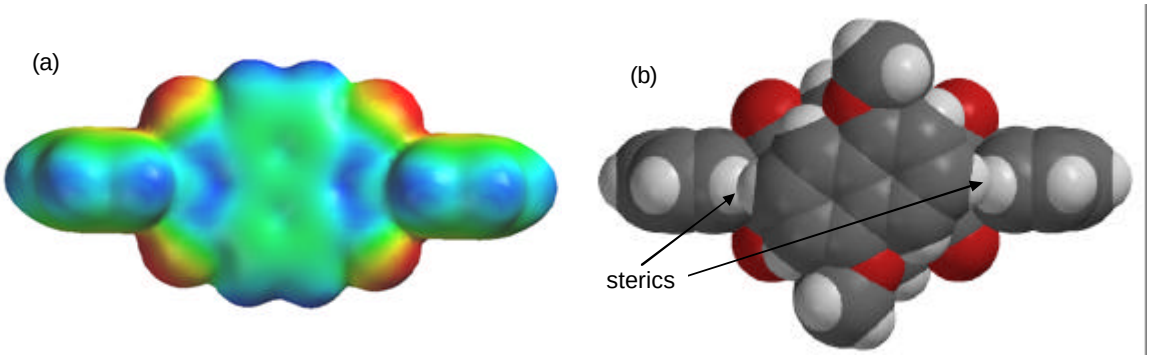

Figure 3.15 (a) Electrostatic surface potential of compound **3.12**. Shows no observable difference from other Ndi compounds. (b) Spacefilling model of **3.12** with Dan overlayed. The phenyl groups crowd above and below the plane of the Ndi preventing Dan association.

3.4.4 Thermochromic Behavior of Mixtures Containing Dan 3.3

The fact that all the alkyl chain complexes investigated in this study exhibit the same deep red color in the mesophase and isotropic phase suggest that the side chains investigated do not affect the aromatic stacking arrangement in these less ordered phases. However, the mixtures involving Dan **3.3**, with various Ndi derivates, in particular **3.9** all show striking thermochromic behavior in which the deep red mesophase rapidly turns to a light yellow color upon crystallization. It appears that the packing of the side chains can make a difference in the structure of the crystalline phase. Steric interactions

involving the Dan **3.3** isopropyl chains apparently force the aromatic faces apart and thereby disrupt the CT absorbance upon freezing into a crystalline phase (yellow color), although these interactions are not significant enough to prevent face-centered interactions in the isotropic or mesophases (deep red color) as was the case with the phenyl side chains of Ndi **3.12**.

The x-ray powder diffraction data for the **3.3**:**3.9** mixture are consistent with crystallization-induced phase separation. In the crystalline phase of the **3.3**:**3.9** mixture, reflections corresponding to those seen in the Dan **3.3** homo-crystal appear as sharp peaks, and reflections corresponding to those seen in the Ndi **3.9** homo-crystal appear as well, although they are of low intensity and diffuse. These data are consistent with the Dan molecules forcing themselves out of contact with the Ndi molecules in what is likely a sterically induced phase separation. The Dan molecules reorganize and pack with themselves in what appears to be the homo-crystal herringbone arrangement, and the Ndi molecules are forced to reorganize and pack with themselves as well. This leads to many structural defects seen at high magnification. The only new peak (not the sum of the two component spectra) in the **3.3**:**3.9** crystal phase is a very broad one at $2q = 6.2°$ that could be due to the new boundaries introduced between phase separated domains of Dan and Ndi molecules.

Note that the steric effect proposed to be responsible for the thermochromic behavior seen with Dan **3.3** is highly sensitive to structure. Moving the branch one methylene unit farther from the aromatic ring, as in derivatives **3.4** or **3.5**, eliminates the thermochromic behavior.

3.4.5 Tuning Phase Transition Temperatures

As seen in Table 3.1, the relative clearing points of the various donor-acceptor mixtures track with the relative melting/clearing points of the Ndi component independent of the Dan partner. For example, in 1:1 mixtures containing Dan **3.2** as the donor, the clearing points range from 143°C with **3.7** to 127°C with enantiomers **3.9** and **3.10**, with **3.8** coming inbetween. This relative order coincides with the relative melting/clearing points of the independent Ndi components. The variation in the crystallization point for all of these mixtures is essentially constant, varing only by 4°C, illustrating an ability to alter the clearing point of a mesophase predictably, and independently, from the crystallization temperature.

Along the same lines, the relative crystallization points of the 1:1 mixtures track with the melting points of the Dan derivatives. For example, with Ndi **3.8**, the crystallization points range from 79°C with **3.3** to 26°C with **3.4**, with the other derivatives coming inbetween; again in the same relative order as their individual melting points. In the case of the crystallization points, the values for the mixtures are also similar (within ~5° C) in absolute magnitude to the Dan component melting points. The exception is the derivative 1c, in which the crystallization points of the 1:1 mixtures are around 20 °C lower than the melting point of 1c, presumably a phenomenon that is related to the phase separating behavior seen in these mixtures upon crystallization. When comparing the clearing points for these complexes, the temperature is almost constant between mixtures, varying only by 5°C. Similar to the ability to independently adjust the clearing point of the Dan:Ndi mixtures, the crystallization point can be altered without affecting the clearing point.

A straightforward interpretation of these trends is that the 1:1 Dan:Ndi mixture clearing points track in a relative way with restriction of motion of the Ndi side chains, and the crystallization points track with restriction of motion of the Dan side chain component. In other words, there is more order associated with Ndi long axes because the Ndi side chains have more restricted motion in the mesophase, and less order along the Dan long axes because the Dan residues maintain greater freedom of motion in the mesophase. Consistent with this, the mesophase x-ray powder diffraction data for both the **3.3**:**3.9** and **3.4**:**3.9** mixtures show substantially more order (much more intense relative reflection) corresponding to the short plane, previously ascribed to the long axis of the Ndi component. The ability to independently tune phase transition temperatures based on knowledge of component melting/clearing points and structures is a unique and highly desirable feature of Dan:Ndi mixtures.

3.4.6 Titration Affect of Phase Transition Temperatures

Further temperature tuning of the clearing point was affected by altering the molar ratios of the component mixtures as was exhibited in the titration of **3.3** with **3.8** (Figure 3.6a). While the crystallization temperature remained fairly constant, the clearing point ranged from 95°C at 66% 1b to 140°C at 33% 1b. Presumably, the 66% and 33% values indicate 2:1 and 1:2 stoichiometries, in which each aromatic unit is still interacting with at least one complementary unit, and there is still long range face-centered stacking. At mixtures with more extreme molar compositions (>66% or < 33%), this arrangement is

not possible, and the clearing temperatures of the mixtures change more gradually, taking on more the characteristics of the aromatic unit in highest concentration.

3.4.7 Chiral Side Chains

Phase transition temperatures were further modulated by manipulating the chirality of the side chains. While Ndi enantiomers 2c and 2d behave identically by themselves and with any achiral Dan derivative, the diastereomeric mixtures they create upon mixing with chiral Dan **3.5** produced similar mesophase textures, but their phase transition temperatures differed significantly. In particular, the 1:1 mixture of **3.5**:**3.10** (the *S,S : S,S* diastereomeric complex) displayed clearing and crystallization points of 125°C and 38°C, respectively. The 1:1 mixture of **3.5**:**3.9** (the *S,S : R,R* diastereomeric complex) exhibited clearing and crystallization points of 115°C and 17°C, respectively. These latter two values represent the lowest transition temperatures measured of any Dan:Ndi complex in the present study. Interestingly, using a racemic mixture of **3.9** and **3.10** with **3.5** (in a 1:1:2 ratio) resulted in no mesophase being formed. A single isotropic to crystal phase transition occurs at 25°C, in between the crystallization temperatures of the single diastereomeric mixtures, implying that the crystallization event may be an average of the two. The mixture remains a deep red in both phases indicating face-centered Dan:Ndi interactions, yet it appears that any long range order at higher temperature is disrupted by the opposing chirality of the Ndi units, disallowing the existence of a mesophase.

3.4.8 Terniary Mixtures

A potential alternative method of controlling phase transition temperatures is to use more than one Dan mixed with a particular Ndi, for example a 1:1:2 mixture of **3.2**:**3.3**:**3.9**, in hopes of averaging or in some other way affecting the crystallization temperature. However, the result was not a single mesophase with intermediate temperature crystallization points. Instead the mixture exhibited two separate sets of crystallization points (Figure 3a) corresponding roughly to the crystallization temperatures of independent **3.2**:**3.9** and **3.3**:**3.9** mixtures, respectively. The clearing point was that expected for a mixture containing Ndi **3.9**. Similar results were obtained with a 1:1:2 mixture of **3.2**:**3.4**:**3.9**. This result leads to the conclusion that each Dan component interacts independently with the Ndi, creating a mixture that is not homogeneous, but rather a blend of **3.2**:**3.9** and **3.3**:**3.9** domains.

3.4.9 Thoughts on Preliminary Results of Electrical Properties

Measurements made with the multimeter in mV are qualitative and preliminary. However, they are reproducible, and show that electrons are able to traverse the 5μm gap in the Dan:Ndi mixture. The fact that the same results are not observed with either of the two individual components implies that it is the donor-acceptor complex itself that gives the electrical reading, and not an impurity in the sample. It is unclear at this time if the charge carrier mode in through the columnar stacks of complex orbitals, molecular diffusion of a discrete complex, or some combination. The nature of these

complexes may lend to photoconductivity in these materials, and experiments to investigate this should be carried out in the near future (Atwood 1996).

3.5 CONCLUSIONS

Taken together, the results reported in this chapter indicate that a significant amount of predictable control can be exerted over the phase transition temperatures and phase structure of 1:1 Dan:Ndi mixtures. The success of this approach is no doubt related to not only their complementary geometries (both aromatic units are of a similar size) but also the specific electrostatic compatability of their C2 symmetries that facilitates alternating, face-centered stacks with side chains oriented in orthogonal directions. That this orthogonal directionality is apparently maintained in the mesophase is significant, adding further directionality to the Dan:Ndi aromatic donor-acceptor interaction as a design element for supramolecular chemistry. Not only are stacks of face-centered columns assembled, but the relative orientation of the Dan and Ndi units is fixed, allowing the side chains of individual Dan and Ndi units to behave independently. This independent behavior is probably the basis for the predictable behavior of the mesophases corresponding to the Dan and Ndi components, respectively. By "mixing and matching" various derivatives it allows for control of mesophase structure in three dimensions, and control of crystallization and clearing point temperatures independently.

Further, by adjusting the sterics of the side chains next to the rings complexation can be controlled. The inclusion of phenyl groups on the Ndi seems to prevent complexation completely, while isopropyl groups on the Dan unit allows for complexation in the isotropic phase and mesophase, but then prevents crystalline phase

association. The dramatic color change which results from the latter effect could have applications in sensing technology or as a supramolecular switch. The incorporation of chirality two atoms away from the Dan and Ndi aromatic cores produces the interesting observation that different diasteriomeric mixtures have different mesophase behavior, and mixtures racemic in Ndi have drastically different behavior. Further investigations into the affects of chirality on donor-acceptor complex orientation may yield additional design elements and applications. This work establishes the Dan:Ndi aromatic interaction as a new tool for supramolecular phase chemistry. The three-dimensional directionality (i.e. orthogonal side chain stacking) of the interaction offers unprecedented and predictable control over mesophase properties.

3.6 EXPERIMENTAL SECTION

General methods. All starting materials were obtained from Aldrich and used without further purification. Space fill modeling including all electrostatic surface potential mapping was done with Spartan '04. Models of mesophase packing structures were generated in Hyperchem 7. NMR spectra were taken on a Varian Unity +300 spectrometer in solutions of $CDCl_3$. Optical microscopy was carried out using standard glass microscope slides which were first treated in a base bath, rinsed and allowed to air dry, on an Olympus BX60 microscope equipped with a Mettler FP82HT hot stage and digital camera. DSC experiments were performed on a TA Instruments DSC Q100. Variable temperature X-ray data were collected using an Inel CPS 120 position sensitive detector using an XRG 2000 generator (Cu Ka) and a Minco CT 137 temperature

controller. Crushed powder samples were loaded into 1.5 mm thin walled glass capillary tubes and sealed prior to being mounted into the instrument. UV-Vis spectra were taken of samples using standard glass microscope slides on a temperature-regulated Hewlett-Packard 8452A diode array spectrophotometer. Samples were heated above the clearing point outside the instrument then allowed to cool slowly against the heated cell while recording spectra.

1,5-*Bis*-hexyloxy-naphthalene (3.1). 1,5-Dihydroxy naphthalene (4.5 g, 28 mmol), 1-Bromohexane (9.3 g, 56 mmol), potassium carbonate (8 g) were all added to CH_3CN (300 ml). The solution was stirred under reflux for 24 h, allowed to cool, filtered and then concentrated under reduced pressure. The crude product was purified twice by column chromatography (20% CH_2Cl_2/ 80% Hexanes), and recrystalized by vapor diffusion of hexanes into $CHCl_3$ to afford 6.2g (67% yield) of **3.1** as light yellow crystals. Mp 85-87°C; ^{13}C NMR (300 MHz, $CDCl_3$) *d* 154.96, 127.08, 125.31, 114.31, 105.51, 68.43, 31.91, 29.56, 26.23, 22.91, 14.33; ^{1}H NMR (300 MHz, $CDCl_3$) *d* 7.89 (d, *J* = 8.7 Hz, 2H), 7.41 (t, *J* = 7.8 Hz, 2H), 6.87 (d, *J* = 7.5 Hz, 2H), 4.17 (t, 6.3 Hz, 4H), 1.97 (p, *J* = 7.2 Hz, 4H), 1.63 (m, 4H), 1.44 (m, 8H), 0.99 (t, 6.3 Hz, 6H) ppm; ESI –MS (positive-ion) 329 ($[M + H]^+$).

1,5-*Bis*-undecyloxy-naphthalene (3.2). According to the method used for **3.1**, **3.2** was obtained as a white flaky solid in 59% yield. Mp 74-76°C; ^{13}C NMR ($CDCl_3$) *d* 154.95, 127.07, 125.29, 114.31, 105.50, 68.43, 32.17, 29.88 (three coincident peaks), 29.70 (two coincident peaks), 29.59, 26.53, 22.95, 14.38; ^{1}H NMR ($CDCl_3$) *d* 7.89 (d, *J* = 8.7 Hz,

2H), 7.40 (t, *J* = 7.8 Hz, 2H), 6.86 (d, *J* = 7.5 Hz, 2H), 4.17 (t, 6.3 Hz, 4H), 1.97 (p, *J* = 7.2 Hz, 4H), 1.59 (m, 4H), 1.42 (m, 28H), 0.94 (t, 6.6 Hz, 6H) ppm; ESI –MS (positive-ion) 469 ($[M + H]^+$).

1,5-Diisopropoxy-naphthalene (3.3). According to the method used for **3.1**, **3.3** was obtained as yellow crystals in 64% yield. Mp 100-102°C; ^{13}C NMR ($CDCl_3$) *d* 153.71, 128.17, 125.18, 114.62, 107.39, 70.64, 22.40; ^{1}H NMR ($CDCl_3$) *d* 7.89 (d, *J* = 8.1 Hz, 2H), 7.40 (t, *J* = 7.5 Hz, 2H), 6.90 (d, *J* = 7.5 Hz, 2H), 4.76 (m, 2H), 1.49 (d, 6 Hz, 12H) ppm; ESI –MS (positive-ion) 245 ($[M + H]^+$).

1,5-*Bis*-(2-ethyl-butoxy)-naphthalene (3.4). According to the method used for **3.1**, **3.4** was obtained as flat yellow crystals in 54% yield. Mp 30-32°C; ^{13}C NMR ($CDCl_3$) *d* 155.13, 127.12, 125.31, 114.26, 105.34, 70.27, 41.39, 23.99, 11.55; ^{1}H NMR ($CDCl_3$) *d* 7.88 (d, *J* = 8.7 Hz, 2H), 7.40 (t, *J* = 7.8 Hz, 2H), 6.88 (d, *J* = 7.5 Hz, 2H), 4.07 (d, 4H), 1.86 (m, 2H), 1.63 (m, 8H), 1.03 (t, *J* = 7.5 Hz, 12H) ppm; ESI –MS (positive-ion) 329 ($[M + H]^+$).

***(S,S)*-1,5-*Bis*-(2-methyl-butoxy)-naphthalene (3.5).** According to the method used for **3.1**, **3.5** was obtained as clear crystals in 71% yield. Mp 44-46°C; ^{13}C NMR ($CDCl_3$) *d* 155.06, 127.12, 125.32, 114.27, 105.43, 73.13, 35.16, 26.63, 17.08, 11.70; ^{1}H NMR ($CDCl_3$) *d* 7.91 (d, *J* = 8.7 Hz, 2H), 7.41 (t, *J* = 7.8 Hz, 2H), 6.87 (d, *J* = 7.5 Hz, 2H), 4.00 (m, 4H), 2.07 (m, 4H), 1.74 (m, 2H), 1.42 (m, 2H), 1.17 (d, *J* = 6.9 Hz, 4H), 1.06 (t, *J* = 7.2 Hz, 6H) ppm; ESI –MS (positive-ion) 301 ($[M + H]^+$).

1,5-*Bis*-(3-hydroxy-propoxy)-naphthalene (3.6). According to the method used for **3.1**, **3.6** was obtained as long white crystals in 68% yield. M.p.: 141.5-142.0°C ^{13}C NMR (DMSO-d_6) *d* 155.8, 128.1, 126.4, 115.4, 106.7, 66.3, 60.3, 33.5; ^{1}H NMR (DMSO-d_6): *d* 7.80 (d, *J* = 8.6 Hz, 2H), 7.34 (t, *J* = 8.2 Hz, 2H), 6.88 (d, *J* = 7.6 Hz, 2H), 4.65 (t, *J* = 5.8 Hz, 2H), 4.28 (t, *J*= 6.0 Hz, 4H, 3.88 (q, *J*= 6.0 Hz, 4H), 2.05 (quint, *J* = 6.0 Hz, 4H); ESI –MS (positive-ion) 277 ($[M + H]^+$).

2,7-Dihexyl-benzo[*lmn*][3,8]phenanthroline-1,3,6,8-tetraone (3.7). 1,4,5,8-Naphthalenetetracarboxylic dianhydride (3.2g, 12mmol) was placed into a round bottom flask and suspended in isopropanol (150 ml). A mixture of 1-aminohexane (2.6g, 25mmol), TEA (2.6g, 25mmol), and isopropanol (50ml) was slowly added and the solution was allowed to stir at room temperature for 30 min, and then heated at reflux for 12 hours. The solution was allowed to cool to room temperature and the precipitate was filtered, and purified by column chromatography (70% CH_2Cl_2/ 26% Hexanes/ 4% Acetone) to afford **3.7** (3.6g, 69% yield) as pink crystals. Mp 203-205°C; ^{13}C NMR ($CDCl_3$) *d* 163.06, 141.11, 131.15, 126.87, 41.23, 31.73, 28.27, 26.98, 22.78, 14.28; ^{1}H NMR ($CDCl_3$) *d* 8.76 (s, 4H), 4.20 (t, *J* = 7.5 Hz, 4H), 1.75 (p, *J* = 7.2 Hz, 4H), 1.45 (m, 4H), 1.36 (m, 8H), 0.91 (t, *J* = 6.9 Hz, 6H) ppm; ESI –MS (positive-ion) 435 ($[M + H]^+$).

2,7-Diundecyl-benzo[*lmn*][3,8]phenanthroline-1,3,6,8-tetraone (3.8). According to the method used for **3.7**, **3.8** was obtained as light pink flaky crystals in 72% yield. Mp

161-163℃; ^{13}C NMR ($CDCl_3$) *d* 163.10, 141.09, 131.17, 126.89, 41.25, 32.14, 29.83, 29.78, 29.56 (three coincident peaks) 28.32, 27.32, 22.92, 14.34; ^{1}H NMR ($CDCl_3$) *d* 8.78 (s, 4H), 4.21 (t, *J* = 7.8 Hz, 4H), 1.76 (p, *J* = 7.5 Hz, 4H), 1.40 (m, 4H), 1.28 (m, 28H), 0.90 (t, *J* = 6.0 Hz, 6H) ppm; ESI –MS (positive-ion) 574 ($[M + H]^+$).

(*R*,*R*)-(+)-2,7-*Bis*-(1-methyl-hexyl)-benzo[*lmn*][3,8]phenanthroline-1,3,6,8-tetraone (3.9). According to the method used for **3.7**, **3.9** was obtained as light yellow flaky crystals in 74% yield. Mp 158-160°C; $[a]^{24}_D$+82.2 (*c* 0.6, CH_2Cl_2); ^{13}C NMR ($CDCl_3$) *d* 163.57, 141.10, 131.12, 127.05, 50.67, 33.63, 31.82, 26.94, 22.75, 18.52, 14.22; ^{1}H NMR ($CDCl_3$) *d* 8.74 (s, 4H), 5.28 (m, 2H), 2.19 (m, 2H), 1.91 (m, 2H), 1.61 (d, *J* = 7.2 Hz, 6H), 1.30 (m, 12H), 0.85 (t, *J* = 7.5 Hz, 6H) ppm; ESI –MS (positive-ion) 463 ($[M + H]^+$).

(*S*,*S*)-(-)-2,7-*Bis*-(1-methyl-hexyl)-benzo[*lmn*][3,8]phenanthroline-1,3,6,8-tetraone (3.10). According to the method used for **3.7**, **3.10** was obtained as light yellow flaky crystals in 72% yield. Mp 158-160°C; $[a]^{24}_D$-82.2 (*c* 0.6, CH_2Cl_2); ^{13}C NMR ($CDCl_3$) *d* 163.57, 141.10, 131.12, 127.05, 50.67, 33.63, 31.82, 26.94, 22.75, 18.52, 14.22; ^{1}H NMR ($CDCl_3$) *d* 8.74 (s, 4H), 5.28 (m, 2H), 2.19 (m, 2H), 1.91 (m, 2H), 1.61 (d, *J* = 7.2 Hz, 6H), 1.30 (m, 12H), 0.85 (t, *J* = 7.5 Hz, 6H) ppm; ESI –MS (positive-ion) 463 ($[M + H]^+$).

2,7-Di(ethoxy-ethyl)-benzo[*lmn*][3,8]phenanthroline-1,3,6,8-tetraone 3.11. According to the method used for **3.7**, **3.11** was obtained as long pink crystals in 82% yield. ^{13}C

NMR (DMSO-d_6) *d* 171.5, 138.9, 135.1, 134.8, 81.2, 69.3, 60.9, 49.4; ^{1}H NMR (DMSO-d_6) *d* 8.63 (s, 4H), 4.57 (t, *J* = 6.4 Hz, 4H), 4.26 (t, *J* = 7.2 Hz, 4H), 3.70 (t, *J* = 7.6 Hz, 4H) 3.49 (m, 8H); ESI –MS (positive-ion) 443 ($[M + H]^+$).

***N,N'*-bis-phenyl-1,4,5,8-naphthalenediimide (3.12).** According to the method used for **3.7**, **3.12** was obtained as a fine orange powder 64% yield. ^{13}C NMR ($CDCl_3$) *d* 163.73, 133.80, 132.15, 129.95, 129.85, 128.29, 127.19, 126.88; ^{1}H NMR ($CDCl_3$) *d* 8.88 (s, 4H), 7.57 (m, 4H), 7.42 (m, 2H), 7.32 (d, *J* = 0.6 Hz, 4H); ESI –MS (positive-ion) 419 ($[M + H]^+$).

CHAPTER 4

Neutral Solution Phase Dan Oligomers

4.1 CHAPTER SUMMARY

Introduction. The naphthyl oligomers involved in discrete duplex formation driven by Dan:Ndi association, described in chapter 1, are solubilized in aqueous solution by negatively charged carboxylates appended off of the aromatic linkers. Chapter 2 described the association of negatively charged Dan and Ndi polymers. Both of these associations are successful in spite of the fact that they force several negative charges into close proximity in the complexation events. This chapter investigates the synthesis, solubility, and association of neutral Dan oligomers to be used in studies to determine the role of charge repulsion in Dan:Ndi complex formation.

Goals. Previously, all aedamers and naphthyl oligomers have been synthesized to include negative formal charges via solid phase synthesis. It is the immediate goal of work in this chapter to design a facile solution phase synthesis for water soluble Dan oligomers and to study their interaction with Ndi oligomers.

Approach. Tetraethylene glycol was chosen as the neutral linker for the solution phase Dan oligomers as the length is consistent with the previous linkers used in oligomer

synthesis. A synthetic scheme was chosen which allowed for a minimal number of steps in the synthesis of dimer, trimer and tetramer oligomers. These oligomers were tested for aqueous solubility by NMR with comparison to internal standards. The most soluble oligomer was combined with the charged NDI oligomer in preliminary ITC investigations.

Results. Dan oligomers with tetraethylene glycol linkers were synthesized in solution. The synthetic route developed in this chapter allows for the assembly of several Dan monomer into oligomers of defined length. The maximum solubility of the oligomers in aqueous solution was found to be in the μM range by NMR. Preliminary ITC experiments were carried out, however the solubility of the neutral Dan oligomers proved to be too low for a detailed analysis. Nevertheless, a qualitative inspection of the data indicated greatly increased binding of the neutral Dan tetramer to a charged Ndi tetramer.

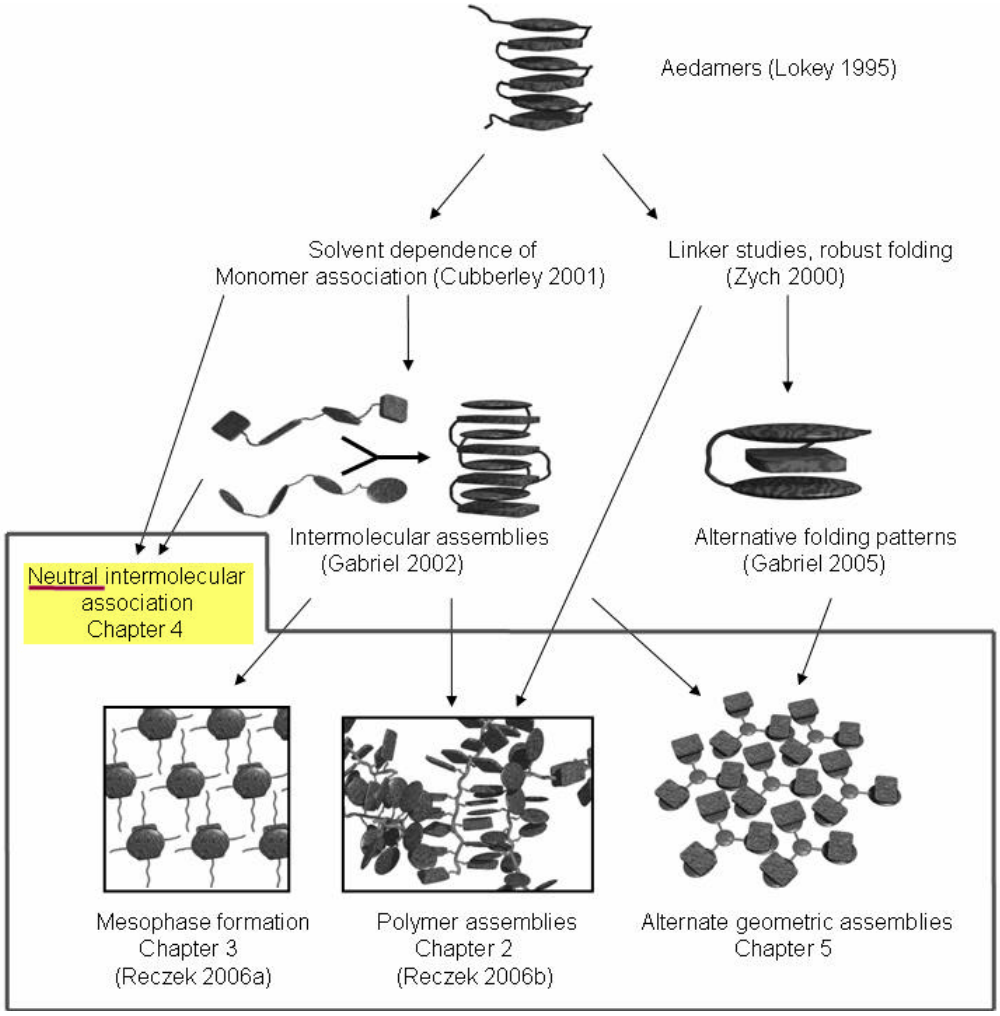

Chart 4.1 Aromatic donor-acceptor molecular assembly in the Iverson group.

4.2 BACKGROUND

4.2.1 Monomer Association

Experiments were discussed in chapter 1 in which the affect of solvent polarity on the association of neutral Dan and Ndi monomers were investigated by previous members of the Iverson group. These studies measured an association constant of ~2000 M^{-1} (? *G*°

= -4.5 kcal/mol) by NMR titration for the neutral monomers in aqueous solution, shown in figure 4.1a (Cubberley 2001). Negatively charged Dan and Ndi oligomers were also investigated, and exhibited association constants ranging from ~3000 M^{1} (? *G*° = -5.0 kcal/mol) for dimers, then increasing by a factor of 10 with each additional aromatic unit up to ~3 x 10^{5} M^{-1} that was seen with tetramers (Gabriel 2002). It is striking that the association constant of the charged dimers is on the same order of magnitude as that of the neutral monomers. When NMR titrations were performed on the charged monomers shown in figure 4.1b, an association constant of 300 M^{-1} (? *G*° = -3.1 kcal/mol) was obtained, in concert with the trend of an order of magnitude in association per aromatic unit in the charged oligomers. It was thus implied that forcing the negative charges of the charged monomers into close proximity during Dan:Ndi complexation cost about an order of magnitude in association. The exact extrapolation of the affect of charges on oligomer assembly is in question, and so the synthesis of neutral oligomers is desired to understand the affect of charge repulsion of association. In so doing, it should be possible to shine light on the full potential of the Dan:Ndi complex to serve as a tool for supramolecular chemistry in water.

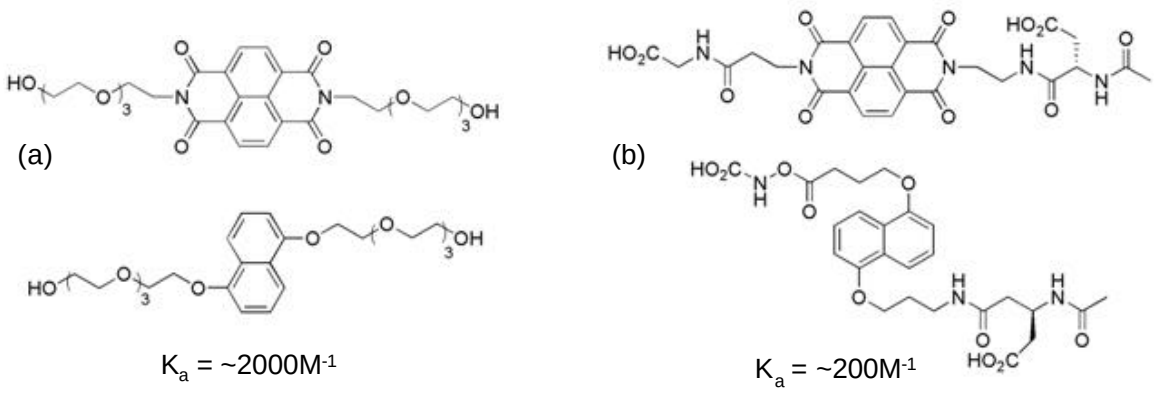

Figure 4.1 Neutral (a) and charged (b) monomer pairs with their association constant in buffered D_2O as measured by NMR titration.

4.2.3 Solid Phase Neutral Aedamers

Previous attempts in the Iverson group at the synthesis of neutral aedamers via the solid phase synthetic procedures used for the charged systems have met with little success (Cubberley 2000). Amino acid derivatives incorporating tetra(ethylene glycol monomethyl ester) were designed and used in the solid phase synthesis of a neutral aedamer dimer (Figure 4.2). Much work was done on optimizing the conditions for the overall synthesis of the amino acids, but yields remained low. The solid phase synthesis was also optimized, but conditions and in particular cleavage from the resin proved inefficient and the products difficult to separate. At the conclusion of this prior work the parent ion mass of the desired product was observed in mass spec analysis of the crude product, but it could not be isolated in pure form.

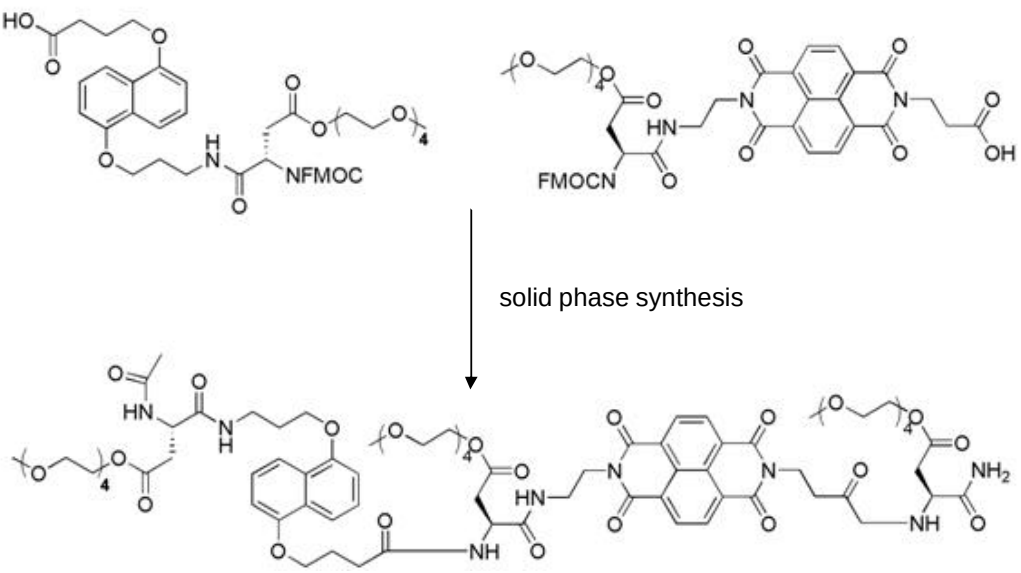

Figure 4.2 Dan and Ndi amino acids and the neutral solid phase dimer that could not be isolated.

4.3 RESULTS AND DISCUSSION

4.3.1 Theorized Propagation of Charge Repulsion

Based on the monomer associations measurements the propagated affect of charge repulsion on oligomer association would be significant. If the cost in terms of K_a is an order of magnitude for every four like charges brought together on a compound, then the anticipated association constant for a neutral tetramer should be much higher than the value of ~3 x 10^5 M^{-1} that was measured for the charged species.

A crude estimation of the energy cost for each like-charge interaction can be made using the equation for the energy of a single charge-charge interaction:

$$?E = k_c \, a \, \frac{q^1 \, q^2}{e \, r}$$

Here **q** is the charge of an electron in coulombs, **k** is the coulomb force constant for the permittivity of free space, **a** is Avogadro's number, **e** is a unitless shielding constant of the environment which is estimated at 80 for buffered water, and **r** is the distance between two charges in meters. Figure 4.3 shows the charged monomers in a geometrically minimized stacked position and gives the average distance between the two closest charges on opposing monomers (a) and the two further charges (b) which average out to be 12Å and 17Å respectively. These distances are plugged into the above equation to give energies of charge-charge repulsion for each individual interaction as follows:

close charge repulsion

$$?E = (9x10^{9})(6.02x10^{23}) \frac{(1.6x10^{-19})^2}{80 \, (12x10^{-10})} = 1.45 \text{ kJ/mol} = .345 \text{ kcal/mol}$$

far charge repulsion

$$?E = (9x10^{9})(6.02x10^{23}) \frac{(1.6x10^{-19})^2}{80 \, (17x10^{-10})} = 1.02 \text{ kJ/mol} = .243 \text{ kcal/mol}$$

When the four charge repulsion interactions shown in figure 4.3, two close and two far, are added together a total of 1.2 kcal/mol is obtained as the energy cost of charge-charge repulsion for charged monomer association. This is remarkably close to the experimentally calculated energy difference between association of charged and neutral monomers of ? *G*° of 1.4 kcal/mol!

This calculation supports the theory that the difference between the associations of the charged vs. neutral monomers is primarily a result of charge-charge repulsion.

With oligomers, each additional aromatic unit per molecule involved in association will add one close and one far charge-charge repulsion interaction. This amounts to a cost of about 0.6 kcal/mol to the ? *G*° for each aromatic unit, propagated in tetramers to a total of 4.8 kcal/mol lost to charge-charge repulsion. This predicts a possible association constant of approximately 1 x 10^9 at room temperature for a tetramer duplex involving a neutral oligomer!

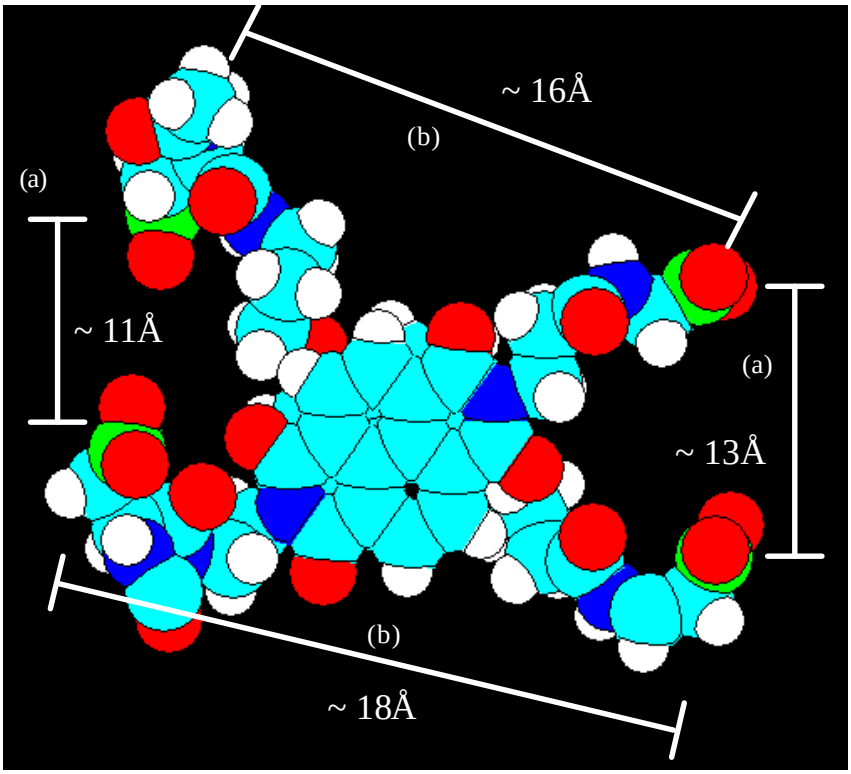

Figure 4.3 Hyperchem model of charged monomer association. The carbonyl carbon of each carboxylate group is highlight in green. (a) Distance to the closest charge on complementary monomer. (b) Distance to farther charge on complementary monomer.

4.3.2 Design and Synthesis of Neutral Dan Oligomers

The impressive aqueous solubility of the neutral monomers shown in figure 4.1 indicated that the use of tetra(ethylene glycol) (TEG) as the neutral linker could be a successful design element for oligomer synthesis. It is of matching length with previous linkers, and inexpensive at ($25.00/1Kg). Synthesis of the Dan oligomer was carried out according to scheme 4.1.

Tetra(ethylene glycol) was monotosylated by reacting it in 20 times excess with *p*-toluenesulfonyl chloride. Compound **4.1** was then reacted with 1.5 equivalents of Dhn to yield the mono-TEG electron rich aromatic **4.2**. This stoichiometry was used as it gave the highest yield after purification. Using more of compound **4.1** gave the obvious result of the di-TEG Dan as the dominant product. Using one molar equivalent gave mostly the mono-TEG product, but separation for the leftover Dhn starting material proved messy and difficult.

Di-tosylated TEG was reacted with Dhn in a 5:1 stoichiometry. This gave a decent yield of mono-Dan compound **4.3** at 56%, and also a reasonable amount of the di-Dan compound **4.4**, giving precursors to the di, tri, and tetra-Dan oligomers all in one reaction. **4.4** was then hydrolyzed to give the dimer **4.5**, **4.3** was reacted with compound **4.2** to give trimer **4.6**, and **4.4** was reacted with **4.3** to yield tetra-Dan compound **4.7**. The purification of Dan oligomers was nontrivial by column chromatography using a concentration gradient of acetone and CH_2Cl_2 as the eluting solvents. The seemingly low yields represent pure isolated products.

The synthesis of the Dan oligomers could be optimized for any number of repeat units. However as dimers, trimers, and tetramers were all desired this scheme represents a quick and efficient route to obtaining all oligomers with minimal time and material.

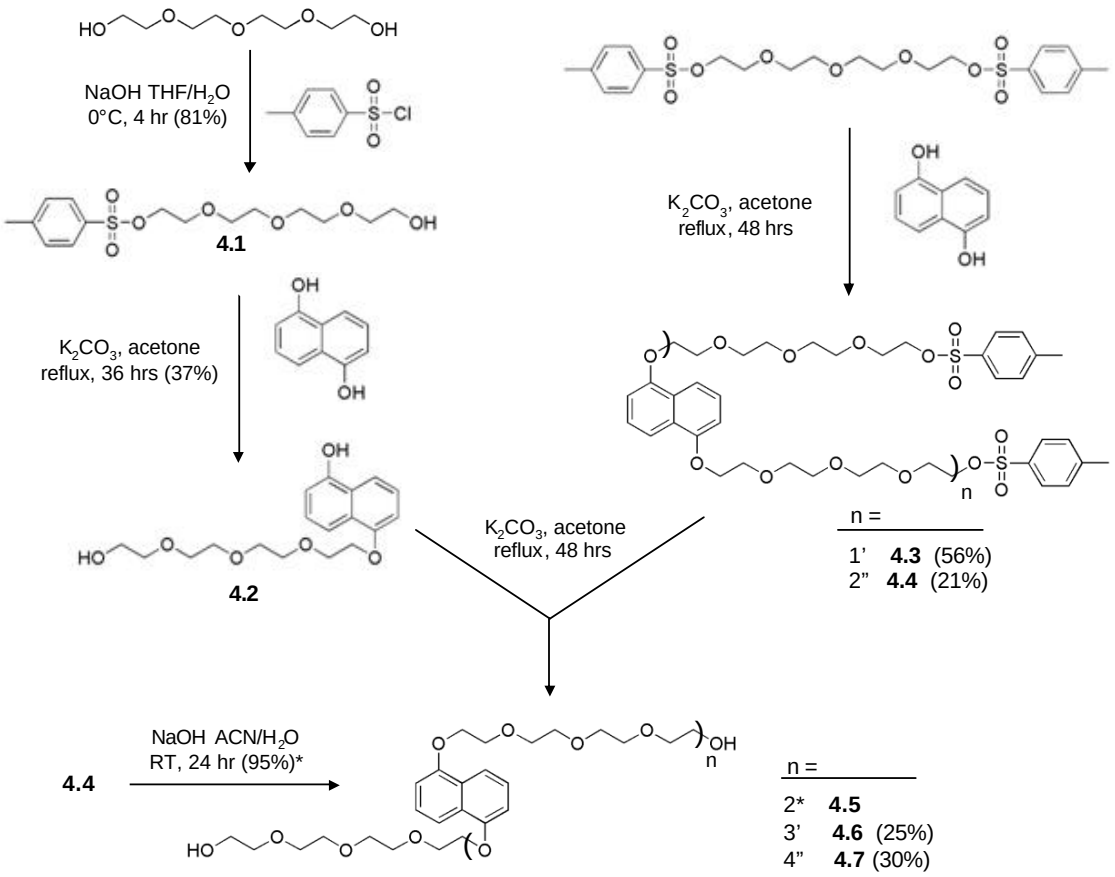

Scheme 4.1 Synthesis of neutral Dan oligomers.

4.3.3 Maximum Solubility by NMR Analysis

It was immediately apparent that the TEG-Dan oligomers were not as water soluble as hoped. While the neutral Dan monomer is soluble in concentrations exceeding

100mM, none of the Dan oligomers appeared to dissolve at all in aqueous solution. In order to determine the maximum solubility of the compounds, NMR spectroscopy in D_2O with an internal standard was used. Small amounts of each oligomer were placed into a solution that was 1mM in 3-aminopropanol as an internal standard in D_2O. The solubility for all oligomers was in the µM range, limiting the accuracy of the measurements, particularly in the case of the dimer, which was surprisingly found to be the least soluble oligomer at < 1 µM. The trimer's maximum solubility was estimated at ~ 1 µM, and the tetramer was most soluble at ~ 1.5 µM.

4.3.4 ITC Experiment and Analysis of Tetramer Association

The extremely low solubility of the TEG-Dan oligomers was not only surprising, but also detrimental to analysis by ITC (Wiseman 1989, Microcal, Inc. 1999). Experiments were attempted in which the charged Ndi oligomer was injected into a solution of **4.7** at its maximum solubility. As expected at such a low concentration, it proved difficult to obtain any measurable heat signal from titration experiments, and impossible to obtain any quantitative data. However, by quick injections of a relatively large amount of the charged Ndi tetramer into a solution of **4.7**, a single injection estimated value for ? *H*° of -21.4 kcal/mol was obtained. This is significantly less than the measured ? *H*° value of the charged system of -19.3 kcal/mol.

There are fewer atoms, and fewer possible degrees of freedom, present in the neutral Dan tetramer compared to the charged Dan tetramer. It is therefore likely that restraining the neutral oligomer in a bound complex would cost less in entropy than

restraining the charged oligomer. However, it is difficult to estimate how much less negative ? *S*° would be with the neutral Dan tetramer, so the value measured for the charged system of -35.3 cal/mol was used with the measured ? *H*° value to determine a tentative ? *G*° of -10.2 kcal/mol. Using this ? *G*° to solve for an association constant yields 1.04 x 10^7 for the K_a of complexation for a charged Ndi tetramer with a neutral Dan tetramer.

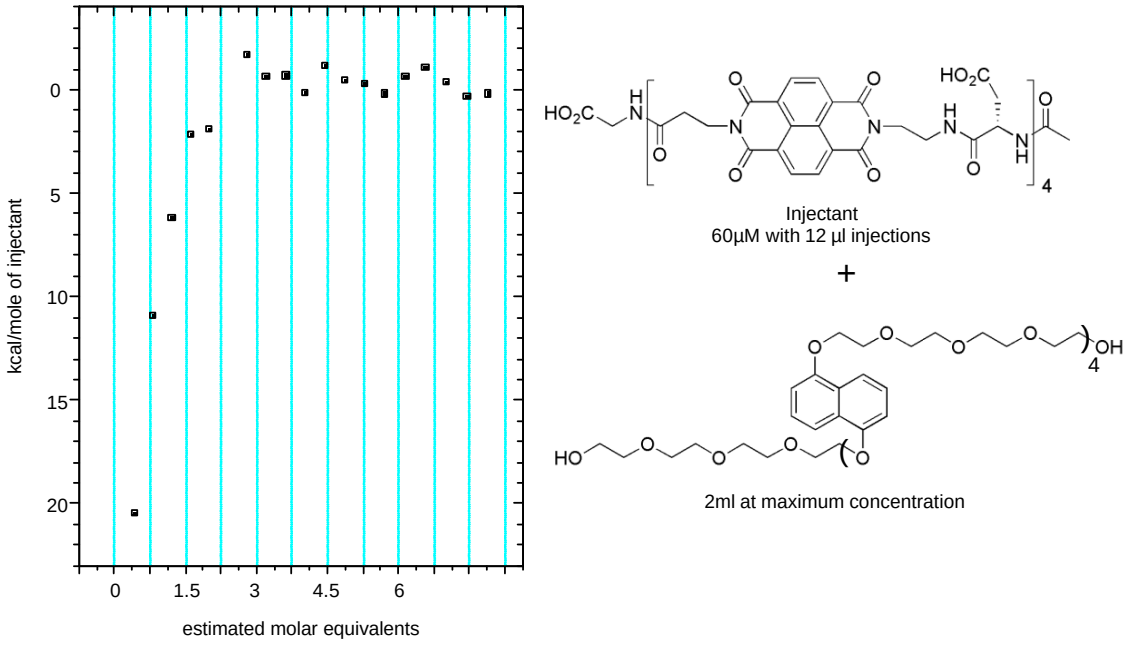

Figure 4.4 Preliminary ITC data for the injection of the charged Ndi tetramer shown into Dan oligomer **4.7**.

4.4 CHAPTER CONCLUSIONS

The model and calculations for the affect of charge repulsion on the association of Dan and Ndi oligomers in water presented in this chapter predicts a possible increase of the K_a of up to four orders of magnitude by replacing the charged system with a neutral one. This certainly warrants the study of neutral systems to further explore the potential of directed aromatic-aromatic interactions as supramolecular chemistry tool. Unfortunately, the neutral TEG-Dan oligomers synthesized for this purpose were not sufficiently water soluble for extensive study, only capable of making solutions at μM concentrations. Still, the limited enthalpy data obtained suggests that there is a significantly larger heat release of at least 2 kcal/mol for the neutral systems.

Further study on the association of neutral oligomers requires serious thought into designing a soluble system. The linker length along with steric bulk of the oligomer must still allow for facile complexation of the Dan and Ndi units. Like the polymer work of chapter 2, a branched design may be beneficial to the solubility characteristics, allowing for solubility both off of the linkers, and the appended aromatic units. Work being done currently in the Iverson group with rigid water soluble linkers is promising in this regard, and will hopefully shine more light on association potential for neutral Dan and Ndi oligomers.

4.5 EXPERIMENTAL SECTION

General Procedures. All starting materials were obtained from Aldrich and used without further purification. Charged NDI tetramer was obtained from Greg Gabriel of the

Iverson group (Gabriel 2004). Flash chromatography was performed ^{1}H and ^{13}C NMR spectra were recorded on a Varian Unity Plus 200 MHz spectrophotometer in the indicated solvent. Chemical shifts are expressed in parts per million (ppm, d) relative to tetramethylsilane (TMS) (d = 0.00 ppm). ITC experiments were performed on a VP-ITC microcalorimeter from Microcal Inc. (Northhampton, MA 01060) in 50 mM sodium phosphate and followed the experimental setups detailed in literature (Wiseman 1998). 12µl volumes of a 60 µM Ndi charged tetramer solution were titrated into the Dan neutral tetramer at maximum solubility.

Toluene-4-sulfonic acid 2-{2-[2-(2-hydroxy-ethoxy)-ethoxy]-ethoxy}-ethyl ester (4.1). Sodium hydroxide (4.9g, 122 mmol) in water (30 ml) was added to a solution of tetra(ethylene glycol) (200ml) in THF (40 ml). The mixture was cooled to 0 °C in an ice bath and *p*-toluenesulfonyl chloride (14.32 g, 75.3 mmol) in THF (100 ml) was slowly added over 4 hours, under argon, via an addition funnel. The mixture was stirred at 0 °C for 3 h, and then poured into water (500 ml). CH_2Cl_2 was added (200 ml) and the layers separated. The aqueous layer was extracted with CH_2Cl_2 (2 x 100 ml) and the combined organic portions were washed with water (200 ml), brine (100 ml), and then concentrated under reduced pressure. The product was dried under vacuum over night to yield a viscous yellow oil (21.3 g, 81%): ^{13}C NMR ($CDCl_3$) d 144.6, 132.7, 129.6, 127.7, 72.3, 70.4, 70.2, 70.0, 69.1, 68.4, 61.4, 21.4144.6, 132.7, 129.6, 127.7, 72.3, 70.4, 70.2, 70.0, 69.1, 68.4, 61.4, 21.4; ^{1}H NMR ($CDCl_3$) d 2.40 (s, 3H), 2.54 (br s, 1H), 3.53-3.67 (comp, 14H), 4.11 (t, *J* = 4.6 Hz, 2H), 7.30 (d, *J* =8.2 Hz, 2H), 7.75 (d, *J* = 8.2 Hz, 2H); ESI –MS (positive-ion) 349 ($[M + H]^+$).

1-hydroxy-5-tetra(ethylene glycol) naphthalene (4.2). Potassium hydroxide (6.34 g, 46 mmol) was added to1,5-dihydroxy naphthalene (3.27 g, 20.4 mmol) dissolved in CH_3CN (150 ml). The solution was heated to 70 °C and **5** (10.66 g, 30.6 mmol) in CH_3CN (200 ml) was added drop wise under argon. The solution was refluxed for 32 h, filtered, and then concentrated under reduced pressure. The dark brown oil was dissolved in CH_2Cl_2 (200 ml), washed with water (2 x 50 ml), brine (50 ml) and then concentrated under reduced pressure. Purification of the crude product by column chromatography, eluting with acetone, yielded the title compound as a brown oil. (2.4 g 37%): ^{13}C NMR ($CDCl_3$) d 157.1, 156.4, 128.4, 127.0, 126.4, 125.3, 114.9, 113.8, 109.7, 104.8, 72.7, 70.6 (2C), 70.5 (2C), 70.3, 70.1, 61.4; ^{1}H NMR ($CDCl_3$) d 2.59 (br, s, 1H), 3.61-3.84 (comp, 13 H), 3.99 (t, *J* = 4.8 Hz, 2H), 4.28 (t, *J* = 4.5 Hz, 2H), 6.79 (d, *J* = 7.5 Hz, 1 H), 6.84 (d, *J* = 7.8 Hz, 1H), 7.226 (t, *J* = 7.5 Hz, 1H), 7.32 (t, *J* = 7.8 Hz, 1H), 7.77 (d, *J* = 3 Hz, 1H), 7.80 (d, *J* = 3.3 Hz, 1H); ESI –MS (positive-ion) 337 ($[M + H]^+$).

Toluene-4-sulfonic acid 2-[2-(2-{2-[5-(2-{2-[2-(2-toluenesulfonyloxy-ehtoxy)-ethoxy]-ethoxy}-ethoxy)-naphthalene-1-yloxy]-ethoxy}-ethoxy)-ethoxy]-ethyl ester (4.3). Tetraethylene glycol ditosylate (38.8 g, 77 mmol) and 1,5-dihydroxynaphthalene (2.43g 15.2 mmol) In acetone (300 ml) was added drop wise over 4 h to a refluxing solution of K_2CO_3 (15.3 g) in acetone (300 ml). After 48 hours the mixture was allowed to cool, filtered, and concentrated under reduced pressure. The resulting oil was dissolved in CH_2Cl_2 (300 ml) washed with water (200 ml), 2 N NaOH (200 ml), brine (100 ml), and concentrated under reduced pressure. Purification of the crude product by column

chromatography, eluting with EtOAc/hexanes (3/1-9/1 gradient) provided the title compound as a light yellow oil (6.9 g, 56%): ^{1}H NMR ($CDCl_3$) d 2.39 (s, 6H), 3.54-3.68 (comp, 16H), 3.75-3.78 (m, 4H), 3.97 (t, *J* = 4.9 Hz, 4H), 4.11 (t, *J* = 4.7 Hz, 4H), 4.27 (t, *J* = 5.0 Hz, 4H), 6.83 (d, *J* = 7.7 Hz, 2H), 7.31 (t, *J* = 7.4, 2H), 7.35 (d, *J* = 8.5 Hz, 4H), 7.74 (d, *J* = 7.5 Hz, 4H), 7.85 (d, *J* = 8.5 Hz, 2H); ESI –MS (positive-ion) 822 ($[M + H]^+$).

Di-1-[toluene-4-sulfonic acid-tetra(ethylene glycol)-naphthalene]-5- tetra(ethylene glycol) (4.4). Same procedure as above, elutes off the column during purification after **4.3**. Yields **4.4** as a light yellow solid (3.68 g, 21%): Mp 71-74°C; ^{1}H NMR ($CDCl_3$) d 2.41(s, 6H), 2.06-3.82 (comp, 28H), 3.98 (t, *J* = 5.1, 8H), 4.13 (t, *J* = 4.8, 4H), 4.25-4.29 (comp, 8H), 6.82 (d, *J* = 7.2, 4H), 7.28-7.36 (comp, 8H), 7.77-7.89 (comp, 8H); ESI –MS (positive-ion) 1140 ($[M + H]^+$).

Di-[1-tetra(ethylene glycol)-naphthalene]-5- tetra(ethylene glycol) (4.5). 4.4 (0.5 g, 0.43 mmol) was dissolved in CH_2Cl_2 (25 ml) and CH_3CN (25 ml) and then added to a 6M NaOH solution (50 ml). The biphasic mixture was allowed to stir vigorously for 24 h, and the layers were separated. The aqueous layer was washed with CH_2Cl_2 (2 x 25 ml), and the combined organic layers were washed with 2M NaOH (25 ml), water (25 ml), brine (25 ml), and then concentrated under reduced pressure to yield **4.5** as a light brown amorphous solid (0.34 g, 95%): Mp 72-75°C; ^{1}H NMR ($CDCl_3$) d 3.57-3.81 (comp, 32H), 3.99 (t, *J* = 4.8 Hz, 8H), 4.28 (t, *J* = 5.1 Hz, 8H), 6.83 (d, *J* = 7.2 Hz, 4H), 7.34 (t, *J* = 7.7, 4H), 7.87 (d, *J* = 8.4, 4H); ESI –MS (positive-ion) 832 ($[M + H]^+$).

Di-{1-tetra(ethylene glycol)-naphthalene-5-}[1,5-tetra(ethylene glycol)-naphthalene] (4.6). **4.2** (0.779 g, 2.4 mmol) and **4.3** (0.945 g, 1.15 mmol) were dissolved in acetone (100 ml) and CH_2Cl_2 (25 ml). Potassium carbonate (0.63 g, 4.6 mmol) was added and the solution was stirred, while refluxing under argon, for 48 h. The solution was allowed to cool, filtered, and concentrated under reduced pressure. The brown oil was then dissolved in CH_2Cl_2 (100 ml) and then washed with 2M NaOH (25 ml), water (25 ml), brine (25 ml), and then concentrated under reduced pressure. The crude product was purified by column chromatography, eluting with EtOAC/MeOH (0-5% gradient MeOH) to yield **4.6** as a dark reddish solid (0.32 g, 25%): Mp 78-81°C; ^{1}H NMR ($CDCl_3$) d 2.43 (br, s, 2H), 3.61-3.81 (comp, 40H), 3.96-3.99 (comp, 12H), 4.24-4.33 (comp, 12H), 6.78-6.87 (comp, 6H), 7.31-7.41 (comp, 6H), 7.86-7.9 (comp, 6H); ESI –MS (positive-ion) 1166 ($[M + H]^+$)

Di-{1-tetra(ethylene glycol)-naphthalene-5-[1-tetra(ethylene glycol)-naphthalene]-5-ethylene glycol} (4.7). **4.2** (0.464 g, 1.45 mmol) and **4.4** (0.839 g, 0.737 mmol) were dissolved in acetone (100 ml) and CH_2Cl_2 (25 ml). Potassium carbonate (0.40 g, 2.9 mmol) was added and the solution was stirred, while refluxing under argon, for 72 h. The solution was allowed to cool, filtered, and concentrated under reduced pressure. The brown oil was then dissolved in CH_2Cl_2 (100 ml) and then washed with 2M NaOH (25 ml), water (25 ml), brine (25 ml), and then concentrated under reduced pressure. The crude product was purified by column chromatography, eluting with EtOAc/MeOH (0-8% gradient MeOH) to yield **4.7** as a dark brown amorphous solid (0.33 g, 30%): Mp 71-

76°C; ^{1}H NMR ($CDCl_3$) d 2.19 (s, 2H), 3.65-3.81 (comp, 44), 3.98 (comp, 18H), 4.26 (comp, 18H), 6.80 (d, *J* = 7.8 Hz, 8H), 7.28-7.36 (comp, 8H), 7.87 (d, J = 8.4 Hz, 8H); ESI –MS (positive-ion) 1484 ($[M + H]^+$).

CHAPTER 5

Variations on the Precursors of Dan and Ndi Assemblies

5.1 CHAPTER SUMMARY

Introduction. The previous chapters have expanded the scope of Dan:Ndi interactions in the Iverson group to affecting polymer macrostructure, controlling mesophase formation and properties, and maximizing association by limiting charge repulsion. This chapter describes preliminary experiments on C_3 symmetric trimers and other synthetic designs to complement and enhance prior and current work on the study and application of Dan and Ndi assemblies.

Goals. It is the aim of experiments in this chapter to explore alternative synthetic motifs in the design of supramolecular aromatic donor-acceptor interactions. The short-term goal is to initiate the investigation of molecular architectures that could further address general issues such as enhanced structural control, cooperativity, and solubility. Long-term, new architectures will allow for further control over the properties and utilities of aromatic donor-acceptor interactions in solution and bulk.

Approach. A number of synthetic approaches towards advances in supramolecular aromatic donor-acceptor chemistry were initiated. C_3 symmetric cores were functionalized with various Dan or Ndi units to create relatively rigidified C_3 trimers for control over association geometry in solution and bulk phase. A double cope

rearrangement was explored to give additional functional handles in the 2,6 positions of the Dan unit, and a tetra-substituted benzene was used as a core for specifically designed solubilizing pieces. New diimide and dialkoxy compounds with extended conjugation were synthesized.

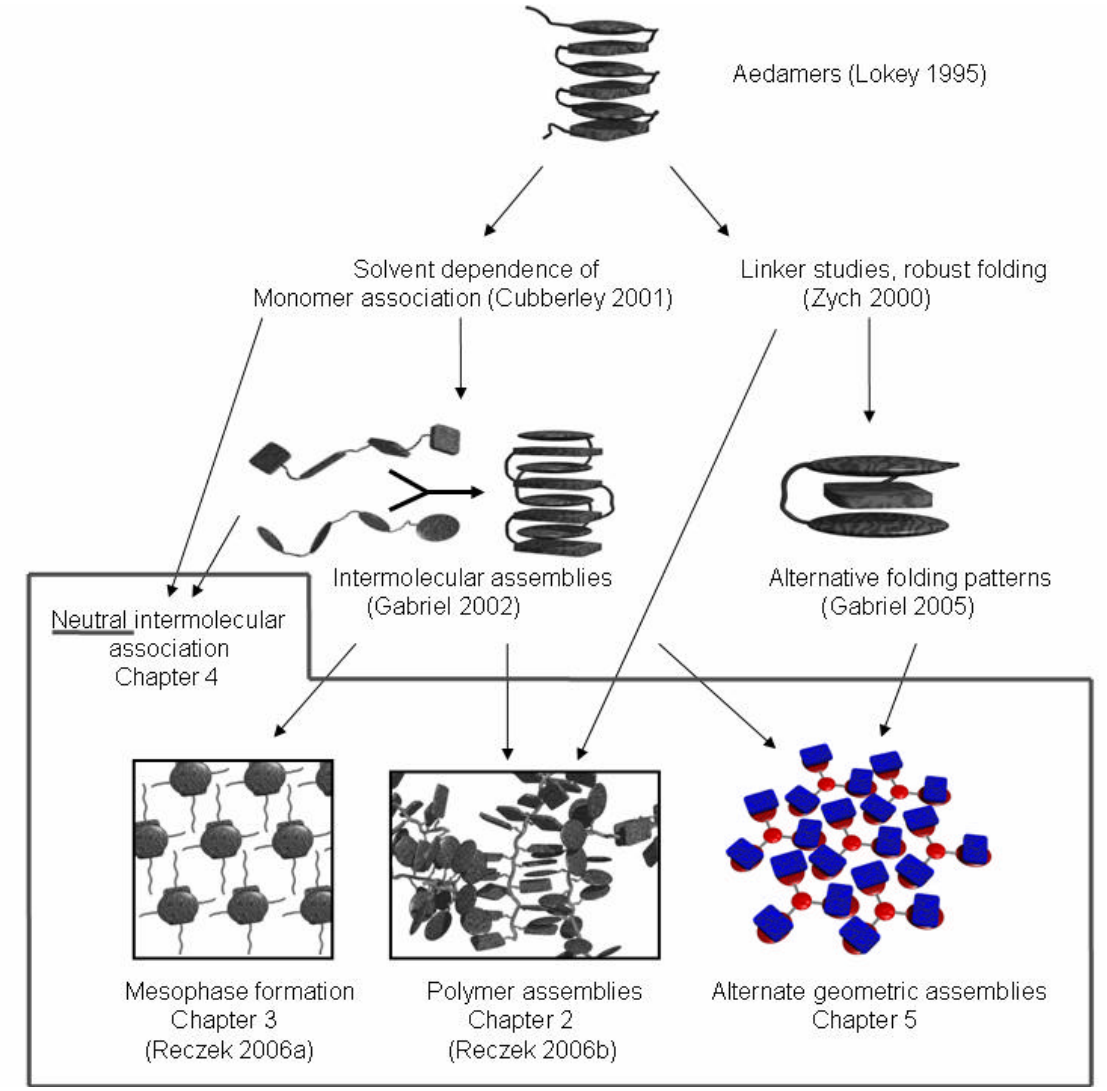

Chart 5.1 Aromatic donor-acceptor molecular assembly in the Iverson group.

5.2 RIGIDIFIED MULTIVALENCY: PLANER TRIMERS

5.2.1 Background

Based upon analysis of the binding of naphthyl oligomers investigated previously in the Iverson group, it appears that the binding energy of sequential Dan:Ndi interactions is non-cooperative (Gabriel 2004). That is, after initial association the binding of additional naphthyl units is additive, each binding event is essentially equal in energy to the one before it. This is distinct from positive cooperativity, in which subsequent binding events shown an enhancement over previous ones. A prominent example of this is the tetrameric protein hemoglobin, which binds four oxygen molecules, each with increasing affinity over the last (Eaton 1999). Positive cooperativity is an important phenomena in biology, and increasingly so in molecular self-assembly for structural control, molecular recognition, and molecular machines, yet it is poorly understood, and few synthetic systems are available for its study (Archer 2002, Ercolani 2003, Badjic 2005).

Changing from a flexible linear system to a relatively flat C_3 symmetric architecture for naphthyl oligomers may enhance the potential for positive cooperativity with Dan:Ndi complexation. With the linear system, the initial binding event brings all of the naphthyl units into proximity, but not necessarily the correct orientation. Multimeric binding adds additional constraints to the molecules and therefore causes a substantial decrease in entropy for each additional binding unit (Figure 5.1a). There is also the possibility for molecules to fold the wrong way, falling into kinetic traps, which need to be dynamically overcome to reach a thermodynamic minimum. Finally, with the

linear oligomer system, the terminal aromatic units of the stack can wag on or off with no affect on the other interactions. This weakens the overall association and has presented some difficulty on the characterization of folding and binding (Lokey 1997, Gabriel 2004). In the case of the C_3 trimer, after an initial binding event, the molecules are pre-organized to further interact by simple sliding or rotation (Figure 5.1b). This should require minimal entropy cost. Further, the third binding event can gain additional association by designed interactions between the molecular cores. A result of the relative rigid design for the trimers could be that no one interaction can break apart without affecting the other 3 (or 4), greatly strengthening the overall association. With these considerations, this system could exhibit positive cooperativity, and exhibit a significantly increased association constant for Dan and Ndi trimers.

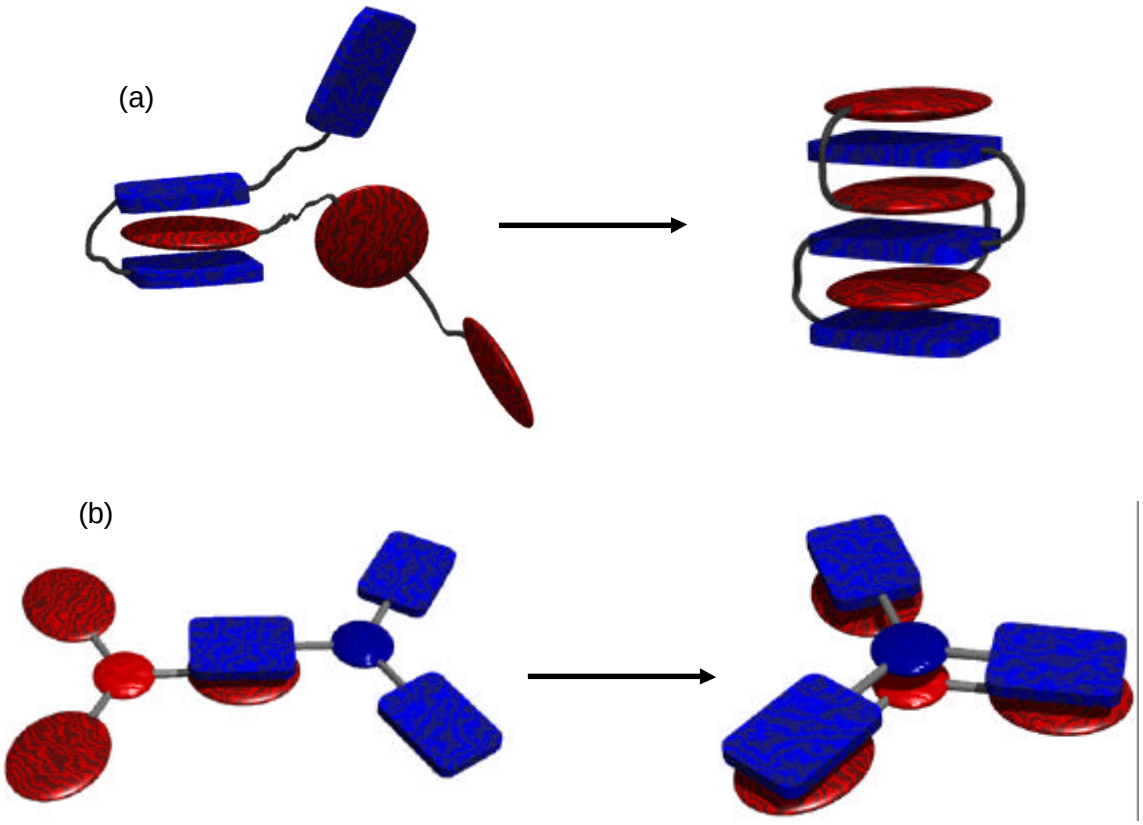

Figure 5.1 Schematic of the binding of Dan and Ndi trimers. (a) Linear trimers must constrain themselves to completely bind. (b) C_3 trimers pay little extra entropy cost for constraining the molecule upon multiple binding events.

The association of the C_3 trimers in bulk may also display interesting characteristics. As with the work discussed in chapter 3, melts of Dan and Ndi trimers should interact to form donor-acceptor columnar mesophases (Figure 5.2a). It is possible that larger components with increased association will add stability to the phase, and may enhance the temperature range of the phase transitions. Further, it is proposed that the C_3 trigonal shape of the molecules would promote a hexagonal packing geometry of the

columns, and perhaps allow for more single crystal data that would lend insight into the Dan:Ndi complexation (Figure 5.2b).

Building flat trimers with two donors and one acceptor, and *visa-versa*, could allow for an additional element of control in the stacking geometry, both in solution and the bulk phase. The nature of the resultant stacking would give fixed relative positions for the trimer molecules within a column, and perhaps allow for control of *inter*-column interactions, templating structures, and/or interactions with other molecules such as proteins (Figure 5.2c,d).

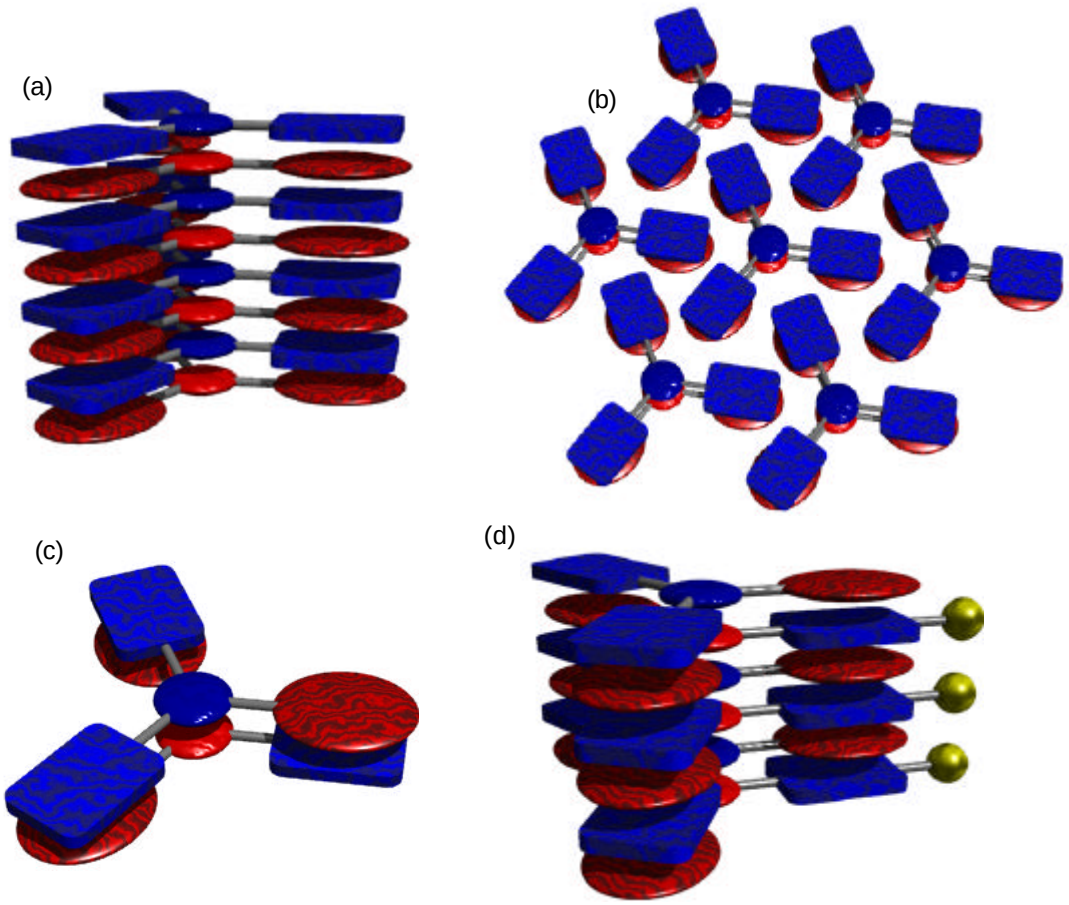

Figure 5.2 Representations of rigidified trimers (a) Columnar stacking with three dependant Dan:Ndi interactions and an additional core interaction. (b) Hexagonal packing in the melt. (c) Asymmetric trimer association. (d) Stack of asymmetric trimers, the yellow balls illustrating the relative fixed orientation of the trimers.

5.2.2 Design and Synthesis

5.2.2.1 C_3 Dan trimers

Phloroglucinol was chosen as an electron rich trivalent central core for the Dan trimer. Initial attempts at synthesizing the trimer involved reacting three equivalents

of Dan monomer **5.2** with phloroglucinol (Scheme 5.1). Mono and di-substituted phloroglucinol were obtained in low yields, but none of the desired trimer could be isolated. It is likely that the close proximity of the nucleophilic sites, along with the bulkiness of the electrophile prevented formation of the desired product.

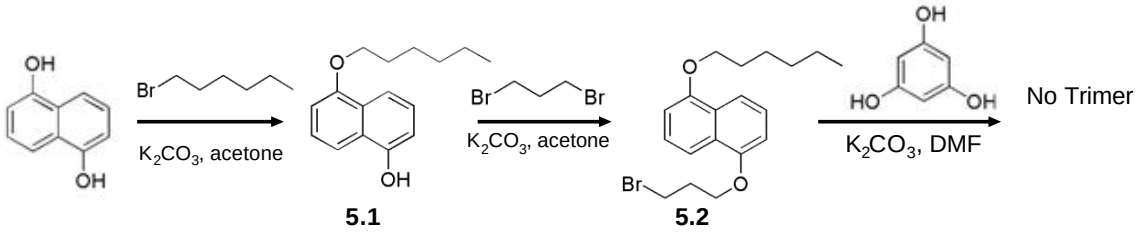

Scheme 5.1 Unsuccessful tri-Dan synthesis.

It was thought that by spreading out the reactive sites on the core, steric barriers to synthesis of the trimer could be minimized. Reacting phloroglucinol with an excess of 1,3-dibromopropane yielded compound **5.3**. This was reacted with three equivalents of monoalkylated Dhn **5.4** to afford the desired trimer product **5.6** in decent yields. Apparently spreading out the reactive sites on the core sterically allowed for the formation of the timer. Trimer **5.7** was synthesized in a similar fashion from the mono-alkylated Dhn compound **5.5**, and then hydrolyzed to yield tri-acid Dan trimer **5.8**.

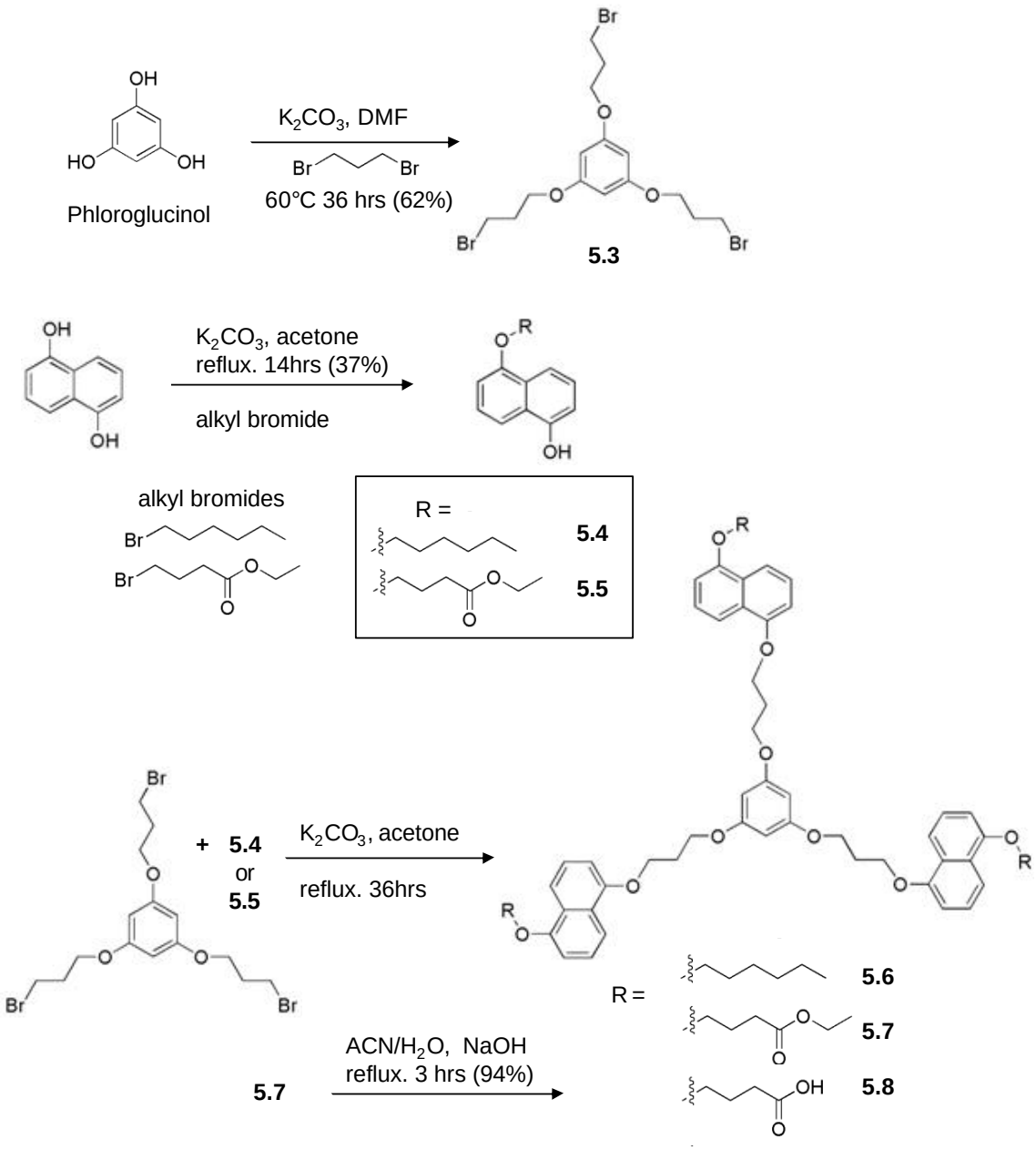

Scheme 5.2 Synthesis of C_3 Dan trimers.

5.2.2.2 C_3 Ndi Trimers

Initial attempts at synthesis of the Ndi trimer employed a Heck coupling with three equivalents of asymmetric alkene Ndi **5.9** and 1,3,5-tribromobenzene. This reaction gave a large number of products, at least 7 by TLC, and the trimer mass appeared as a very minor peak in the mass spec analysis and could not be isolated. It is likely that a number of diastereomers and conformational isomers were present in the crude reaction mixtures. It was proposed that switching to the coupling with alkyne Ndi **5.10** would eliminate isomers, however no coupling was observed. It was determined that **5.10** was complexing with the Pd catalyst, probably through an allyl system after deprotonation of the hydrogens a to the alkyne. Scheme 5.3 shows these ultimately unsuccessful synthetic paths.

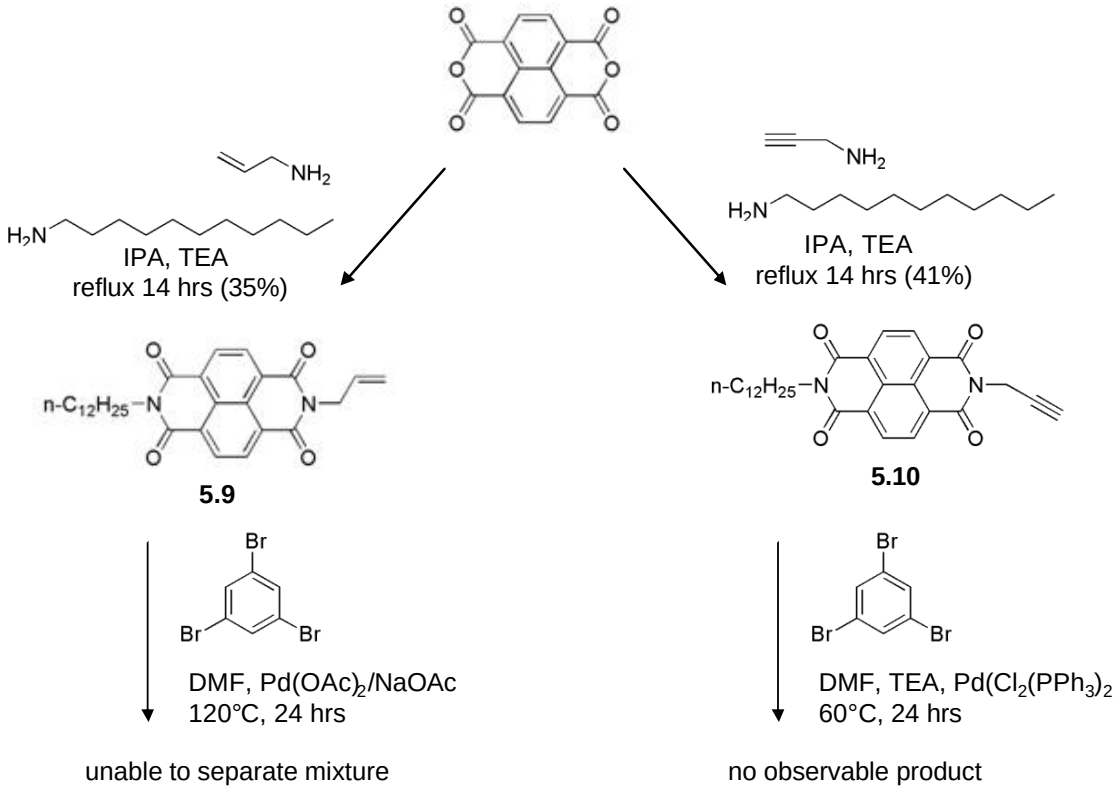

Scheme 5.3 Route towards rigid Ndi trimers.

The transition metal coupling reactions of three Ndi units to one core were abandoned for a reaction scheme that could be more easily monitored. Trimesic acid was activated with pentaflurophenol (PFP) to give the reactive core compound **5.11**. It was thought that this compound would react cleanly with asymmetric monoamine Ndi compounds **5.12-5.15** and **5.18**. The synthesis of these compounds is detailed in scheme 5.4.

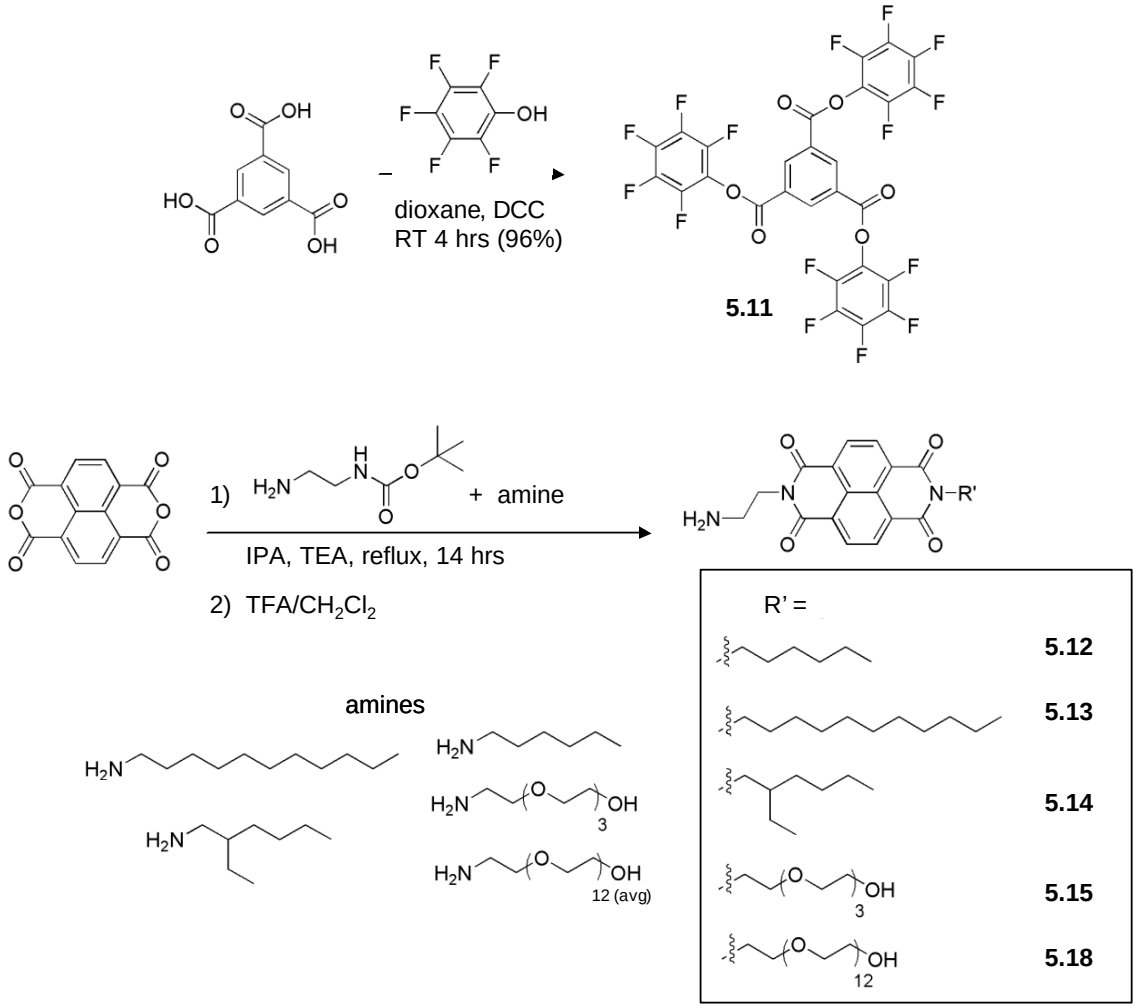

Scheme 5.4 Synthesis of an activated C_3 core and asymmetric Ndi amines.

Reactions of **5.11** with Ndi amines are detailed in scheme 5.5. In the reactions of **5.11** with compounds **5.12** and **5.13** a precipitate formed in the reaction that was completely insoluble in any solvent. The Ndi monomers and some PFP were present in the filtered solution by TLC, leading to the conclusion that the first condensation took place to yield an insoluble product, frustrating the proposed reaction scheme. Compound

5.14 was synthesized in hopes that the branching on the side would increase solubility, and **5.15** was designed to increase the affinity of the compounds for the DMF solvent. Unfortunately, a completely insoluble powder precipitated from the reaction. However, monitoring the course of the reaction revealed a new spot by TLC which grew and then decreased in intensity over the course of the reaction. Mass spec analysis of the solution revealed the mass expected for one condensation, and it was reasoned that the monomer was formed and soluble, but that upon further condensation the dimer crashed out of the reaction as a completely insoluble compound.

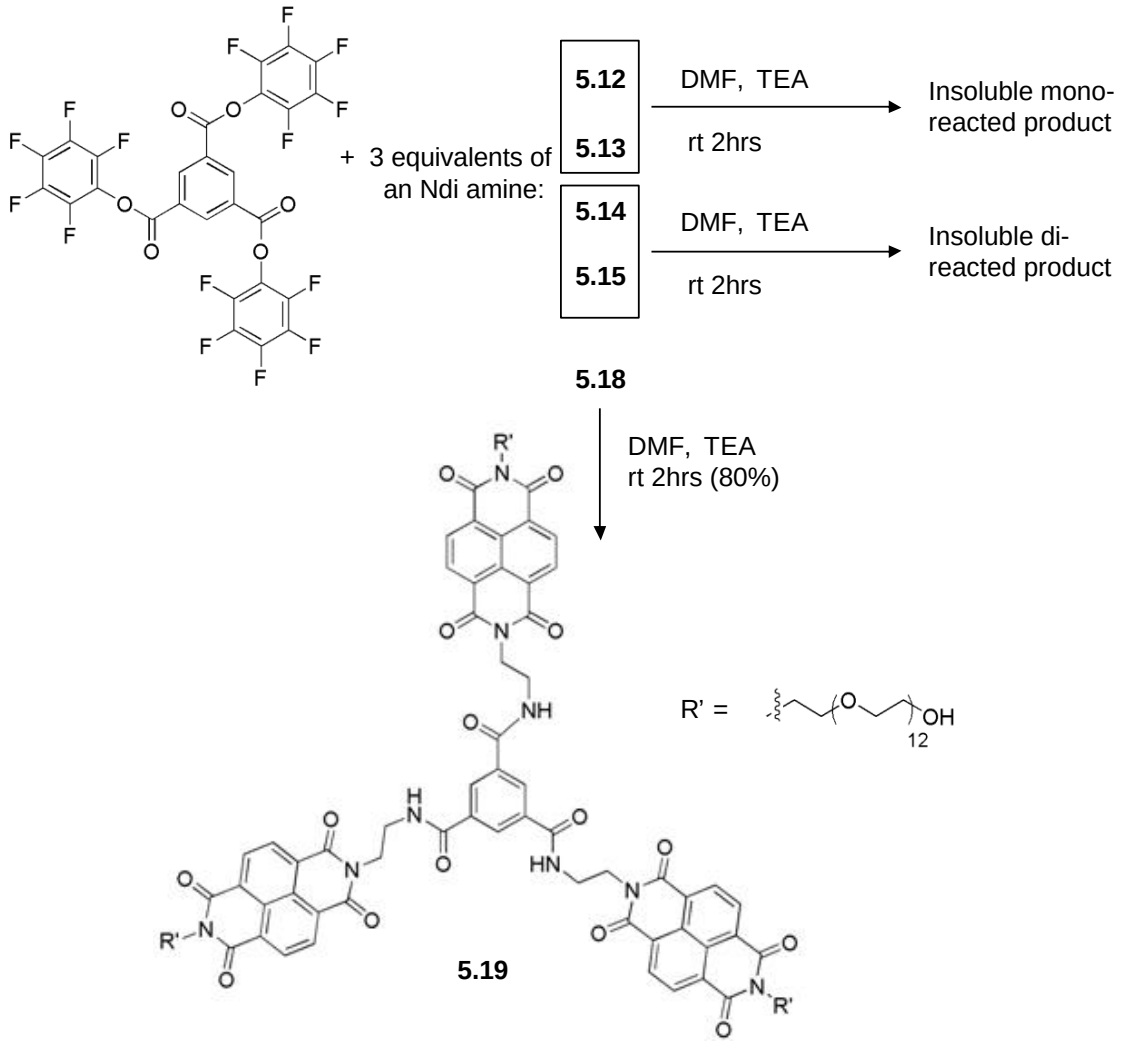

Scheme 5.5 Synthesis of C_3 Ndi trimer.

Compound **5.17** was synthesized according to scheme 5.6 from low molecular weight poly(ethylene glycol) and used in the synthesis of Ndi **5.18** (scheme 5.4). It is not ideal to have an inexact mass for the Ndi reagent, but with the encouraging result from the reaction with **5.15**, the possible success of this route in synthesizing a soluble trimer was explored. Following the reaction by TLC revealed two spots which successively

grew and then faded in intensity, presumed to be the mono and di-Ndi compounds. The final product precipitated from solution, but upon isolation was found to be slightly soluble in DMSO and was ultimately confirmed as the Ndi trimer **5.19** (Scheme 5.5).

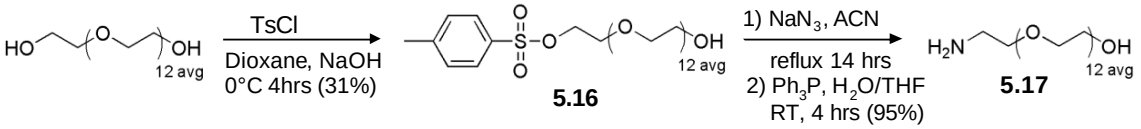

Scheme 5.6 Synthesis of amine terminated PEG.

5.2.2.3 Asymmetric Cores

Initial work towards asymmetric planer trimers was carried out with the synthesis of functionalized cores according to scheme 5.7. Phloroglucinol was fully acylated with and excess of acetic anhydride to yield compound **5.20**, and then partially reduced to give both the di and mono-acylated products **5.21** and **5.22**. Quenching the reaction immediately upon the appearance of phloroglucinol in the reaction resulted in the easiest purification and highest yields of both compounds. The compounds were then protected with benzyl bromide and the acyl groups hydrolyzed to yield the electron-rich asymmetric cores **5.23** and **5.34**. The diethyl protected trimesic acid was activated with PFP to give **5.25**, ready to be functionalized as the electron-poor asymmetric cores. This gives both an electron-rich and electron-poor core which can be functionalized according to the chemistry of the C_3 trimers mentioned above in a step wise fashion to yield the asymmetric designs in figure 5.2b and c.

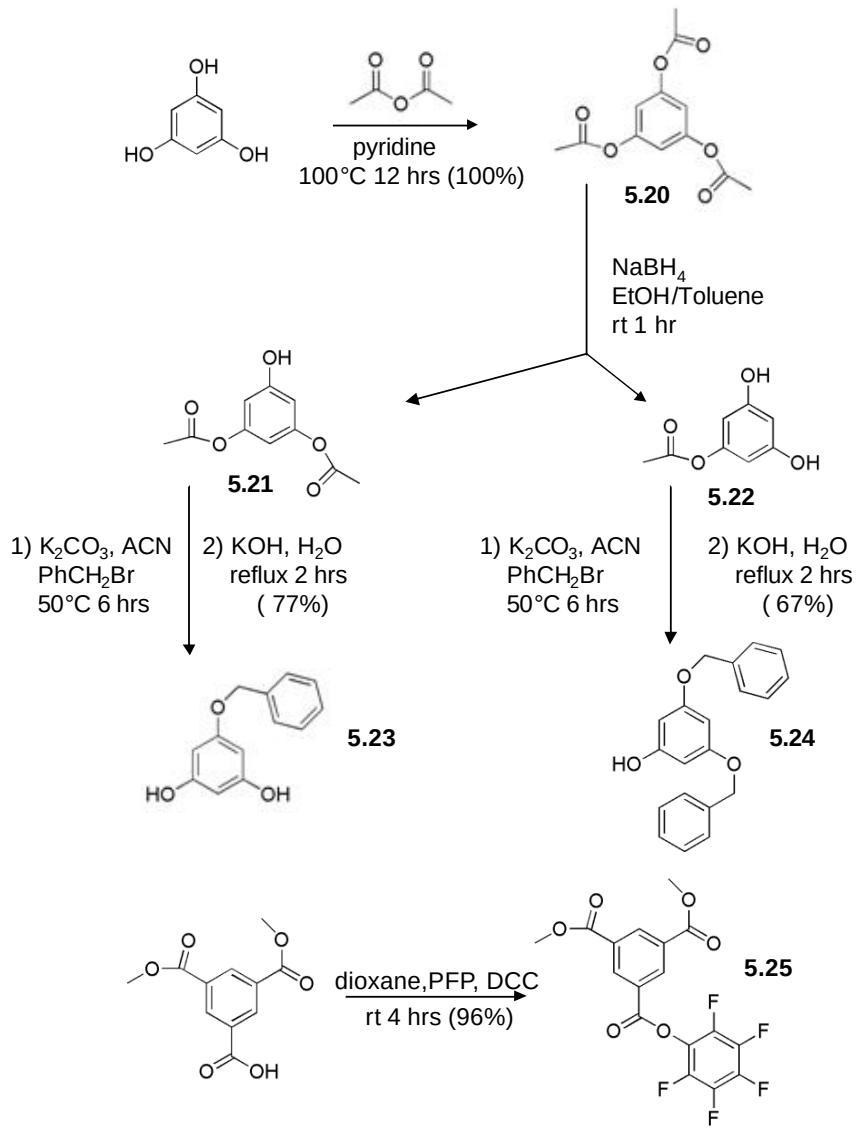

Scheme 5.7 Synthesis of cores for asymmetric trimers.

5.2.3 Results and Discussion

5.2.3.1 Solubility of Trimers

The two Dan trimers **5.6** and **5.7** are both moderately soluble in polar organic solvents including DMF and DMSO. Surprisingly, compound **5.7** exhibits no solubility in either neutral or basic aqueous solution. The inability to synthesize any Ndi trimer except for **5.19**, which has three 500 mW PEG chains attached, highlights that in future designs of multi-Ndi molecules, solubility must be specifically addressed, whether for use in water, organic solvents, or as a melt. The relatively long PEG chains on Ndi **5.18** finally allowed for the synthesis of compound **5.19,** but it displayed only a moderate solubility in DMSO (~10 mM), and a solubility of about 10μM in water.

5.2.3.2 Solubility of mixtures and UV-Vis Data with Monomers

Equal molar quantities of compounds **5.8** and **5.19** were added to buffered aqueous solution. The sample was sonicated for one hour, and then stirred overnight. The Dan trimer **5.7** remained completely insoluble and no enhancement of **5.19** solubility was observed. UV-Vis analysis of the sample showed no evidence of any Dan:Ndi complexation.

The soluble Dan and Ndi neutral monomers (Figure 4.1a) were added to the complementary trimers **5.19** and **5.8** in order to affect their solubility and detect the possibility of complexation. There was no observable effect on aqueous suspension of Dan trimer **5.8** with addition of up to 1mM of the Ndi monomer. No absorbance of the Dan unit or charge transfer band was detected.

At 3 and 10 equivalents of the Dan monomer with Ndi trimer **5.19** no effect was observed by UV-Vis. However, at 1mM concentration of the Dan monomer, a two nanometer red shift and a charge transfer band were detected in the UV-Vis spectra of the solution indication that there was some Dan:Ndi complexation (Figure 5.3). No or very little difference in the solubility of compound **5.19** was observed.

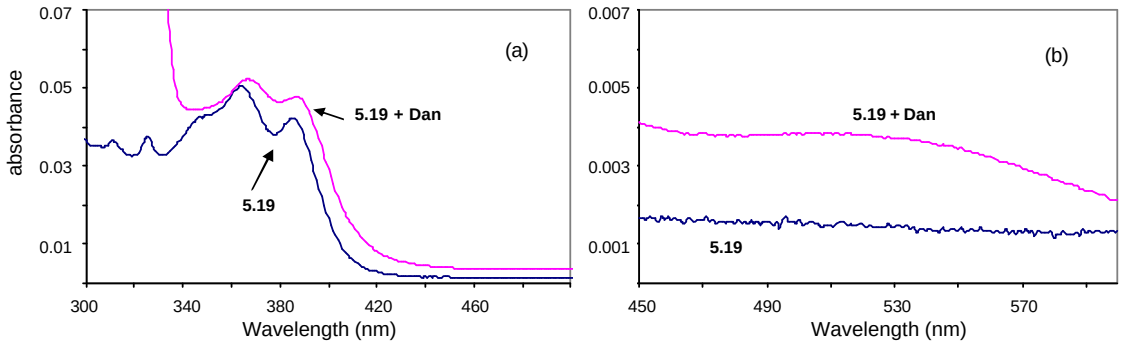

Figure 5.3 UV-Vis absorption spectra of aqueous solutions of **5.19** and **5.19** in 1mM Dan monomer at maximum solubility of the trimer. (a) Slight hypochromism of Ndi units with Dan monomer. (b) Charge transfer band in the Ndi trimer Dan mixture.

It is mildly surprising that Dan trimer **5.8**, with three negative charges, is not at all soluble in any aqueous solution. Even with addition of an excess of water soluble Ndi monomer, a technique successful in solubilizing polyDan compound 2.10, no solubility was observed. The hydrophobic area of the molecule must simply be too large for the charges to pull it into solution, and perhaps it is kinetically too difficult to solvate the trimer with added monomer. The observed complexation of Ndi trimer **5.19** with an excess of the neutral Dan at least shows that there can be complexation in the trimer geometry.

5.2.3.3 Melts with C_3 Trimers

Dan trimer **5.6** with the alkyl chains was combined in a vial with Ndi trimer **5.19** and then melted to observe any complexation or mesophase formation. Compound **5.6** melted maintaining a light yellow color, but no interaction was observed with **5.19** which remained a solid throughout heating to 250°C. Similar results of no Dan:Ndi interaction were observed when mixtures of **5.19** and Dan monomers **3.2** and **3.3** were heated together.

Compound **5.6** was melted together with an equal aromatic equivalent of Ndi monomers **3.8** and **3.9**. In both cases the mixture immediately changed in color from off white to a deep red, indicative of a donor-acceptor interaction. Polarized optical microscopy of the mixture of **5.6** with chiral monomer **3.9** on cooling revealed a sheet-like structure for the mesophase, similar to the B_1 phase texture of the mixtures with compound **3.9** in chapter 3 (Figure 5.5a). Cooling from the melt of the **5.6**:**3.8** mixture exhibited a mesophase texture completely unique from any previously observed. Anisotropic domains radiate outward from a point in a circular pattern, shown in figure 5.5b. This type of texture is diagnostic of hexagonal packing in the columnar mesophase (Demus 1996). The experiments in chapter 3 detail the C_2 symmetric monomers which exhibit controllable oblique rectangular columnar packing. As expected, no evidence of columnar hexagonal packing was observed. This exciting result highlights that additional elements of control over mesophase properties are possible with Dan:Ndi complexation by the rational synthetic design of the components. It is also apparent that having only

one component with a specifically designed structure, in this case the Dan trimer, is all that is necessary for structural control, illustrated in figure 5.5c.

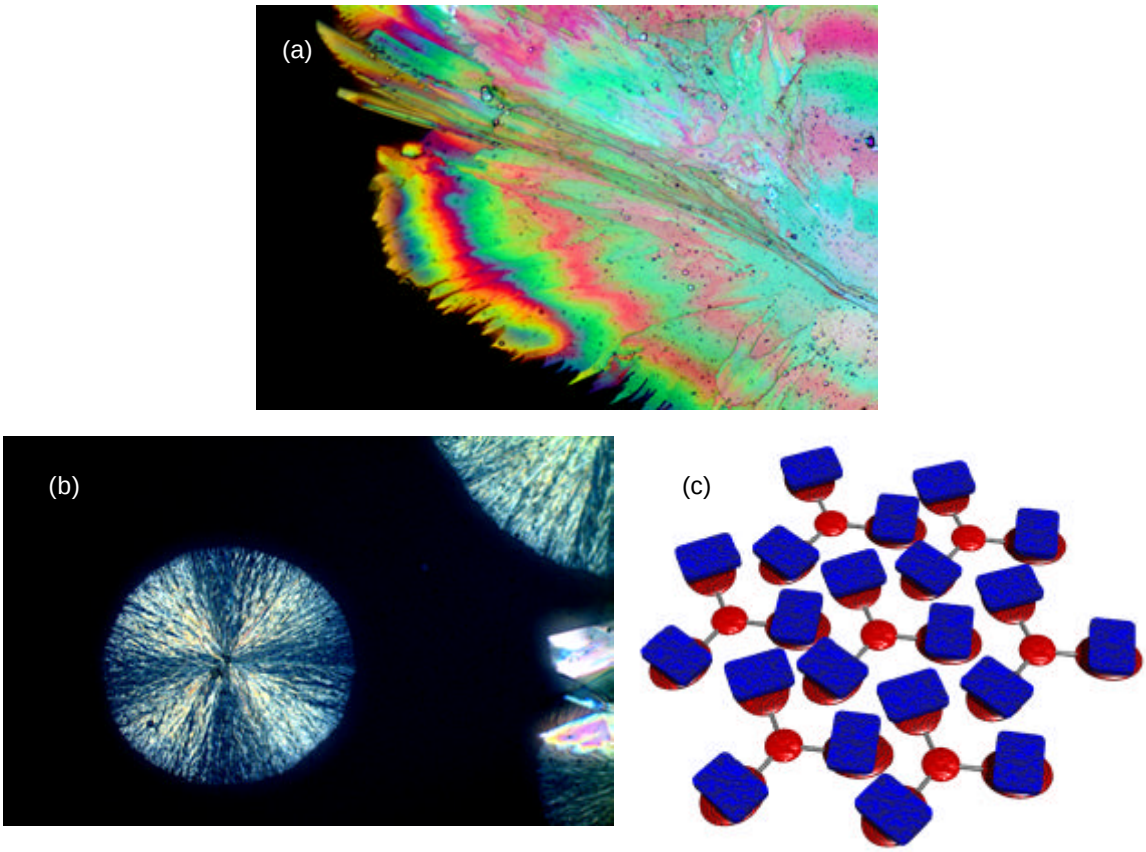

Figure 5.5 (a) Polarized optical microscopy of the chiral B_1 phase of the equal aromatic equivalent mixture of **5.6** and **3.9**. (b) Polarized optical microscopy of the Col_h phase of the equal aromatic equivalent mixture of **5.6** and **3.8**. (c) schematic of the proposed packing of Dan trimer **5.6** interacting with Ndi monomer.

5.3 DESIGNS TOWARD INCREASING SOLUBILITY

The difficulty with solubility for the polymers of chapter 2, the neutral oligomers of chapter 4, and the trimers discussed above have made it quite clear that any synthetic

manipulation of Dan or Ndi molecules for association in, or processing from, aqueous solution requires attention to solubilizing groups. Two ways in which this can be addressed are: 1) adding functionality to the Dan or Ndi units in order to allow for the appendage of additional solubilizing groups, and 2) maximizing the effectiveness of any solubilizing groups used.

5.3.1 Side Chains in the 2,6 Position of the Dan Unit

The addition of functional handles to the Dan molecule would allow for connection of extra groups for solubilizing Dan oligomers, and also increase the connectivity options for the synthesis of alternative designs. By appending additional hydrophilic groups to the Dan core, such as carboxylic acids or PEG chains, Dan oligomers and polymers may become water soluble. New covalent handles for connectivity would allow for additional geometric assemblies of Dan molecules, and therefore further options in mesophase and polymer designs.

A successful route towards Dan funtionalization was achieved according to scheme 5.8. Dhn was di-alkylated with allyl bromide to give compound **5.26**. This was then heated to 180°C over 2 hours to afford compound **5.27** via a double Cope rearrangement in good yield. The resulting compound has alkene functionality in the 2,6 positions of the Dhn, in addition to the 1,5 hydroxy groups. The allyl groups can be added one at a time for control of asymmetric products.

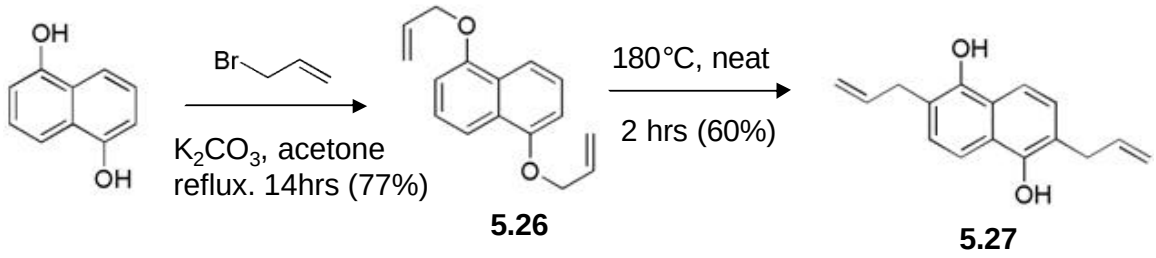

5.26 **5.27**

Scheme 5.8 Synthesis of 2,6 substituted Dhn.

The alkenes in the 2,6 positions of the Dhn can serve as a means for adding aqueous solubilizing groups such as carboxylic acids or PEG chains to the Dan core, or as alternative connection points for new oligomers or polymers designs (Figure 5.6). Examples of possible applications include oxidation to the diacid to serve as charged solubilizing groups, or further addition of peg chains for neutral solubilizing groups. The alkenes could also be used as sites for metathesis polymerizations of the Dan unit.

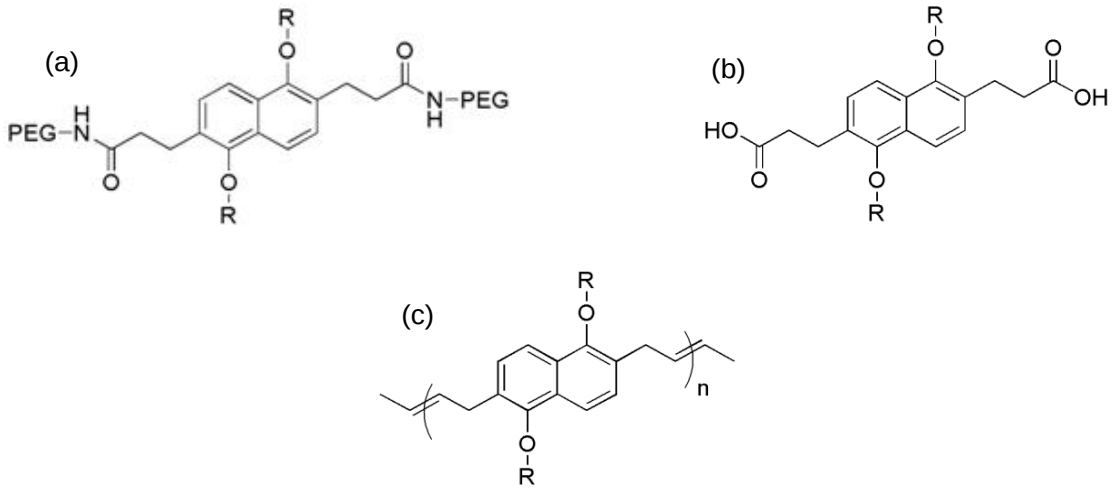

Figure 5.6 (a) Two additional PEG chains on the Dan unit. (b) Two additional negative charges on the Dan unit. (c) Oligomer and polymer formation via metathesis.

5.3.2 Tri-Chain Solubilizing Groups

Compact molecules with relatively facile synthesis that could be attached to Dan and Ndi molecules as solubilizing pieces would be extremely valuable to future designs. Derivatives of the commercially available ethyl gallate could serve as such solubilizing molecules (Brunsveld 2000). By reacting the three hydroxyl groups with alkyl chains or PEG chains, molecules should become stericly frustrated and unable to pack well due to congestion immediately next to the ring, while at the same time giving an increased area for solvation, along with degrees of freedom for mesophase applications. The ester can then be deprotected and activated to attach the molecule to various Dan and Ndi designs. The synthesis of tri-TEG and tri-hexane molecules to serve as solubilizing groups in aqueous solution or in a melt are shown in scheme 5.9.

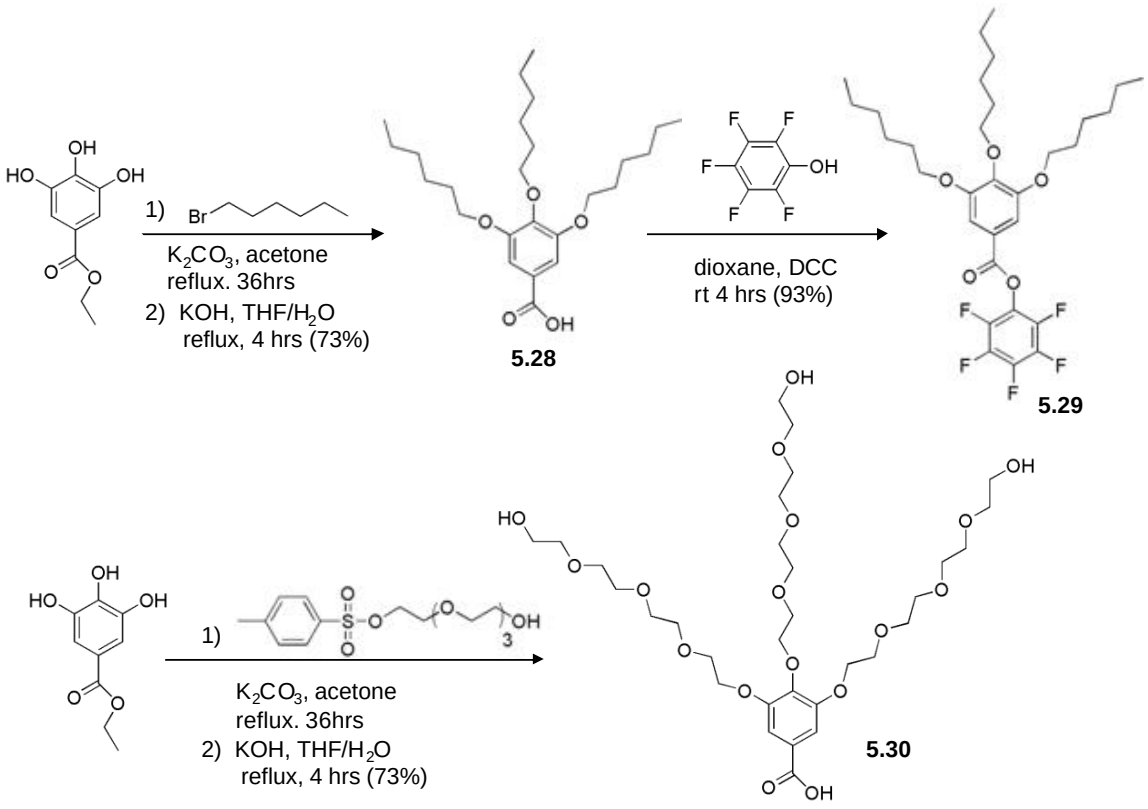

Scheme 5.9 Synthesis of potential solubilizing groups.

Figure 5.7 shows an energy minimized computer model in which the alkyl chains are forced to point in opposing directions to minimize crowding next to the ring. This should hinder crystal packing and promote solubility. These molecules can be easily appended to any of the geometries discussed here, and future designs, to affect solubility and processing.

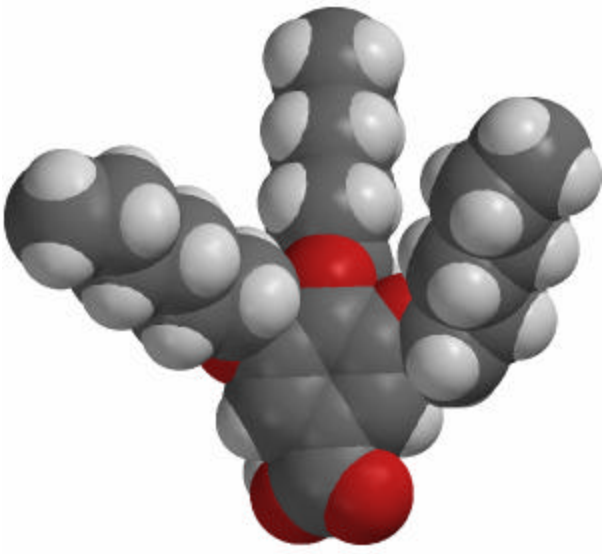

Figure 5.7 Space filling model of tri-hexane compound **5.28**.

5.4 SPACER FOR EXTENDED CONJUGATION

Increasing the conjugated surface area of the donor and acceptor molecules may lead to greater orbital overlap and association of complexed molecules. Extending the conjugated area should also lower the energy of the molecular orbitals, and perhaps allow for a more efficient charge-transfer interaction. This calamitic design may offer a route to additional liquid crystalline donor-acceptor phases such as columnar smectic or nematic (Demus 1996). An asymmetric conjugated design, with electron rich and electron deficient aromatics on opposite sides, could lead to systems with ferroelectric properties.

Dan and Ndi molecules were elongated with a conjugated spacer according to scheme 5.10. 1-hydroxy-5-bromonaphthalene was not commercially available, so the 2-6 molecule was used as a replacement in this initial experiment. *p*-Divinyl benzene was

purified from the commercially available isomeric mixture by bromination, selective crystallization, and then debromination. It was then reacted with either compound **5.31** or **5.32** via Heck coupling to yield compounds **5.33** and **5.34** respectively. **5.33** exhibits blue fluorescence, and **5.34** yellow under longwave UV light.

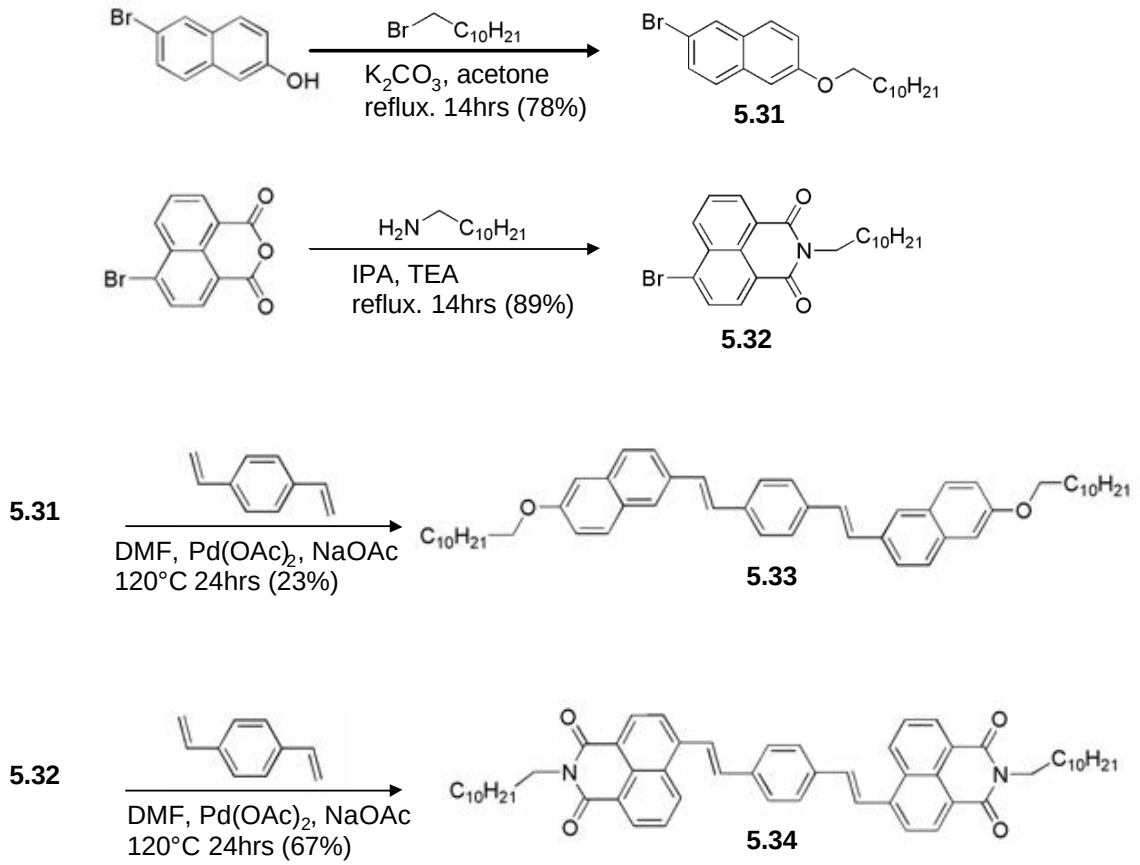

Scheme 5.10 Synthesis of pi extended Dan and Ndi.

A proposed asymmetric compound from this scheme, and its electrostatic surface potential, is shown in figure 5.8. This molecule should be ferroelectric if a liquid crystalline phase can be obtained, and could stack in both an intra and inter-molecular

geometries. Use of the tri-hexyl group **5.29** may aid in mesophase formation. Further research into extended conjugation of asymmetric aromatic donor-acceptor molecules, specifically finding ones that are well geometrically and electrostatically matched, could prove useful in moving towards molecular electronics and responsive devices.

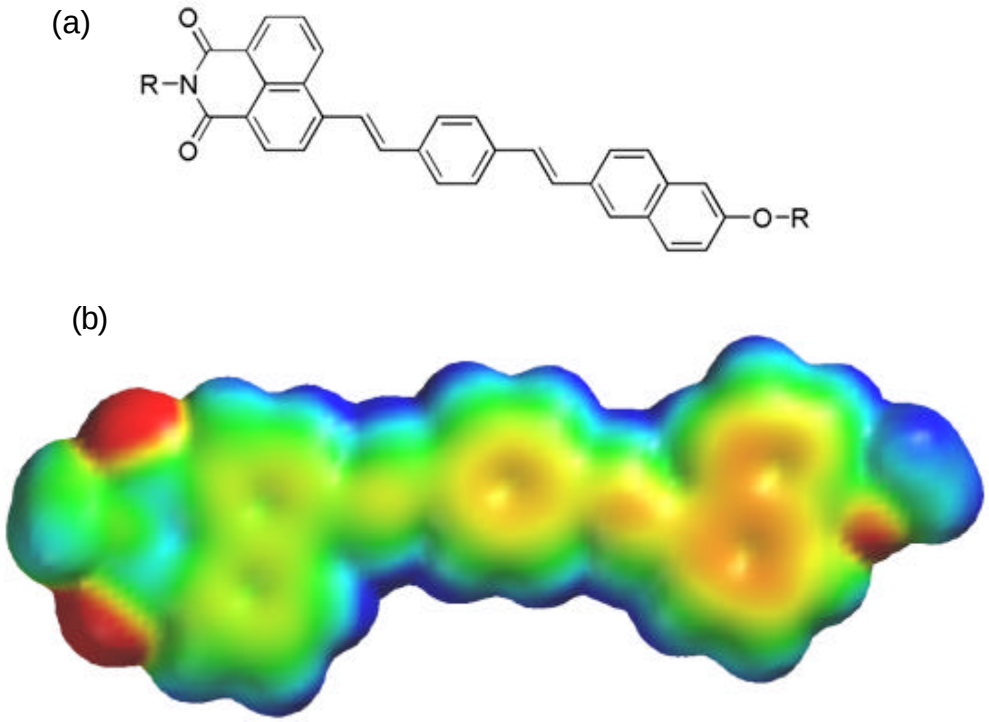

Figure 5.8 (a) Proposed asymmetric conjugated donor-acceptor. (b) Electrostatic surface potential.

5.5 CONCLUSIONS

The work leading to the C_3 trimers of this chapter highlights once again the necessity of specifically addressing the issue of solubility for synthesizing aqueously

soluble Dan and Ndi molecules. In particular for derivatives with Ndi, solubility should be addressed in order to ensure that the target molecule can be made at all. Before any other Ndi molecular architectures are attempted, a plan for solubility at all stages should be drawn up, perhaps utilizing the proposed molecules **5.29** and **5.30**. Further investigations into cooperativity and the asymmetric designs should hold for confidence in solubility.

The apparent success of creating hexagonal packing in a mesophase with C_3 Dan trimer **5.5** and Ndi monomers is inspiring. Intelligently designed control over the properties and structures of mesophases and crystalline phases is highly desirable and it looks as though it might be achieved with only one component, namely the Dan, directing assembly. One can imagine additional studies that could include new C_3 trimers, tetramers, straight and bent dimers, and any other accessible geometries.

5.6 EXPERIMENTAL

General procedures. (2-Amino-ethyl)-carbamic acid *tert*-butyl ester was synthesized according to work previously published in the Iverson group (Cubberley 2000).

1-Hexyl-5-hydroxy-naphthalene 5.1. 1,5-Dihydroxynaphthalene (5.0 g, 31 mmol), 1-bromohexane (7.2 g, 44 mmol), and catalytic amounts of LiI and 18-crown-6 were added to acetone (100 ml). The solution was degassed with argon, and K_2CO_3 (6.1g, 45 mmol) added. The mixture was heated to reflux and allowed to stir under argon for 14 hours. The brown mixture was filtered, concentrated under reduced pressure and then CH_2Cl_2

(150 ml) was added. The solution was heated and stirred, then filtered and concentrated under reduced pressure. The brown sludge was then purified by column chromatography (60% CH_2Cl_2, 25% hexanes, 15% acetone) to yield the product as a thick brown oil in 31% yield. ^{13}C NMR (300 MHz, $CDCl_3$) *d* 157.0, 156.6, 129.2, 127.0, 126.5, 125.3, 114.5, 113.5, 109.7, 104.8, 69.5, 29.0, 25.7, 31.5, 22.9, 14.5; ^{1}H NMR (300 MHz, $CDCl_3$) *d* 7.83 (d, *J* = 8.2 Hz, 1H), 7.71 (d, *J* = 8.3 Hz, 1H), 7.26 (m, 2H), 6.69 (d, 7.3 Hz, 1H), 6.60 (d, *J* = 7.2 Hz, 1H), 4.97 (b, 1H), 3.96 (t, *J* = 5.9 Hz, 2H), 1.71 (p, *J* = 5.7 Hz, 2H) 1.30 (m, 6H), 1.01 (t, *J* = 5.1 Hz, 3H) ppm; ESI –MS (positive-ion) 245 ($[M + H]^+$).

5-Hexyl-1-(3-bromopropyl)hydroxy-naphthalene 5.2. **5.1** (1.74 g, 7.1 mmol) 1,3-dibromopropane (6 ml) and a catalytic amount of 18-crown-6 were added to acetone (100 ml). The solution was degassed with argon, and K_2CO_3 (1 g, 7.2 mmol) added. The mixture was heated to reflux and allowed to stir under argon for 14 hours. The brown mixture was filtered, concentrated under reduced pressure and purified by column chromatography (70% CH_2Cl_2, 25% hexanes, 5% acetone) to yield the product as a light brown solid in 82% yield. ^{13}C NMR (300 MHz, $CDCl_3$) *d* 157.1, 156.9, 128.4, 128.3, 125.2, 125.0, 115.0, 114.5, 104.6, 103.9, 69.5, 67.7, 32.0, 30.5, 30.3, 29.4, 25.7, 22.6, 14.3; ^{1}H NMR (300 MHz, $CDCl_3$) *d* 7.78 (d, *J* = 8.0 Hz, 2H), 7.21 (t, *J* = 7.8 Hz, 2H), 6.68 (d, 7.3 Hz, 2H), 4.21 (t, *J* = 6.4 Hz, 2H), 4.02 (p, *J* = 5.5 Hz, 2H), 3.61 (p, *J* = 5.4 Hz, 2H), 1.98 (p, *J* = 5.2 Hz, 2H) 1.71 (p, *J* = 6.2 Hz, 2H) 1.27 (m, 6H), 0.96 (t, *J* = 5.1 Hz, 3H) ppm; ESI –MS (positive-ion) 365 ($[M + H]^+$).

1,3,5-*tris*-(3-bromobutoxy)benzene 5.3. Phloroglucinol (4.0 g, 32 mmol) 1,3-dibromopropane (40 ml) and a catalytic amount of 18-crown-6 were added to DMF (40 ml). The solution was degassed with argon, and K_2CO_3 (15 g, 108 mmol) added. The reaction was heated to 40°C for and allowed to stir under argon for 16 hours (DO NOT OVERHEAT). The mixture was then filtered, concentrated under reduced pressure (DO NOT OVERHEAT), left under high vacuum at room temp. for 14 hours and purified by two iterations of column chromatography (toluene 80%, hexanes 15%, acetone 5%) to yield the title compound as yellow crystals (62%). Mp 37-40°C; ^{13}C NMR (300 MHz, $CDCl_3$) *d* 160.9, 94.7, 66.0, 32.6, 31.9; ^{1}H NMR (300 MHz, $CDCl_3$) *d* 6.15 (s, 3H), 4.05 (t, *J* = 6.0 Hz, 6H), 3.35 (t, 6.6 Hz, 6H), 2.23 (p, *J* = 6.3 Hz, 6H) ppm; ESI –MS (positive-ion) 487 ($[M + H]^+$).

Ethyl-4-(1-hydroxynaphthalen-5-yloxy)butanoate 5.5. According to the method used for **5.1**, **5.5** was obtained as a brown solid in 28% yield. ^{13}C NMR (300 MHz, $CDCl_3$) *d* 174.5, 158.3, 157.0, 128.4, 127.2, 126.3, 125.1, 114.3, 113.8, 109.1, 104.2, 68.3, 60.9, 30.4, 24.2, 14.3; ^{1}H NMR (300 MHz, $CDCl_3$) *d* 7.81 (d, *J* = 8.0 Hz, 1H), 7.71 (d, *J* = 7.9 Hz, 1H), 7.31 (m, 2H), 6.67 (m, 2H), 4.23 (q, *J* = 6.2 Hz, 2H), 3.92 (t, *J* = 5.4 Hz, 2H), 2.31 (t, *J* = 5.1 Hz, 2H), 2.06 (p, *J* = 5.2 Hz, 2H) 1.34 (t, *J* = 4.9 Hz, 3H) ppm; ESI –MS (positive-ion) 275 ($[M + H]^+$).

1,3,5-tris(3-(1-(hexyloxy)naphthalene-5-yloxy)benzene 5.6. **5.1** (0.94 g, 3.2 mmol), **5.3** (0.43 g, 1.0 mmol), and a catalytic amount of 18-crown-6 were added to acetone. The solution was degassed with argon, and K_2CO_3 (0.5 g, 3.6 mmol) added. The solution

was allowed to stir at reflux under argon for 36 hours, allowed to cool and then filtered. The filtrate was concentrated under reduced pressure, and the brown sludge was purified via column chromatography to yield the title compound as an off-white flakey solid in 83% yield. M.p. 78-82°C ^{13}C NMR (300 MHz, $CDCl_3$) *d* 161.0, 154.9, 154.6, 127.1, 127.0, 125.4, 125.2, 114.6, 114.2, 105.6, 105.5, 94.5, 68.4, 65.1, 64.9, 31.9, 29.6, 29.5, 26.2, 22.9, 14.3; ^{1}H NMR (300 MHz, $CDCl_3$) *d* 7.91 (d, *J* = 8.4 Hz, 3H), 7.88 (d, *J* = 9.3 Hz, 3H), 7.35 (m, 6H), 6.88 (d, *J* = 8.6 Hz, 3H), 6.83 (d, *J* = 7.8 Hz, 3H), 6.19 (s, 3H), 4.31 (t, *J* = 6.2 Hz, 6H), 4.23 (t, *J* = 5.6 Hz, 6H) 4.14 (t, *J* = 5.4 Hz, 6H), 2.38 (p, *J* = 5.2 Hz, 6H), 1.95 (p, *J* = 5.3 Hz, 6H), 1.61 (p, *J* = 5.1 Hz, 6H), 1.43 (m, 12H) 0.98 (t, *J* = 5.7 Hz, 9H) ppm; ESI –MS (positive-ion) 979 ($[M + H]^+$).

1,3,5-tris[Ethyl-4-(1-hydroxynaphthalen-5-yloxy)butanoate]benzene 5.7. According to the method used for **5.6**, **5.7** was obtained as a white solid in 68% yield. M.p. 92-96°C ^{13}C NMR (300 MHz, $CDCl_3$) *d* 173.5, 161.0, 154.6, 126.9, 125.4, 114.5, 105.7, 105.6, 94.5, 67.2, 65.0, 64.9, 60.7, 31.3, 29.6, 25.0, 14.5; ^{1}H NMR (300 MHz, $CDCl_3$) *d* 7.86 (d, *J* = 8.4 Hz, 6H), 7.36 (m, 6H), 6.88 (d, *J* = 8.6 Hz, 3H), 6.81 (d, *J* = 8.4 Hz, 3H), 6.16 (s, 3H), 4.30 (t, *J* = 6.2 Hz, 6H), 4.19 (m, 12H) 2.64 (t, *J* = 7.2 Hz, 6H), 2.38 (p, *J* = 5.8 Hz, 6H), 2.27 (p, *J* = 5.6 Hz, 6H), 1.28 (t, *J* =7.2 Hz, 9H), 1.43 (m, 12H) ppm; ESI –MS (positive-ion) 1070 ($[M + H]^+$).

1,3,5-tris[4-(1-hydroxynaphthalen-5-yloxy)butanoic acid]benzene 5.8. 5.7 (0.4 g, 0.37 mmol) was dissolved in ACN (30 ml) and 1 M KOH solution (15 ml) added. The solution was allowed to reflux for 2 hours, allowed to cool and then neutralized with 2 M

HCl. The ACN was removed under reduced pressure, and the brown solid filtered and washed with 1 M HCL (30 x 2 ml) and distilled water (30 x 5 ml) to yield the title compound as a brown solid in 94% yield. ^{13}C NMR (300 MHz, DMSO) *d* 177.3, 158.9, 157.5, 156.1, 128.2, 128.3, 125.5, 125.3, 114.6, 114.5, 104.5, 104.3, 92.3, 68.7, 65.6, 65.2, 32.4, 29.1, 24.1; ^{1}H NMR (300 MHz, DMSO) *d* 7.74 (d, *J* = 8.7 Hz, 3H), 7.73 (d, *J* = 8.6 Hz, 6H), 7.35 (m, 6H), 6.99 (d, *J* = 8.2 Hz, 3H), 6.89 (d, *J* = 8.4 Hz, 3H), 6.16 (s, 3H), 4.25 (t, *J* = 6.0 Hz, 6H), 4.14 (m, 12H) 2.51 (t, *J* = 7.1 Hz, 6H), 2.27 (p, *J* = 5.8 Hz, 6H), 2.07 (p, *J* = 5.6 Hz, 6H) ppm; ESI –MS (positive-ion) 986 ($[M + H]^+$).

2-propene-7-Dihexyl-benzo[*lmn*][3,8]phenanthroline-1,3,6,8-tetraone (5.9). 1,4,5,8-Naphthalenetetracarboxylic dianhydride (3.2g, 12mmol) was placed into a round bottom flask and suspended in isopropanol (150 ml). A mixture of 1-aminododecane (2.3g, 12 mmol), allyl amine (0.68 g, 12 mmol), TEA (2.6g, 25mmol), and isopropanol (70ml) was slowly added and the solution was allowed to stir at room temperature for 30 min, and then heated at reflux for 12 hours. The solution was allowed to cool to room temperature and purified by column chromatography (70% CH_2Cl_2/ 26% Hexanes/ 4% Acetone) to afford **5.9** (2.1 g, 35% yield) as an off-white solid. ^{13}C NMR ($CDCl_3$) *d* 159.8, 159.5, 139.8, 139.7, 135.2, 135.1, 134.3, 116.2, 41.6, 40.5, 31.5, 29.8, 29.7, 29.6, 29.5, 29.4, 27.4, 26.8, 22.9, 14.2; ^{1}H NMR ($CDCl_3$) *d* 8.38 (s, 4H), 5.83 (m, 1H), 5.27 (m, 2H), 4.76 (d, *J* = 7.8 Hz, 2H), 3.94 (t, *J* = 7.4 Hz, 2H), 1.76 (p, *J* = 7.5 Hz, 2H), 1.40 (m, 4H), 1.28 (m, 14H), 0.94 (t, *J* = 6.0 Hz, 3H) ppm; ESI –MS (positive-ion) 475 ($[M + H]^+$).

2-propyne-7-Dihexyl-benzo[*lmn*][3,8]phenanthroline-1,3,6,8-tetraone (5.10). According to the method used for **5.9**, **5.10** was obtained as light pink flaky crystals in 41% yield. ^{13}C NMR ($CDCl_3$) *d* 159.8, 159.5, 139.8, 139.7, 135.2, 135.1, 78.1, 71.1, 40.5, 31.5, 29.8, 29.7, 29.6, 29.5, 29.4, 28.5, 27.4, 26.8, 22.9, 14.2; ^{1}H NMR ($CDCl_3$) *d* 8.82 (m, 4H), 5.01 (s, 2H), 4.46 (t, *J* = 6.8 Hz, 2H), 2.23 (s, 1H), 1.76 (p, *J* = 7.5 Hz, 2H), 1.40 (m, 4H), 1.28 (m, 14H), 0.94 (t, *J* = 6.0 Hz, 3H) ppm; ESI –MS (positive-ion) 474 ($[M + H]^+$).

Tris(perfluorophenyl) benzene-1,3,5-tricarboxylate 5.11. Trimesic acid (4 g, 19 mmol) and pentafluorophenol (10.5 g, 57 mmol) were dissolved in dioxane (300 ml) and then 1,3-dicyclohexylcarbodiimide (DCC) (11.7 g, 56 mmol) was added. The mixture was stirred at room temperature for 4 hours, and then the dicyclohexylurea was filtered off, the filtrate concentrated under reduced pressure, and purified via column chromatography (CH_2Cl_2 70%, acetone 30%) to yield the title compound in 96% yield. ^{13}C NMR ($CDCl_3$) *d* 165.2, 150.3, 142.0, 140.0, 137.7, 135.9, 130.1; ^{1}H NMR ($CDCl_3$) *d* 9.31 (s, 3H); ESI –MS (positive-ion) 709 ($[M + H]^+$).

2-(2-amino ethyl)-7-hexyl-benzo[*lmn*][3,8]phenanthroline-1,3,6,8-tetraone (5.12). 1,4,5,8-Naphthalenetetracarboxylic dianhydride (2.1g, 7.8 mmol) was placed into a round bottom flask and suspended in isopropanol (50 ml). A mixture of (2-Amino-ethyl)-carbamic acid *tert*-butyl ester (1.25 g, 7.8 mmol), hexylamine (0.79 g, 7.8 mmol), TEA (3 ml), and isopropanol (30ml) was slowly added and the solution was allowed to stir at room temperature for 30 min, and then heated at reflux for 12 hours. The mixture was

allowed to cool and then concentrated under reduced pressure. The pink solid was dissolved in a 50:50 mixture of CH_2Cl_2:TFA (80 ml) and allowed to stir at room temperature for six hours. The solvent was removed under reduced pressure, and ethanol was added (50 x 3 ml) and removed under reduced pressure, followed by an ethanol:TEA (90:10, 50ml) mixture, which was rotovaped down. The resulting pink sludge was purified via column chromatography (CH_2Cl_2 80%, acetone 10%, hexanes 9%, TEA 1%) to yield the title compound as a pink solid (31%). ^{13}C NMR ($CDCl_3$) *d* 159.5, 159.1, 139.9, 139.7, 135.2, 135.1, 120.7, 120.6, 52.1, 40.4, 37.9, 31.6, 27.4, 26.5, 22.8, 14.2; ^{1}H NMR ($CDCl_3$) *d* 8.28 (s, 4H), 4.20 (t, *J* = 7.5 Hz, 2H), 3.96 (t, *J* = 5.8 Hz, 2H) 2.95 (t, *J* = 6.4 Hz, 2H) 1.75 (p, *J* = 7.2 Hz, 2H), 1.45 (m, 2H), 1.36 (m, 4H), 0.91 (t, *J* = 6.9 Hz, 3H) ppm; ESI –MS (positive-ion) 395 ($[M + H]^+$).

2-(2-amino ethyl)-7-undecyl-benzo[*lmn*][3,8]phenanthroline-1,3,6,8-tetraone (5.13). According to the method used for **5.12**, **5.13** was obtained as off white crystals in 35% yield. ^{13}C NMR ($CDCl_3$) *d* 159.3, 159.2, 139.6, 139.5, 135.4, 135.2, 120.9, 120.8, 52.1, 40.5, 37.9, 31.9, 29.7, 29.7, 29.6, 29.5, 29.4, 29.3, 27.7, 26.8, 22.8, 14.1; ^{1}H NMR ($CDCl_3$) *d* 8.35 (s, 4H), 4.12 (t, *J* = 6.8 Hz, 2H), 3.79 (t, *J* = 5.6 Hz, 2H) 2.95 (t, *J* = 6.4 Hz, 2H) 1.75 (p, *J* = 7.2 Hz, 2H), 1.41 (m, 4H), 1.36 (m, 12H), 0.90 (t, *J* = 6.2 Hz, 3H) ppm; ESI –MS (positive-ion) 464 ($[M + H]^+$).

2-(2-amino ethyl)-7-(2-ethylhexyl)-benzo[*lmn*][3,8]phenanthroline-1,3,6,8-tetraone (5.14). According to the method used for **5.12**, **5.14** was obtained as a light pink solid in 29% yield. ^{13}C NMR (DMSO) *d* 161.3, 160.5, 140.8, 140.5, 136.1, 136.0, 121.2, 121.1,

54.0, 42.5, 31.5, 29.7, 28.5, 27.4, 26.8, 22.9, 14.2, 12.0; ^{1}H NMR (DMSO) *d* 8.63 (s, 4H), 4.10 (t, *J* = 6.3 Hz, 2H), 3.98 (t, *J* = 6.8 Hz, 2H), 2.87 (t, *J* = 6.9 Hz, 2H), 1.76 (p, *J* = 7.5 Hz, 2H), 2.83 (m, 1H), 1.29 (m, 8H), 0.87 (m, 6H) ppm; ESI –MS (positive-ion) 423 ($[M + H]^+$).

2-(2-amino ethyl)-7-{2-[2-(2-(2-hydroxy-ethoxy)-ethoxy]-ethoxy}-ethyl-benzo[*lmn*][3,8]phenanthroline-1,3,6,8-tetraone (5.15). According to the method used for **5.12**, **5.15** was obtained as an orange solid in 28% yield. ^{13}C NMR ($CDCl_3$) *d* 159.8, 159.5, 139.8, 139.7, 135.2, 135.1, 78.1, 71.1, 40.5, 31.5, 29.8, 29.7, 29.6, 29.5, 29.4, 28.5, 27.4, 26.8, 22.9, 14.2; ^{1}H NMR ($CDCl_3$) *d* 8.82 (s, 1H), 8.80 (s, 1H), 4.46 (t, *J* = 6.2 Hz, 2H), 3.88 (t, 2H), 3.72 (m, 2H), 3.68 (t, *J* = 5.3 Hz, 2H), 3.61 (m, 6H), 3.53 (t, *J* = 5.4 Hz, 2H), 2.81 (t, *J* = 6.5 Hz, 2H), 0.94 (t, *J* = 6.0 Hz, 3H) ppm; ESI –MS (positive-ion) 487. ($[M + H]^+$).

Toluene-4-sulfonic acid-poly(ethylene glycol) 5.16. According to the method used for **4.1**, **5.16** was obtained as a thick clear oil in 68% yield. ^{1}H NMR ($CDCl_3$) d 7.75 (d, *J* = 8.2 Hz, 2H), 7.30 (d, *J* =8.2 Hz, 2H), 4.11 (t, *J* = 4.6 Hz, 2H), 3.53-3.67 (comp, 48H), 2.40 (s, 3H); ESI –MS (positive-ion) 702 (also prevalent: 746, 790, 658) ($[M + H]^+$).

Amino ethyl poly(ethylene glycol) 5.17. 5.16 (2.5 g, ~3.5 mmol) was dissolved in ACN (50 ml) and sodium azid (0.5 g, 7.7 mmol) was added. The solution was heated to reflux under argon, and allowed to stir for 14 hours. The solution was then allowed to cool, concentrated under reduced pressure, and then H_2O (50 ml) was added. The aqueous

solution was extracted with CH_2Cl_2 (9 x 30 ml) and the combined organic portions were dried (Na_2SO_4) and concentrated under reduced pressure. The yellow oil was then dissolved in THF (25 ml) and H_2O (0.2 ml) and triphenyl phosphine (1.0 g, 4 mmol) were added under argon. The solution was allowed to stir at room temperature for 8 hours, and then concentrated under reduced pressure. The oil was dissolved in 0.2 M HCl and then filtered, and washed with Ch_2Cl_2 (4 x 20 ml). The aqueous layer was then neutralized with NaOH and then concentrated under reduced pressure. CH_2Cl_2 (50 ml) was added to the residue, and the solution was then filtered and concentrated to yield the title compound as a clear oil in 80% yield. ^{1}H NMR ($CDCl_3$) *d* 3.54 (m, 44H), 2.85 (t, *J* = 5.1 Hz, 2H), 2.46 (t, *J* = 4.8 Hz, 2H) ppm; ESI –MS (positive-ion) 546 (also prevalent: 690, 734, 502) ($[M + H]^+$).

2-(2-amino ethyl)-7-poly(ethylene glycol)-benzo[*lmn*][3,8]phenanthroline-1,3,6,8-tetraone (5.18). According to the method used for **5.12**, **5.18** was obtained as a thick orange oil in 31% yield. ^{1}H NMR ($CDCl_3$) *d* 8.72 (s, 4H), 4.46 (t, *J* = 6.3 Hz, 2H), 4.13 (t, *J* = 6.8 Hz, 2H), 3.72 (7, *J* = 6.5 Hz, 2H), 3.54 (m, 48H) ppm; ESI –MS (positive-ion) 838 (also prevalent: 883, 927, 794) ($[M + H]^+$).

Tris-[Poly(ethylene glocol)-Ndi]-benzene-1,3,5-tricarboxylate 5.19. 5.11 (0.2 g, 0.28 mmol) was dissolved in dry DMF (10 ml) and degassed with argon. A solution of **5.18** (0.8 g, 0.95 mmol) and TEA (1 ml) in DMF (10 ml) was added dropwise over 1 hour via an addition funnel. The solution was allowed to stir at room temperature for 4 hours, forming an orange precipitate. The solution was filtered, and the precipitated washed

will cold DMF (3 x 20 ml) to yield the title compound as an orange solid (95%). ^{1}H NMR ($CDCl_3$) *d* 9.10 (br, 3H), 8.62 (s, 12H), 8.12 (s, 3H), 4.23 (m, 6H), 3.71 (t, *J* = 6.8 Hz, 6H), 3.52 (m, 6H), 3.43 (m, 124H) ppm; ESI –MS (positive-ion) 2671 (also prevalent: 2715, 2759, 2803, 2847, 2891, 2627, 2583) ($[M + H]^+$).

Tris-1,3,5-acetyl benzene 5.20. Phloroglucinol (10 g, 79 mmol) was dissolved in ACN (100 ml) and acetic anhydride (100 ml) was added. The solution was allowed to stir at room temperature for 4 hours, and then water (700 ml) was slowly added. The precipitate was filtered and dried giving the title compound in quantitative yield. ^{13}C NMR ($CDCl_3$) *d* 169.0, 152.2, 111.8, 20.4; ^{1}H NMR (DMSO) *d* 6.85 (s, 3H), 2.29 (s, 9H) ppm; ESI –MS (positive-ion) 253 ($[M + H]^+$).

5-Hydroxy-1,3-phenyl-bis-acetate 5.21 and 3,5-dihydroxy phenyl acetate 5.22 (4 g, 15.9 mmol) was dissolved in toluene (100 ml) and ethanol (75 ml) and $NaBH_4$ (0.4 g, 10 mmol) was added. The reaction was heated to 40°C under argon and allowed to stir for 1 hour. H_2O was added, and the solution extracted with CH_2Cl_2 (3 x 100 ml). The organic layers were combined, concentrated under reduced pressure, and then purified via column chromatography to yield **5.21** and **5.22** (39% and 34%). **5.21**: ^{13}C NMR ($CDCl_3$) *d* 169.4, 159.1, 153.1, 107.8, 106.2, 20.4; ^{1}H NMR ($CDCl_3$) *d* 6.69 (s, 1H), 6.52 (s, 2H), 5.21 (br, 1H), 2.23 (s, 6H) ppm; ESI –MS (positive-ion) 211 ($[M + H]^+$). **5.22**: ^{13}C NMR (DMSO) *d* 168.4, 159.1, 154.5, 102.8, 100.2, 20.3; ^{1}H NMR (DMSO) *d* 6.57 (s, 2H), 6.52 (s, 1H), 5.21 (br, 1H), 2.13 (s, 3H) ppm; ESI –MS (positive-ion) 169 ($[M + H]^+$).

3,5-dihydroxy benzyloxy benzene 5.23. Benzyl bromide (0.6 g, 3.5 mmol), K_2CO_3 (0.6 g) and a catalytic amount of 18-crown-6 were dissolved in ACN and degassed with

argon. **2.21** (0.72 g, 3.4 mmol) was dissolved in ACN and the solution was degassed with argon and then the two solutions were combined. The mixture was heated to 50°C and allowed to stir under argon for 14 hours, allowed to cool, filtered, and then concentrated under reduced pressure. The residue was then dissolved in dioxane (40 ml) and 2 M KOH (40 ml) was added. The solution was stirred at reflux for two hours, allowed to cool, and then extracted with CH_2Cl_2 (5 x 30 ml). The combined organic phases were concentrated under reduced pressure and purified via column chromatography (toluene 70 %, acetone 30%) to yield the title compound (77%). ^{13}C NMR (DMSO) *d* 164.1, 161.2, 141.3, 129.9, 128.3, 128.1, 96.0, 94.2, 70.1; ^{1}H NMR (DMSO) *d* 7.23 (m, 5H), 5.91 (s, 2H), 5.88 (s, 1H), 5.21 (s, 2H) 4.84 (br, 2H) ppm; ESI –MS (positive-ion) 217 ($[M + H]^+$).

5-dihydroxy-1,3-bis-benzyloxy benzene 5.24 According to the method used for **5.23**, **5.24** was obtained as white crystals in 67% yield. ^{13}C NMR (DMSO) *d* 163.5, 161.2, 142.6, 129.1, 128.1, 127.6, 94.9, 93.1, 70.3; ^{1}H NMR (DMSO) *d* 7.23 (m, 10H), 5.91 (s, 1H), 5.86 (s, 2H), 2.33 (s, 4H), 4.89 (br, 1H) ppm; ESI –MS (positive-ion) 307 ($[M + H]^+$).

1,3-diethyl 5-perfluorophenyl benzene-1,3,5-tricarboxylate 5.25. According to the method used for **5.11**, **5.25** was obtained as white crystals in 96% yield. ^{13}C NMR (DMSO) *d* 166.0, 165.2, 150.3, 142.1, 140.3, 137.6, 135.1, 134.6, 130.4, 130.2, 60.9, 14.7; ^{1}H NMR (DMSO) *d* 9.16 (s, 2H), 8.90 (s, 1H), 4.38 (q, *J* = 6.2 Hz, 4H), 1.44 (t, *J* = 5.2 Hz, 6H) ppm; ESI –MS (positive-ion) 433 ($[M + H]^+$).

1,5-bis(allyloxy)naohthalene 5.26. According to the method used for **3.1**, **5.26** was obtained as yellow crystals in 77% yield. ^{13}C NMR ($CDCl_3$) *d* 158.2, 133.9, 128.7, 125.1,

115.6, 119.2, 73.3; ^{1}H NMR ($CDCl_3$) *d* 7.94 (d, *J* = 7.8 Hz, 2H), 7.39 (t, *J* = 8.4 Hz, 2H), 6.88 (d, *J* = 7.2 Hz, 2H) 6.20 (m, 2H), 5.48 (m, 4H), 4.74 (d, *J* = 5.4 Hz, 4H) ppm; ESI –MS (positive-ion) 241 ($[M + H]^+$).

2,6-diallylnaphthalene-1,5-diol 5.27. 5.26 (3 g, 12.4 mmol) was placed into a flask and put in sand in an electric heater. Under argon, the reaction was heated to 160°C for 2 hours (DO NOT OVERHEAT). The white solid was purified via column chromatography (CH_2Cl_2 70%, acetone 30%) to yield the title compound (60%). ^{13}C NMR ($CDCl_3$) *d* 153.2, 139.1, 126.1, 125.7, 117.8, 117.4, 115.8, 39.1; ^{1}H NMR ($CDCl_3$) *d* 7.73 (d, *J* = 8.4 Hz, 2H), 7.23 (d, *J* = 8.4 Hz, 2H), 6.08 (m, 2H), 5.52 (br, 2H), 5.27 (m, 4H), 3.59 (d, *J* = 6.3 Hz, 4H) ppm; ESI –MS (positive-ion) 241 ($[M + H]^+$).

3,4,5-tris(hexyloxy)benzoic acid 5.28. Ethyl-3,4,5-trihydroxybenzoate (4 g, 20.2 mmol) and 1-bromohexane (10 g, 62 mmol) was dissolved in acetone (100 ml) and catalytic amounts of LiI and 18-crown-6 were added. The solution was degassed with argon, and then K_2CO_3 (9 g) was added. The solution was allowed to stir at reflux under argon for 36 hours, then allowed to cool, filtered, and concentrated under reduced pressure. The off-white solid was then dissolved in ACN (100 ml) and 1 M KOH (75 ml) added. The solution was refluxed for 4 hours under argon, made slightly acidic with 2 M HCl, and concentrated under reduced pressure. The white solid was washed with CH_2Cl_2 (5 x 40 ml), filtered, and the organic washes concentrated. The white solid was purified via column chromatography to yield **5.28** in 81% yield. ^{13}C NMR ($CDCl_3$) *d* 171.4, 149.6, 142.1, 123.8, 106.9, 69.7, 69.3, 31.9, 29.7, 25.7, 22.9, 14.4; ^{1}H NMR ($CDCl_3$) *d* 10.04 (br, 1H), 7.31 (s, 2H), 4.03 (t, *J* = 6.0 Hz, 6H), 1.80 (m, 6H), 1.49 (p, *J* = 6.9 Hz, 6H), 1.35 (m, 12H), 0.91 (d, *J* = 6.9 Hz, 9H) ppm; ESI –MS (positive-ion) 423 ($[M + H]^+$).

Perfluorophenyl 3,4,5-tris(hexyloxy)benzoate 5.29. According to the method used for **5.11**, **5.29** was obtained as white crystals in 93% yield. ^{13}C NMR ($CDCl_3$) *d* 167.2, 151.0, 148.1, 142.9, 141.4, 140.0, 137.2, 124.6, 106.8, 69.5, 69.2, 31.9, 29.7, 25.7, 22.9, 14.4; ^{1}H NMR ($CDCl_3$) *d* 7.11 (s, 2H), 3.98 (t, *J* = 5.8 Hz, 6H), 1.80 (m, 6H), 1.44 (p, *J* = 6.4 Hz, 6H), 1.32 (m, 12H), 0.90 (d, *J* = 6.6 Hz, 9H) ppm; ESI –MS (positive-ion) 589 ($[M + H]^+$).

3,4,5-tris[tetra(ethylene glycol)]benzoic acid 5.30. Ethyl-3,4,5-trihydroxybenzoate (4 g, 20.2 mmol) and **4.1** (21.1 g, 61 mmol) were dissolved in acetone and a catalytic amounts of 18-crown-6 was added. The solution was degassed with argon, and then K_2CO_3 (9 g) was added. The reaction was allowed to stir at reflux under argon for 36 hours, and then cooled, filtered, and concentrated under reduced pressure. The oil was purified via column chromatography (toluene 40%, acetone 52%, ethanol 8%) and then placed in 1M KOH (100 ml) and refluxed for 4 hours. The solution was allowed to cool, and then made slightly acidic with 2M HCl, concentrated under reduced pressure, and ACN (5 x 40) was added and filtered. The washes were combined and concentrated to give a clear oil as the title compound in 73% yield. ^{13}C NMR (DMSO) *d* 171.2, 147.8, 142.2, 124.6, 107.3, 76.2, 73.1, 71.3, 71.0, 70.5, 71.4, 70.3, 62.7; ^{1}H NMR (DMSO) *d* 10.72 (br, 1H), 7.10 (s, 2H), 4.21 (t, *J* = 6.4 Hz, 6H), 3.82 (m, 6H), 3.61 (comp, 42H), ppm; ESI –MS (positive-ion) 698 ($[M + H]^+$).

2-bromo-6-(undecyloxy)naphthalene 5.31 According to the method used for **3.1**, **5.31** was obtained as white crystals in 73% yield. ^{13}C NMR ($CDCl_3$) *d* 158.2, 135.6, 130.2, 129.9, 128.4, 128.3, 127.6, 120.0, 118.6, 105.2, 69.2, 29.7, 29.6, 29.3, 26.0, 14.2; ^{1}H

NMR ($CDCl_3$) *d* 7.93 (s, 1H), 7.63 (m, 2H), 7.51 (m, 1H), 7.18 (m, 1H), 7.11 (s, 1H), 4.08 (t, *J* = 6.6 Hz, 2H), 1.82 (p, *J* = 5.7 Hz, 2H), 1.47 (comp, 16H), 0.92 (t, *J* = 5.1 Hz, 3H) ppm; ESI –MS (positive-ion) 377 ($[M + H]^+$).

1,8-dicarboxyundecylimide-(4-bromo)-naphthalene 5.32. According to the method used for **3.7**, **5.32** was obtained as orange crystals in 82% yield.^{13}C NMR ($CDCl_3$) *d* 161.4, 139.0, 137.7, 137.2, 133.4, 132.9, 130.6, 129.2, 126.2, 124.6, 40.7, 32.1, 30.0, 29.9, 29.8, 29.7, 29.6, 27.2, 26.9, 23.1, 14.3; ^{1}H NMR ($CDCl_3$) *d* 8.67 (d, *J* = 7.2 Hz, 1H), 8.57 (d, *J* = 8.4 Hz, 1H), 8.42 (d, *J* = 7.8 Hz, 1H), 8.05 (d, *J* = 8.1 Hz, 1H), 7.86 (t, *J* = 7.5 Hz, 1H), 4.18 (t, *J* = 7.5 Hz, 2H), 1.75 (p, *J* = 6.9 Hz, 2H), 1.30 (comp, 16H), 0.90 (t, *J* = 6.3 Hz, 3H); ESI –MS (positive-ion) 430 ($[M + H]^+$).

1,4-bis(2-(-2-(undecyloxy)naphthalene-6-yl)vinyl)benzene 5.33. *p*-Divinylbenzene (0.11 g, 0.8 mmol) after purification via tetrabromination, selective recrystallization, and debromination, **5.31**, palladacycle (56 mg, 0.06 mmol) and NaOAc (0.16 g, 2 mmol) were added to DMF (25 ml) and stirred for 16 hours under argon at 120°C. The solution was concentrated under reduced pressure, dissolved in CH_2Cl_2 and then washed with water (2 x 20 ml) and brine (20 ml), dried (Na_2CO_3) and concentrated under reduced pressure. The sludge was then purified via column chromatography (CH_2Cl_2 60%, hexanes 20%, acetone 20%) to yield the title compound (23%). ^{13}C NMR (DMSO) *d* 158.6, 135.3, 135.0, 132.1, 129.9, 129.7, 127.6, 127.4, 126.8, 125.2, 124.6, 124.2, 116.4, 110.3, 68.9, 32.1, 30.0, 29.9, 29.8, 29.7, 29.6, 27.2, 26.9, 23.1, 14.3; ^{1}H NMR (DMSO) *d* 7.81 (br, 2H), 7.72 (m, 4H), 7.49 (dd, J_1 = 8.4 Hz, J_2 = 19.8 Hz, 4H), 7.18 (m, 4H), 6.75 (m, 2H), 5.80 (m, 1H), 5.27 (m, 1H), 4.10 (t, *J* = 6.6 Hz, 4H), 1.82 (p, *J* = 5.7 Hz, 4H), 1.47 (comp, 32H), 0.92 (t, *J* = 5.1 Hz, 6H); ESI –MS (positive-ion) 724 ($[M + H]^+$).

1,4-bis(4-(1,8-dicarboxyundecylimide)vinyl)benzene 5.34. According to the method used for **5.33**, **5.34** was obtained as orange crystals in 67% yield. ^{13}C NMR (DMSO) *d* 164.5, 164.2, 141.3, 137.3, 134.8, 131.5, 131.3, 130.1, 129.8, 128.9, 127.9, 124.3, 124.2, 123.5, 122.0, 40.8, 32.2, 29.9, 29.7, 28.4, 27.4, 22.9, 14.4; ^{1}H NMR (DMSO) *d* 8.64 (m, 6H), 8.00 (m, 4H), 7.83 (t, *J* =7.5 Hz, 2H), 7.73 (s, 4H), 7.40 (m, 2H), 4.20 (t, *J* = 7.8 Hz, 4H) 1.74 (p, *J* = 5.7 Hz, 4H), 1.34 (comp, 32H), 0.90 (t, *J* = 5.1 Hz, 6H), ESI –MS (positive-ion) 830 ($[M + H]^+$).

References

Albrecht, M.; Van Koten, G. “Platinum Group Organometallics Based on "Pincer" Complexes: Sensors, Switches, and Catalysts” Angew. Chem., Int. Ed. (2001), 40, 3750.

Amabilino, D. B.; Ashton, P. R.; Brown, C. L.; Cordove, E.; Godinez, L. A.; Goodnow, T. T.; Kaifer, A. E.; Newton, S. P.; Pietraszkiewicz, M.; Philp; Raymo, F. M.; Reder, A. S.; Rutland, M. T.; Slawin, A. M. Z.; Spencer, N; Stoddart, J. F. “Molecular meccano. 2. Self-assembly of [n]catenanes” J. Am. Chem. Soc. (1995), 117, 1271.

Amabilino D. B., Stoddart J. F. “Interlocked and intertwined structures and superstructures” Chem. Rev. (1995b), 95, 2725.

Anelli, P. L; Ashton, P. R.; Ballardini, R.; Balzani, V.; Delgado, M.; Gandolfi, M. T.; Goodnow, T. T.; Kaifer, A. E.; Philp, D.; Pietraszkiewicz, M.; Prodi, L.; Reddington, M. V.; Slawin, A. M. Z.; Spencer, N.; Stoddart, F. J.; Vicent, C.; Willams, D. J. “Molecular Meccano. 1 [2]Rotaxanes and a [2]Catenane Made to Order” J. Am. Chem. Soc. (1992), 114, 193.

Archer, E. A.; Gong, H.; Krische, M. J. “Hydrogen bonding in noncovalent synthesis: Selectivity and the directed organization of molecular strands” Tetrahedron (2001), 57, 1139.

Archer, E. A.; Cauble, D. F.; Lynch, V.; Krische, M. J. “Synthetic duplex oligomers: Optimizing interstrand affinity through the use of a noncovalent constraint” Tetrahedron (2002), 58, 721.

Arico, Fabio; Badjic, Jovica D.; Cantrill, Stuart J.; Flood, Amar H.; Leung, Ken C.-F.; Liu, Yi; Stoddart, J. Fraser. “Templated synthesis of interlocked molecules.” Topics in Current Chemistry (2005), 249, 203.

Atwood, J. L.; Davies, J. E. D.; MacNicol D. M.; Vögtle, F.; Lehn, J.-M., Eds. “Comprehensive Supramolecular Chemistry” (1996), Vol 9, Pergamon, Oxford.

Badjic, J. D.; Nelson, A.; Cantrill, S. J.; Turnbull, W. B.; Stoddart, J. F. “Multivalency and Cooperativity in Supramolecular Chemistry” Acc. Chem. Res. (2005), 38, 723.

Bengs, H.; Ebert, M.; Karthaus, O.; Kohne,B.; Praefcke, K.; Ringsdorf, H.; Wendorff, J.; Wüstefeld, R. "Induction and variation of discotic columnar phases through doping with electron acceptors." Adv. Mater. (1990), 2, 141.

Braga, D.; Grepioni, F.; Desiraju, G. R. "Crystal Engineering and Organometallic Architechture" Chem. Rev. (1998), 98, 1375.

Branham, K. E.; Mays J. W.; Gray, G. M.; Bharara, P. C.; Byrd, H.; Bittinger, R.; Farmer, B. "Polycondensation of Dimethyl Phosphonate with Diols: SEC and ^{1}P and ^{13}C NMR Spectroscopic Studies" Polymer (2000), 41, 3371.

Brenner, M.; Seebach, D. "Synthesis and CD spectra in MeCN, MeOH, and H_2O of γ-oligopeptides with hydroxy groups on the backbone" Helv. Chem. Acta (2001), 84, 1181.

Brunsveld, L.; Zhang, H.; Glasbeek M.; Vekemans, J. A. J. M.; Meijer, E. W. "Hierarchical Growth of Chiral Self-Assembled Structures in Protic Media" J. Am. Chem. Soc. (2000), 122, 6175.

Carmichael, M.; Vidu, R.; Maksumov, A.; Palazoglu, A.; Stroeve, P. "Using Wavelets To Analyze AFM Images of Thin Films: Surface Micelles and Supported Lipid Bilayers." Langmuir (2004), 20, 11557.

Cheney, J.; Lehn, J.-M.; Sauvage, J. P.; Stubbs, M. E. "[3]-Cryptates: Metal Cation Inclusion Complexes with a Macrotricyclic Ligand" J.C.S. Chem. Comm. (1972), 1101.

Ciferri, A. ed. "Supramolecular polymers" Marcel Dekker: New York (2000)

Cubberley, M. S.; Iverson, B. L. "1H NMR investigation of solvent effects in aromatic stacking interactions" J. Am. Chem. Soc. (2001), 123, 7560.

Cubberley, M. S. Ph.D. thesis, "Investigation of solvent effects in aromatic electron donor-acceptor interactions" The University of Texas at Austin (2000).

Demus, D.; Goodby, J.; Gray, G. W.; Spiess, H.-W.; Vill, V. Eds. "Hanbook of Liquid Crystals, Vol 2B" (1998), Wiley-VCH, Weinheim.

Eaton, W. A.; Henry, E. R.; Hofrichter, J.; Mozzarelli, A. "Is Cooperative Oxygen Binding by Hemoglobin Really Understood?" Nat. Struct. Biol. (1999), 6, 351.

Edelmann, F. T.; Haiduc, I. "Supramolecular Organometalic Chemistry" (1999), Wiley-VCH, Weinheim.

Ercolani, G. "Assessment of cooperativity in self-assembly" J. Am. Chem. Soc. (2003), 125, 16097.

Fouquey, Claudine; Lehn, Jean Marie; Levelut, Anne Marie. Molecular recognition directed self-assembly of supramolecular liquid crystalline polymers from complementary chiral components. Adv. Mater. (1990), 2(5), 254.

Fukuda, M.; Kawai, H.; Horii, F.; Kitamaru, R. "CP/MAS Carbon-13 NMR Study for the Characterization of Water Sorbed in poly(p-phenyleneterephthalamide) fiber (Kevlar 49)." Polymer Communications (1988), 29, 97.

Gabriel, G. J.; Iverson, B. L. "Aromatic oligomers that form hetero duplexes in aqueous solutions" J. Am. Chem. Soc. (2002), 124, 15174.

Gabriel, G. J. Ph.D. thesis, "Exploiting Aromatic Donor-Acceptor Recognition in the Folding and Binding of Naphthyl Oligomers" The University of Texas at Austin (2004).

Gabriel, G. J.; Sorey, S.; Iverson, B. L. "Switching the folding patterns of naphthyl trimers" J. Am. Chem. Soc. (2005), 127, 2637.

Gellman, S. H. "Foldamers: A manifesto" Acc. Chem. Res. (1998), 31, 173.

Gellman, S. H. "Structure and function in foldamers" Polymer Preprints (2005), 46, 169.

Gionis, V.; Fugnitto, R.; Meyer, G.; Strzelecka, H.; Dubois, J. C. "Synthesis and redox properties of mesomorphic pi-donors" Mol. Cryst. Liq. Cryst. (1982), 90, 153.

Ghosh, S.; Ramakrishnan, S. "Aromatic donor-acceptor charge-transfer and metal-ion-complexation-assisted folding of a synthetic polymer" Angew. Chem., Int. Ed. (2004), 43, 3264.

Ghosh, S.; Ramakrishnan, S. "Small-Molecule-Induced Folding of a Synthetic Polymer" Angew. Chem., Int. Ed. (2005), 44, 5441.

Greene, R. N. "18-Crown-6: A Strong Complexing Agent for Alkali Metal Cations" Tet. Lett. (1972) 18, 1793.

Gührs, K.-H.; Weisshart, K.; Grosse, F. "Lessons from Nature-Protein Fibers" Rev. in Mol. Biotech. (2000), 74, 121.

Hamelton, D. G.; Sanders, J. K. M.; Davies, J. E.; Clegg, W.; Teat, S. J. "Neutral [2] catenanes from oxidative coupling of p-stacked components" Chem. Commun. (1997), 897.

Hamley, I. W.; Connell, S. D.; Collins, S. "In Situ Atomic Force Microscopy Imaging of Adsorbed Block Copolymer Micelles." Macromolecules 2004, 37, 5337.

Helgeson, R. C.; Timko, J. M.; Cram, D. J. "Structural Requirements for the Cyclic Ethers to Complex and Lipophilize Metal Cations or a-Amino Acids" J. Am. Chem. Soc. (1973), 95, 3023.

Hill, D. J.; Mio, M. J.; Prince, R. B.; Hughes, T. S.; Moore, J. S. "A field guide to foldamers" Chem. Rev. (2001), 101, 3893.

Hofmeier, H; Schubert, U. S. "Supramolecular Branching and Crosslinking of Terpyridine-Modified Copolymers: Complexation and Decomplexation Studies in Diluted Solution." Macromol. Chem. Phys. (2003), 204, 1391.

Hunter, C. A.; Sanders, J. K. M. "The nature of π-π interactions" J. Am. Chem. Soc. (1990), 112, 5525.

HyperCube, Inc. HyperChem Computational Chemistry Manual. (Gainesville, FL, 32601) (1996) HyperChem 5.1.

Iijima, T.; Vignon, S. A.; Tseng, H.-R.; Jarrosson, T.; Sanders, J. K. M.; Marchioni, F.; Venturi, M.; Apostoli, E.; Balzani, V.; Stoddart, J. F. "Controllable Donor-Acceptor Neutral [2]Rotaxanes" Chem. Eur. J. (2004), 10, 6375.

Ilhan, F.; Gray, M.; Blanchette, K.; Rotello, V. M. "Control of polymer solution structure via intra- and intermolecular aromatic stacking" Macromolecules (1999), 32, 6159.

Kimizuko, N.; Fujikawa, S.; Kuwahara, H.; Kunitake, T.; Marsh, A.; Lehn, J.-M. "Mesoscopic supramolecular assembly of a 'Janus' molecule and a melamine derivative via complementary hydrogen bonds." J. Chem. Soc. Chem. Commun. (1995), 2103.

Kirshenbaum, K.; Barron, A. E.; Goldsmith, R. A.; Armand, P.; Bradley, E. K.; Truong, K. T. V.; Dill, K. A.; Cohen, F. E.; Zuckermann, R. N. "Sequence-specific polypeptoids: a diverse family of heteropolymers with stable secondary structure" Proc. Natl. Acad. Sci. U. S. A. (1998), 95, 4303.

Kouwer, P. H. J.; Jager, W. F.; Mijs, W. M.; Picken, S. J. Macromolecules (2002) 35, 4322.

Kubik, S. "High-performance fibers from spider silk" Angew. Chem., Int. Ed. (2002), 41, 2721.

Langenhan, J. M.; Gellman, S. H. "Effects of alternative side chain pairings and reverse turn sequences on antiparallel sheet structure in β-peptide hairpins" Org. Lett. (2004), 6, 937.

Lehn, J.-M. "Perspectives in Supramolecular Chemistry - From Molecular Recognition towards Molecular Information Processing and Self-Organization" Angew. Chem. Int. Ed. Engl. (1990), 29, 1304.

Lehn, J.-M. "Supramolecular Polymer Chemistry-Scope and Perspective" Polym. Int. (2002), 51, 825.

Li, X.-Q.; Jia, M.-J.; Wang, X.-Z.; Jiang, X.-K.; Li, Z.-T.; Chen, G.-J.; Yu, Y.-H. "Self-Assembly of a New Series of Quadruply Hydrogen bonded Heterotrimers Driven by the Donor-Acceptor Interaction" Tetrahedron (2005), 61, 9600.

Lokey, R. S.; Iverson, B. L. "Synthetic molecules that fold into a pleated secondary structure in solution" Nature (1995), 375, 303.

Lokey, R. S. Ph.D. thesis, "Aedamers: A synthetic approach to higher-order structure" The University of Texas at Austin (1997).

Matsuda, K.; Stone, M. T.; Moore, J. S. "Helical Pitch of *m*-Phenylene Ethynylene Foldamers by Double Spin Labeling" J. Am. Chem. Soc. (2002), 124, 11836

Microcal Inc. VP-ITC MicroCalorimeter user's manual. ORIGIN software package included. Northhampton, MA 01060, (1999).

Nelson, J. C.; Saven, J. G.; Moore, J. S.; Wolynes, P. G. "Solvophobically driven folding of nonbiological oligomers" Science (1997), 277, 1793.

Park, J. W.; Bak, C. S.; Labes, M. M. "Effects of Molecular Complexing on the Properties of Binary Nematic Liquid Crystal Mixtures" J. Am. Chem. Soc. (1975), 97, 4398.

Park, L. Y.; Hamilton, D. G.; McGehee, E. A.; McMenimen, K. A. "Complementary C3-Symmetric Donor-Acceptor Components: Cocrystal Structure and Control of Mesophase Stability" J. Am. Chem. Soc. (2003), 125, 10586.

Park, T.; Zimmerman, S. C.; Nakashima, S. "A Highly Stable Quadruply Hydrogen-Bonded Heterocomplex Useful for Supramolecular Polymer Blends" J. Am. Chem. Soc. (2005), 127, 6520.

Pedersen, C. J. "Cyclic Polyethers and Their Complexes with Metal Salts" J. Am. Chem. Soc. (1967), 86, 7017.

Philp, D.; Stoddart, J. F. "Self-assembly in natural and unnatural systems" Angew. Chem. Int. Ed. Engl. (1996), 35, 1154.

Pollino, J. M.; Weck, M. "Non-Covalent Side-Chain Polymers: Design Principles, Functionalization Strategies, and Perspectives." Chem. Soc. Rev., 2005, 34, 193.

Prince, R. B.; Brunsveld, L.; Meijer, E. W.; Moore, J. S. "Twist sense bias induced by chiral side chains in helically folded oligomers" Angew. Chem., Int. Ed. (2000a), 39, 228.

Prince, R. B.; Barnes, S. A.; Moore, J. S. "Foldamer-Based Molecular Recognition" J. Am. Chem. Soc. (2000b), 122, 2758.

Reczek, J. J.; Villazor, K. R.; Lynch, V.; Swager, T. M.; Iverson, B. L.; "Tunable Columnar Mesophases Utilizing C_2 Symmetric Aromatic Donor-Acceptor Complexes" J. Am. Chem. Soc. (2006a), 128, 7995.

Reczek, J. J.; Iverson, B. L.; "Using Aromatic Donor Acceptor Interactions to Affect Macromolecular Assembly" Macromolecules (2006b), 39, 5601.

Reinhoudt, D. N.; Crego-Calama, M. "Synthesis Beyond the Molecule" Science (2002), 295, 2403.

Rieth, L. R.; Eaton, R. F.; Coates, G. W. "Polymerization of Ureidopyrimidinone-Functionalized Olefins by Using Late-Transition Metal Ziegler-Natta Catalysts: Synthesis of Thermoplastic Elastomeric Polyolefins." Angewandte Chemie, International Edition (2001), 40, 2153.

Ringsdorf, H.; Wüstefeld, R.; Zerta, M.; Ebert, J.; Wendorff, J. "Induction of Liquid-Crystal Phases: Discotic Systems Obtained by Providing Amorphous Polymers with Electron Acceptors." Angew. Chem. (1989), 101, 934.

Schmidt-Mende, L.; Fechtenkötter, A.; Müllen, K.; Moons, E.; Friend, R.; MacKenzie, J. "Self-organized discotic liquid crystals for high-efficiency organic photovoltaics." Science (2001), 293, 1119.

Seebach, D.; Abele, S.; Gademann, K.; Jaun, B. "Pleated sheets and turns of β-peptides with proteinaceous side-chains" Angew. Chem., Int. Ed. (1999), 38, 1595.

Steed, J. W.; Atwood, J., L. "Supramolecular Chemistry" John Wiley & Sons: New York (2000)

Stone, M. T.; Moore, J. S. "A water-soluble m-phenylene ethynylene foldamer" Org. Lett. (2004), 6, 469.

Tanatani, A.; Mio, M. J.; Moore, J. S. "Chain length-dependent affinity of helical foldamers for a rodlike guest" J. Am. Chem. Soc. (2001), 123, 1792.

Thibault, R. J.; Hotchkiss, P. J.; Gray, M.; Rotello, V. M. "Thermally Reversible Formation of Microspheres throught Non-Covalent Polymer Cross-Linking" J. Am. Chem. Soc. (2003), 125, 11249.

Vollrath, F.; Knight, D. P.; "Liquid Crystalline Spinning of Spider Silk" Nature (2001), 410, 541.

Vollrath, F. "Strength and structure of spiders' silk" Rev. Mol. Biotech. (2000), 74, 67.

Wadso, I. "Isothermal Microcalorimetry Near Ambient Temperature: An Overview and Discussion" Thermochimica Acta (1997), 294, 1.

Waters, M. L. "Aromatic interactions in model systems" Curr. Opin. Chem. Biol. (2002), 6, 736.

Weck, M.; Dunn, A. R.; Matsumoto, K.; Coates, G. W.; Lobkovsky, E. B.; Grubbs, R. H. "Influence of Perfluoroarene-Arene Interactions on Phase Behavior of Liquid Crystalline and Polymeric Materials" Angew. Chem. (1999), 38, 2741.

Whitesides, G. M.; Grzybowski, B. "Self-Assembly at All Scales" Science (2002), 295, 2418.

Winkler, S.; Kaplan, D.L. "Molecular biology of spider silk" Rev. in Mol. Biotech. (2000), 74, 303.

Wiseman, T.; Williston, S.; Brandts, J. F.; Lin, L. N. "Rapid measurement of binding constants and heats of binding using a new titration calorimeter" Anal. Biochem. (1989), 179, 131.

Zhao, X.; Jia, M.-X.; Jiang, X. K.; Wu, L.-Z.; Li, Z.-T.; Chen, G.-J. "Zipper-featured d-peptide foldamers driven by donor-acceptor interaction. Design, synthesis, and characterization" J. Org. Chem. (2004), 69, 270.

Zhou, Q.-Z.; Jiang, X. K.; Shao, X.-B.; Chen, G.-J.; Jia, M.-X.; Li, Z.-T. "First zipper-featured molecular duplexes driven by cooperative donor-acceptor interaction" Org. Lett. (2003), 5, 1955. [Addition/Correction; (2003), 5, 2763.]

Zych, A. J.; Iverson, B. L. "Synthesis and conformational characterization of tethered, self-complexing 1,5-dialkoxynaphthalene / 1,4,5,8-naphthalenetetracarboxylic diimide systems" J. Am. Chem. Soc. (2000), 122, 8898.

Zych, A. J. Ph.D. thesis, "Conformational characterization of non-natural secondary structures based on aromatic stacking" The University of Texas at Austin (2001).

Vita

Joseph James Reczek was born the oldest of three children of Dr. James A. Reczek and Christine A. Reczek on January 31, 1979 in the city of Rochester NY. He graduated from Greece Athena High School in 1997 and attended Cornell University beginning in the fall of that year. He began his research in chemistry in the summer of 1999 as an intern in the polymer research laboratories of The Eastman Kodak company, and joined the group of Professor Geoffrey Coates that fall at Cornell where he worked until receiving his Bachelor of Arts with honors in 2001. He interned at The Eastman Kodak company for his third summer before entering the Graduate School of The University of Texas at Austin in the fall of 2001.

Permanent address: 46 Parkside La., Rochester NY 14612

This dissertation was typed by the author.